



Review

# The Role of Small Molecules and Their Effect on the Molecular Mechanisms of Early Retinal Organoid Development

Philip E. Wagstaff <sup>1,\*</sup> , Andrea Heredero Berzal <sup>2</sup>, Camiel J. F. Boon <sup>2,3</sup>, Peter M. J. Quinn <sup>4</sup> ,  
Anneloor L. M. A. ten Asbroek <sup>1</sup> and Arthur A. Bergen <sup>1,2,5,\*</sup>

<sup>1</sup> Department of Human Genetics, Amsterdam UMC, University of Amsterdam (UvA), 1105 AZ Amsterdam, The Netherlands; a.l.tenasbroek@amsterdamumc.nl

<sup>2</sup> Department of Ophthalmology, Amsterdam UMC, University of Amsterdam (UvA), 1105 AZ Amsterdam, The Netherlands; a.herederobezal@amsterdamumc.nl (A.H.B.); Camiel.boon@amsterdamumc.nl (C.J.F.B.)

<sup>3</sup> Department of Ophthalmology, Leiden University Medical Center (LUMC), 2333 ZA Leiden, The Netherlands

<sup>4</sup> Jonas Children's Vision Care and Bernard & Shirlee Brown Glaucoma Laboratory, Columbia Stem Cell Initiative, Departments of Ophthalmology, Pathology & Cell Biology, Institute of Human Nutrition, Vagelos College of Physicians and Surgeons, Columbia University, New York, NY, USA; Edward S. Harkness Eye Institute, Department of Ophthalmology, Columbia University Irving Medical Center—New York-Presbyterian Hospital, New York, NY 10032, USA; pq2138@cumc.columbia.edu

<sup>5</sup> Netherlands Institute for Neuroscience (NIN-KNAW), 1105 BA Amsterdam, The Netherlands

\* Correspondence: p.e.wagstaff@amsterdamumc.nl (P.E.W.); aabergen@amsterdamumc.nl (A.A.B.)



**Citation:** Wagstaff, P.E.; Heredero Berzal, A.; Boon, C.J.F.; Quinn, P.M.J.; ten Asbroek, A.L.M.A.; Bergen, A.A. The Role of Small Molecules and Their Effect on the Molecular Mechanisms of Early Retinal Organoid Development. *Int. J. Mol. Sci.* **2021**, *22*, 7081. <https://doi.org/10.3390/ijms22137081>

Academic Editors: Beatriz Cubelos, Florencia Cavodeassi and Luisa Sanchez-Arroles

Received: 1 June 2021  
Accepted: 26 June 2021  
Published: 30 June 2021

**Publisher's Note:** MDPI stays neutral with regard to jurisdictional claims in published maps and institutional affiliations.



**Copyright:** © 2021 by the authors. Licensee MDPI, Basel, Switzerland. This article is an open access article distributed under the terms and conditions of the Creative Commons Attribution (CC BY) license (<https://creativecommons.org/licenses/by/4.0/>).

**Abstract:** Early in vivo embryonic retinal development is a well-documented and evolutionary conserved process. The specification towards eye development is temporally controlled by consecutive activation or inhibition of multiple key signaling pathways, such as the Wnt and hedgehog signaling pathways. Recently, with the use of retinal organoids, researchers aim to manipulate these pathways to achieve better human representative models for retinal development and disease. To achieve this, a plethora of different small molecules and signaling factors have been used at various time points and concentrations in retinal organoid differentiations, with varying success. Additions differ from protocol to protocol, but their usefulness or efficiency has not yet been systematically reviewed. Interestingly, many of these small molecules affect the same and/or multiple pathways, leading to reduced reproducibility and high variability between studies. In this review, we make an inventory of the key signaling pathways involved in early retinogenesis and their effect on the development of the early retina in vitro. Further, we provide a comprehensive overview of the small molecules and signaling factors that are added to retinal organoid differentiation protocols, documenting the molecular and functional effects of these additions. Lastly, we comparatively evaluate several of these factors using our established retinal organoid methodology.

**Keywords:** retinal organoids; retinogenesis; cell signaling; human development; disease modeling; stem cells

## 1. Introduction

### *Development of the Retina*

Human eye development can be separated into four main stages: the development of the neural tube, the formation of the optic vesicle, the invagination of the double layered optic cup, and the development of the fully differentiated retina. First, neural tube formation is induced by the developing notochord, a long rod that forms along the anteroposterior axis of the embryo (Figure 1A). The notochord secretes growth factors that prompts the differentiation of the overlying ectoderm into the neural ectoderm via hedgehog, BMP and Wnt signaling [1]. Subsequently, this structure thickens into the neural plate (Figure 1Ai). The lateral edges of the neural plate then rise to form neural folds,

fusing to form the neural tube, which is the precursor to the brain, eye, and spinal cord (Figure 1Aiii). Neural tube formation is known as primary neurulation and occurs by the end of the fourth week of embryonic development.

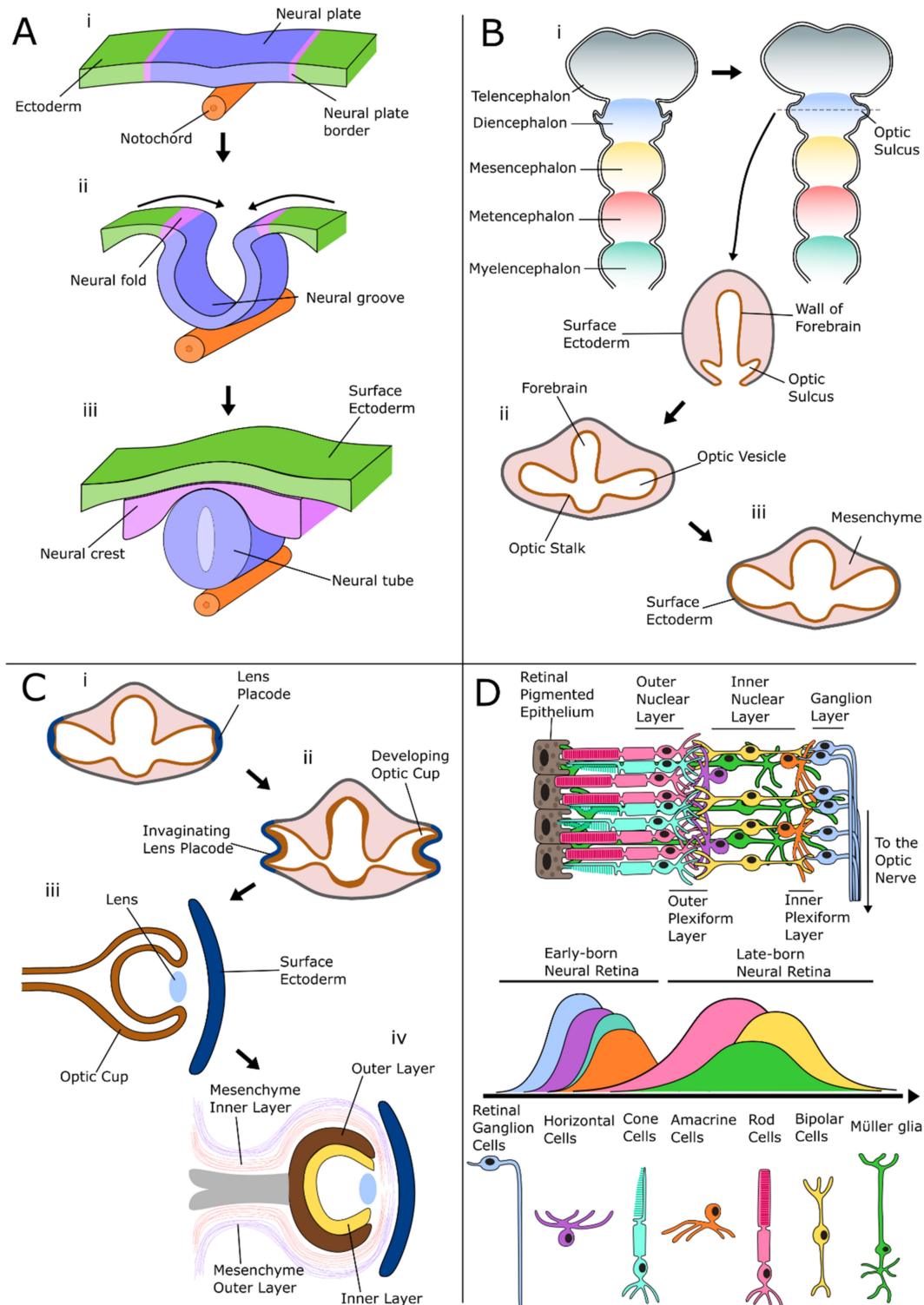


**Figure 1.** The phases of the embryological development of the eye. (A) The first stage of development is the formation of the neural tube. (Ai) The notochord stimulates the neural plate to be drawn inwards from the ectoderm. (Aii,Aiii) The neural folds meet and fuse, creating the neural tube and neural crest. (B) The formation of the optic vesicle. (Bi) The neural tube develops into five secondary vesicles. (Bii) The optic sulcus grows out laterally from the diencephalon, enlarging the

distal area to form the optic vesicle and pinching the proximal area to form the optic stalk. (Biii) The optic sulcus continues to grow until it reaches the surface ectoderm. (C) Development of the major eye structures. (Ci) The area of the surface ectoderm touching the optic vesicle thickens and forms the lens placode. (Cii) The lens placode then invaginates, before pinching off from the surface ectoderm to become the lens. (Ciii) This invagination results in a double-layered optic cup structure. (Civ) The outer layer later becomes the retinal pigmented epithelium, whereas the inner layer develops into the neural retina. The surrounding mesenchyme helps form structures such as the cornea, choroid, and ciliary body. (D) The retina is a laminated structure consisting of many different cells, which can be split into early-born neurons and late-born neurons. The early-born neurons include retinal ganglion cells, horizontal cells, cone cells and amacrine cells, whereas the late-born neurons consist of the rod cells, bipolar cells, and Müller glial cells. These are interconnected in the different layers of the retina, including the outer nuclear layer, the outer plexiform layer, the inner nuclear layer, the inner plexiform layer, and the ganglion layer.

The second major stage towards eye development can be considered as the formation of the optic vesicle. Once the neural tube has been formed, five secondary vesicles appear at the rostral part of the tube. These are the telencephalon, diencephalon, mesencephalon, metencephalon, and the myelencephalon, which give rise to the forebrain (telencephalon and diencephalon), midbrain (mesencephalon), and hindbrain (metencephalon and myelencephalon). Next, the area at the base of the diencephalon, on the border with the mesencephalon, forms a thickened area on either side (Figure 1Bi), which is the first sign of the bilateral separation of the optic tissue [2]. As the area continues to thicken and grow, it bulges and forms the optic sulci at embryonic day 22 (E22) [2,3]. Further in the development process, the distal area of the sulcus enlarges to form an optic vesicle at E24, whereas the proximal area restricts and forms the optic stalk (Figure 1Bii). The optic vesicle continues to grow laterally until it meets the outer surface ectoderm layer, which still surrounds the neural tube (Figure 1Biii) [4].

The third stage of eye development is the invagination of the optic vesicle and subsequent development of the other major eye structures (Figure 1C). Once the optic vesicle meets the outer surface ectoderm layer, the area of the surface ectoderm that overlays the optic vesicle thickens and form the lens placode (Figure 1Ci). The lens placode continues to thicken and move inwards towards the optic vesicle, pinching in to become the lens pit. As the lens pit forms, the optic vesicle also starts to invaginate into a double layered structure known as the optic cup by E32 (Figure 1Cii) [5]. The lens pit detaches from the surface ectoderm, becoming a separate structure that ultimately develops into the lens (Figure 1Ciii). The future choroid and sclera are formed by the mesenchyme, which surrounds the neural tube and optic vesicle throughout development [6]. The mesenchyme exists as two layers: an outer fibrous layer and an inner vascular layer. In eye development, the outer fibrous layer immediately touches the surface ectoderm where the lens placode was once located to form the cornea, along with the current surface ectoderm. In the posterior section, which surrounds the developing retina, the fibrous layer forms the sclera, whereas the inner vascular layer forms the choroid and part of the ciliary body (Figure 1Civ).

Finally, once the outer eye structure has formed, the retina can develop. Two parts of the retina will develop: the retinal pigment epithelium (RPE) and the neural retina (Figure 1D). The neural retina is formed from the inner wall of the optic cup which proliferates and differentiates, forming its multilayered structure. The outer wall remains as a single cuboidal layer which becomes the RPE [7]. The neural retinas go through an early phase and a late phase of development, with different types of cells differentiating and maturing in subsequent waves [8]. The first phase is characterized by the generation of ganglion cells, horizontal cells, cone photoreceptor cells and amacrine cells (Figure 1D). Retinal ganglion cells (RGCs) sit on the innermost layer of the retina and through their topographically mapped axonal projections transmit electrical signals to the brain [9]. Horizontal cells help integrate and regulate the input from multiple photoreceptors and localize to the outer plexus layer of the retina. Cone photoreceptors are located on the outermost layer of the retina and are responsible for distinguishing between colors under normal lighting conditions but cannot perform in areas with dim light. Although they are generally outnumbered in the retina by the rod photoreceptors, they converge in an

area of the neural retina called the fovea. Here, there are no rods present, and this area gives the best visual acuity of the eye. Amacrine cells are the last of the early-born retinal neurons and operate within the inner plexiform layer. Here, they interact with retinal ganglion cells and bipolar cells, affecting the output of the bipolar cells. The late phase of retinogenesis is characterized by the development of rod photoreceptors, Müller glial cells, and bipolar cells. Rod photoreceptors work in tandem with cone photoreceptors, allowing vision in dim light, but do not distinguish color. On the outermost layer of the retina, rods outnumber cones, by roughly 20:1 [10]. Müller glial cells are support cells to the other neural retinal cells. Whilst their cell bodies are located in the inner plexiform layer, Müller glial cell processes span the entire retina, from the inner limiting membrane to the outer limiting membrane. This helps maintain the laminar structure of the retina by providing stability. Müller glial cells also protect the retinal neurons by releasing neurotrophic factors, and maintaining the metabolic and electrophysiological homeostasis of the retina [11]. Bipolar cells are tasked with relaying the electrical stimulus from the photoreceptors to the retinal ganglion cells. Spanning across from the outer plexiform layer into the inner plexiform layer, bipolar cells can be separated into two major groups: Off-bipolar cells and On-bipolar cells. Off-bipolar cells continuously fire in the dark and are suppressed by light, while On-bipolar cells are excited by light and suppressed in the dark.

## 2. The Signaling Pathways of the Developing Retina

In this section, we describe the major signaling pathways involved in the development of the human eye: hedgehog (Section 2.1), BMP (Section 2.2) and Wnt (Section 2.3) signaling all have important functions in the early differentiation of the neural tube. TGF- $\beta$  (Section 2.2) signaling helps protect retinal neurons from apoptosis during early development, and notch (Section 2.4) signaling has a key role in retinal progenitor cell development and the production of distinct retinal populations. We provide an overview of each signaling pathway, with essential steps which can be targeted by small molecule additions.

### 2.1. Hedgehog Signaling

The hedgehog signaling pathway is presented in summary in Figure 2. It is an integral part of human embryonic development and is tasked with ensuring the proper differentiation of embryonic cells. It also initiates the formation of the neural tube after hedgehog signaling initiating factors are secreted by the notochord. Hedgehog signaling is conserved among many species. Vertebrate hedgehog homologues consist of three classes: Desert hedgehog, (Dhh), Indian hedgehog (Ihh), and Sonic hedgehog (Shh). The most well-understood class is Sonic hedgehog, which is involved in the regulation of the central nervous system and induction of motor neuron differentiation [12,13], although all three activate the hedgehog signaling pathway.

#### 2.1.1. Hedgehog Signaling: Mechanism of Action

The process of hedgehog signaling in vertebrates is complex and relies on concentration gradient-based cell to cell signaling. The pathway works through a multistep process. There are cells that secrete the ligand, a protein known as Sonic hedgehog (Shh), and target cells that relay the signal cascade to activate target gene transcription (Figure 2). A location-dependent spatial Shh concentration gradient between secreting cells and target cells determines the mode of action of the signaling pathway. Target cells located close to the secreting cells will receive higher Shh doses than cells further away, and develop into different cell types, which subsequently influences embryonic patterning and brain organization.

The signaling process can be divided into three stages: firstly, secreting cells release the Shh protein into the extracellular matrix. Secondly, the Shh protein binds to a receptor on a target cell that has not yet been targeted by Shh and is therefore in an "OFF State". Thirdly, the target cell becomes activated by Shh and turns into an "ON State", thus activating the transcription of target genes. These stages are described in detail below. The first stage

is characterized by secreting cells that cleave the Shh protein into two parts, N-terminal Shh (N-Shh), and C-terminal Shh (C-Shh) (Figure 2, top). These are released into the extracellular matrix. The second stage is initiated when N-Shh binds to PTCH1 on the target cell. A Shh target cell is, without signaling occurring, in the “OFF state” (Figure 2, left): the transmembrane protein (and receptor of Shh) PTCH1, inhibits Smoothed (Smo), a signal transducer. Smo inhibition allows suppressor of fused (SUFU) to bind to and inactivate the Gli proteins. This activates the transcriptional repressor complex of Gli3 and Glycogen synthase kinase -3 $\beta$  (GSK-3 $\beta$ ), whilst marking Gli1 and Gli2 for degradation, causing a transcriptional repression of hedgehog target genes. The inactivation of Smo, for example, by the selective Smo inhibitor cyclopamine, can cause this loss of expression even in the absence of PTCH1 [14]. The third stage is characterized by the transformation of the target cell into an “ON State” after the binding of N-Shh to PTCH1 (Figure 2, right): the binding of Shh to PTCH1 prevents the repression of Smo. This allows Smo to inhibit both the inactivation of the Gli proteins by SUFU, and the binding of GSK-3 $\beta$  to Gli3. This activates the transduction pathway, whereby the Gli1 and Gli2 transcription factors are activated and translocate to the nucleus, where they control the transcription of target genes, such as *PAX2* and *OTX2* [15–17]. The molecular mechanism by which Smo and Gli activates target gene expression is not fully known, and it has been shown that PTCH1 can also repress target gene transcription through a process independent of Smo [18].

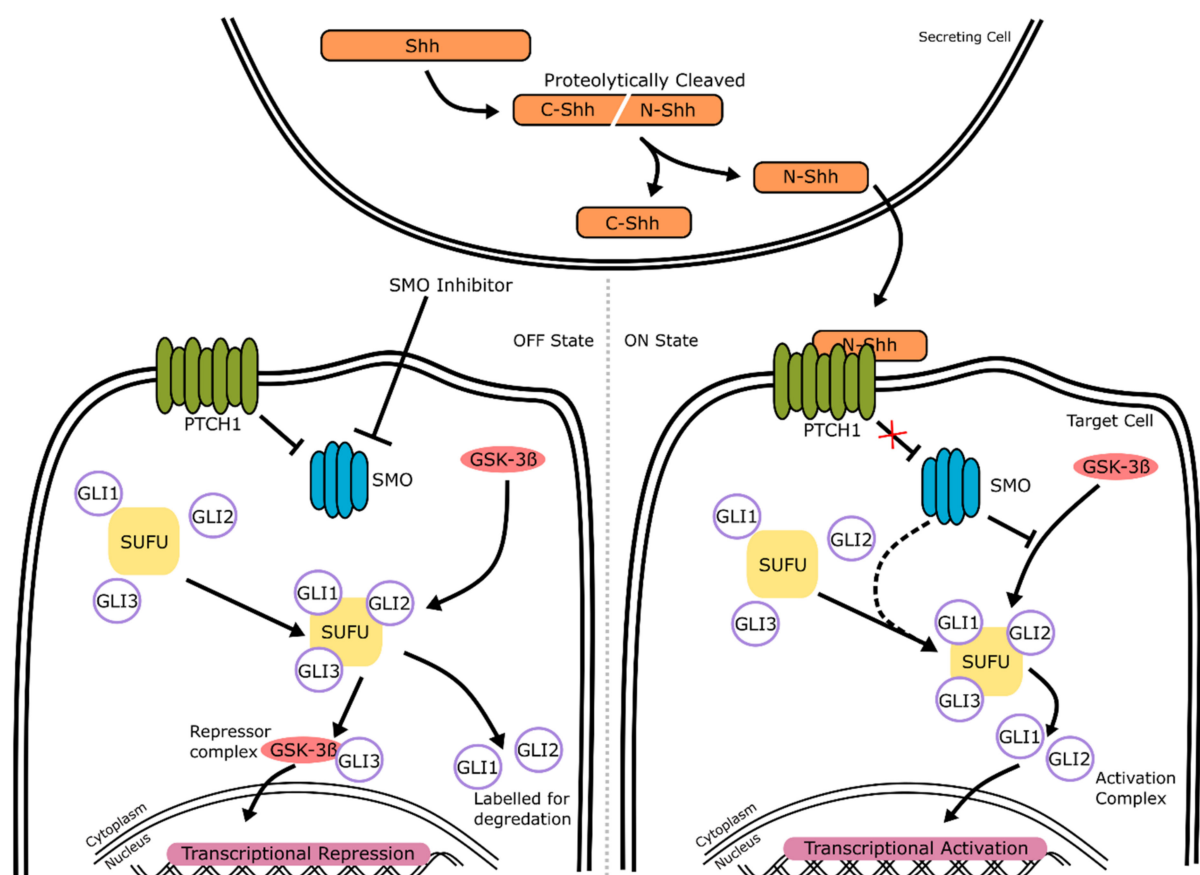


**Figure 2.** The hedgehog signaling pathway. (**Top**—Stage 1): to initiate hedgehog signaling, the secreting cell cleaves the Shh protein into two domains: N-Shh and C-Shh. N-Shh is then secreted into the extracellular domain. (**Left**—Stage 2): cells that have not yet been targeted by Shh exist in an “OFF State”. In this state, PTCH1 inhibits Smo, which allows SUFU to bind the Gli proteins, keeping them in an inactive state. Gli3 forms a repressor complex with GSK-3 $\beta$ , whilst Gli1 and Gli2 are marked for degradation. The repressor complex translocates to the nucleus, where it represses gene transcription. (**Right**—Stage 3): once the N-Shh has bound to the transmembrane protein PTCH1, cells transition into an “ON State”. In this state, PTCH1 no longer inhibits Smo, which in turn stops SUFU-mediated inactivation of the Gli proteins. This impedes the formation of the repressor complex and allows Gli1 and Gli2 to form an activation complex, which translocates to the nucleus and activates the transcription of target genes.

### 2.1.2. Hedgehog Signaling: Neural and Retinal Development

In neural development, the eye field develops from an area of the anterior neural plate that folds into a structure that will become the neural tube. This is stimulated by hedgehog signals secreted from the notochord, which initiates the invagination of the neural plate along the midline. Shh also has an important role in the bilateralization of the neural plate that results in determination of the eye fields, whereby cells acquire different identities depending on their relative spatial position within the eye. Studies in Shh knockout mice showed defects in bilateralization, and mice developed cyclopia [19].

Once the bilateral separation occurs, Shh is still required in the development and formation of the mature eye and specific cell types. Indeed, hedgehog signaling is intrinsically involved in all stages of retinal ganglion cell development. Neumann and Nusslein-Volhard (2000) showed in zebrafish models that a wave of Shh signaling moves throughout the eye, preceding an expressional wave of *atonal*, a known gene involved in early retinal ganglion cell differentiation [20]. Indeed, further experiments in zebrafish models demonstrated that, after initial ganglion cell development, hedgehog signaling was involved in the guidance of retinal ganglion cells axons exiting the eye through the optic nerve. Shh (and Smo) mutations in zebrafish models resulted in abnormal optic nerve growth, and some axons even failed to exit the eye [21]. Furthermore, continued signaling is needed for the maturation of the optic cup, and the inactivation of Shh at this stage leads to a hypoplastic optic nerve in murine models [22]. Finally, Shh signaling might also be involved in the guidance of retinal ganglion cell axons in the optic chiasm through the establishment of nerve fibers crossing along the rostral cranial axis. The addition of Shh causes axonal growth to slow in chick retina explants [23].

Shh signaling does not only affect the neural retina but is also involved in the differentiation and maturation of the RPE, which requires Shh signaling during the later stages of the development of the optic cup [24]. In zebrafish, Shh is temporally highly expressed in the RPE layer immediately before a wave of photoreceptor differentiation, with a reduction in Shh by antisense oligonucleotides inhibiting photoreceptor development [25]. In lens development, hedgehog signaling disrupts the differentiation of fiber cells in mouse models [26].

### 2.2. TGF- $\beta$ /BMP Signaling

The transforming growth factor-beta (TGF- $\beta$ ) signaling pathway is presented in Figure 3. It consists of a large superfamily of interacting proteins, growth factors, and Activins that govern many different cellular processes, from cell development to apoptosis. In humans, the TGF- $\beta$  superfamily consists of over 30 known members that encode for the different TGF- $\beta$  isoforms, bone morphogenetic proteins (BMPs), growth and differentiation factors (GDFs) and Activins [27]. All have differing roles in development and can be split into groups depending on which receptors they bind to. In retinal development, TGF- $\beta$  signaling protects neurons from programmed cell death during development [28]. BMP proteins, along with GDFs, make up a large subset of the TGF- $\beta$  superfamily [29]. The pathway is well conserved between species.

#### 2.2.1. TGF- $\beta$ /BMP Signaling: Mechanism of Action

There are two major branches of this signaling pathway: (1) the TGF- $\beta$ /Activin/Nodal pathway and (2) the BMP/GDF pathway [30]. Both of these branches work through canonical and non-canonical signaling (Figure 3).

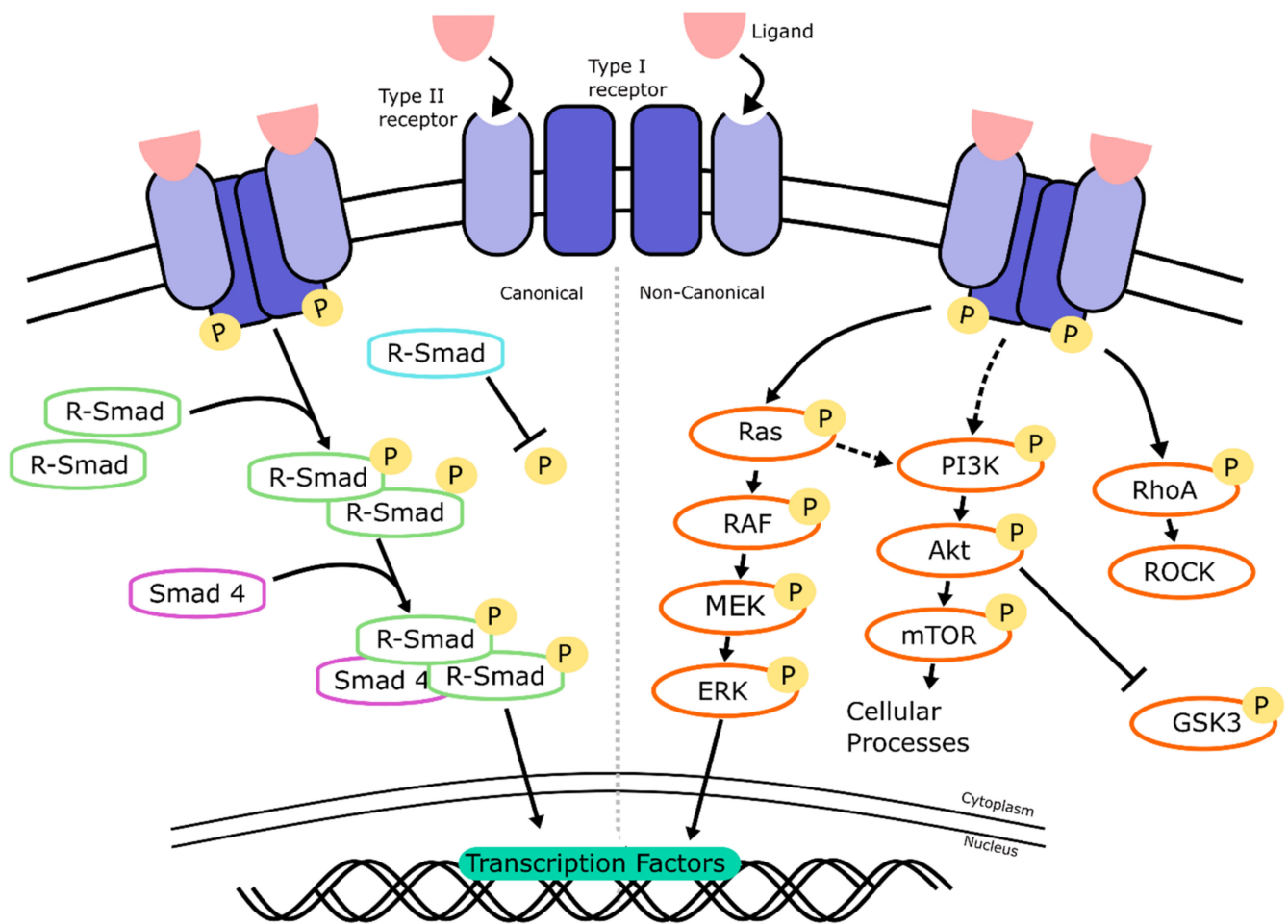


**Figure 3.** The TGF- $\beta$ /BMP signaling pathway. TGF- $\beta$  and BMP ligands bind to two type II receptors, which recruit two type I receptors, and a complex is formed. The type I receptors are phosphorylated (P), initiating both the canonical and non-canonical signaling pathways. **(Left)** In the canonical pathway, phosphorylation of the type I receptors results in the recruitment of two R-Smads. The two R-Smads are phosphorylated and recruit SMAD4, forming a complex which translocates to the nucleus, where it regulates gene transcription. I-Smads inhibit R-Smad phosphorylation. **(Right)** In the non-canonical pathway, Smad-independent interactions occur within different kinase cascades, such as the Ras-ERK-MAPK pathway, the PI3k-Akt-mTOR pathway and the RhoA pathway. This sequential recruitment and phosphorylation of downstream kinases also results in translocation to the nucleus, where transcription of TGF- $\beta$  and BMP target genes is regulated, such as *Sp1*, Forkhead Box (FOX)-related genes, and basic helix-loop-helix (bHLH)-related genes.

The signaling cascade is initiated by the binding of a ligand to a type II cell membrane-bound TGF- $\beta$  receptor, which then recruits a corresponding type I receptor depending on the original ligand (Figure 3). In humans, there are five type II receptors (T $\beta$ R $\beta$ II, ActR $\beta$ II, ActR $\beta$ IIB, BMPR $\beta$ II, AMHR $\beta$ II) and seven type I receptors (ALK-1, -2, -3, -4, -5, -6, -7), which are activated by different TGF- $\beta$  ligands [31] (Figure 4). TGF- $\beta$ , Activin and Nodal ligands generally bind to type I receptors ALK-4, -5, and -7. For example, TGF- $\beta$ 1, 2, and 3 all bind to the receptor type I ALK-1 and ALK-7, and the receptor type II T $\beta$ R $\beta$ II. It is important to understand the specificity of ligands and their target receptors, as pathway agonists or small molecule inhibitors will only target certain receptors, such as SB431542, which is a selective inhibitor of ALK-4, ALK-5, and ALK-7 [32]. BMP ligands work through the type I receptors ALK-1, -2, -3 and -6. For example, BMP-5, -8a, and -8b bind to type I receptors -2, -3, and -6, and type II receptors ActR $\beta$ II, ActR $\beta$ IIB, and BMPR $\beta$ II.

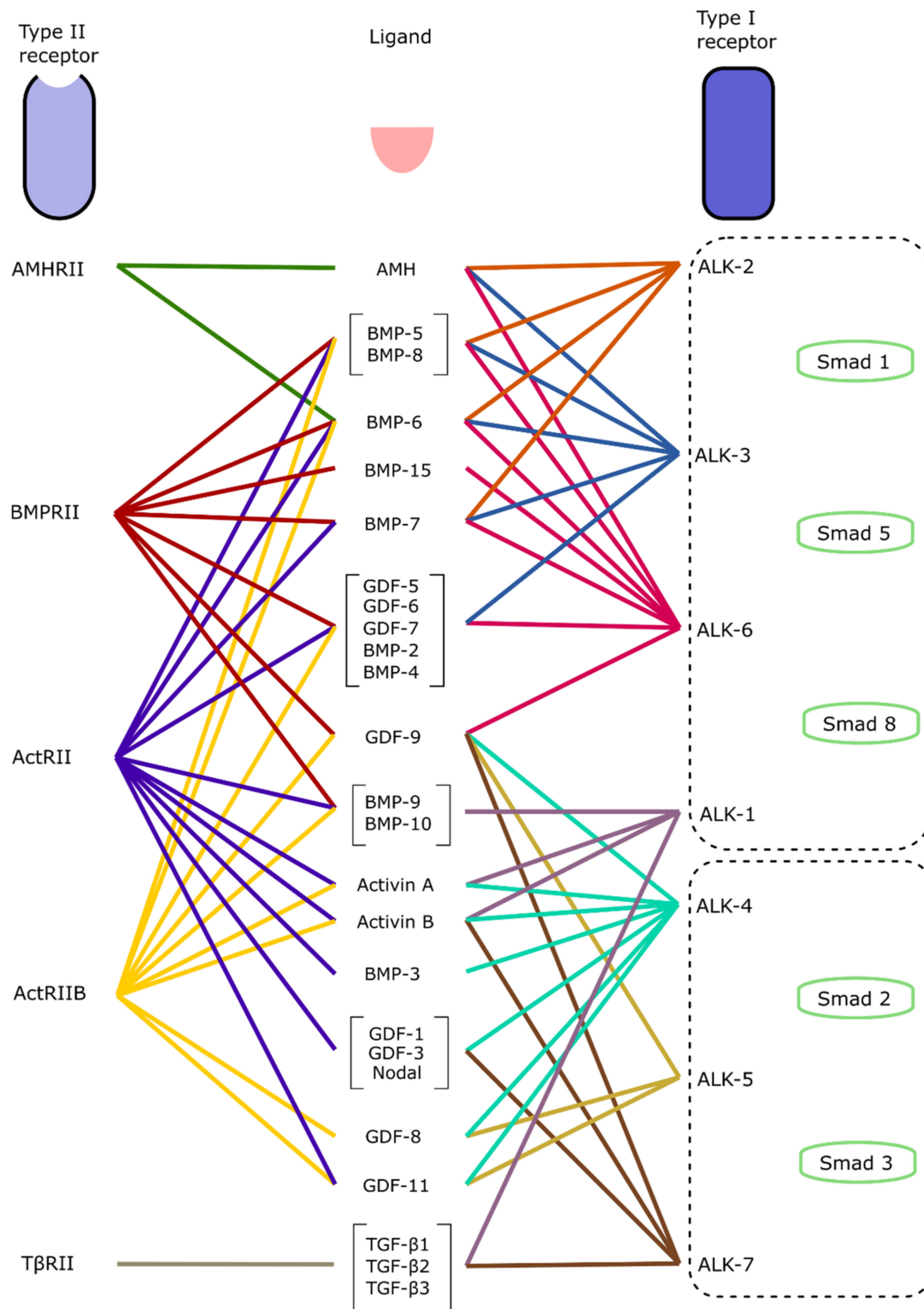


**Figure 4.** TGF-β and BMP signaling: ligand–receptor interactions involved in canonical and non-canonical signaling. TGF-β and BMP ligands can bind to many different combinations of type I and II receptors in both canonical and non-canonical signaling. There are five different type II receptors (**left**) which interact with the many different ligands (**center**). These ligand-bound type II receptors then form a complex with a corresponding type I receptor (**right**). However, in the canonical pathway, the specific type I receptor involved in the complex subsequently determines which R-Smad is recruited. ALK-1, -2, -3, and -6 receptors are commonly used in BMP signaling, and recruit SMAD 1, 5 and 8. The TGF-β branch more commonly works through type I receptors ALK-4, -5, and -7, that recruit SMAD 2 and 3.



Once activated, the signaling cascade can work in a SMAD-dependent (canonical) or SMAD-independent (non-canonical) manner. In the canonical branch of the pathway (Figure 3, left), the binding of a ligand to its receptor results in three subsequent actions: the formation of a type I/II membrane-bound receptor complex, the recruitment of specific R-SMADs, and the formation of R-SMAD/SMAD4 complexes that can enter the nucleus. These actions are next described in more detail: once a ligand binds, a complex of two type I and two type II receptors forms, which triggers the phosphorylation of the type I receptor. Depending on the ligand type, a specific SMAD protein is recruited and phosphorylated (Figure 4). Subsequently, intra-cellular SMAD–protein complexes form that can translocate to the nucleus, and they regulate gene expression. In general, SMADs can be separated into three groups: Receptor-regulated Smads (R-Smads), Common-Smads (Co-Smads), and Inhibitory Smads (I-Smads). R-Smads are the initial proteins that become phosphorylated after the type I/II receptor complex forms, depending on if TGF- $\beta$  or BMP signaling is occurring. SMAD2 and SMAD3 are phosphorylated during TGF- $\beta$  signaling after the recruitment of type I receptors ALK-4, -5, or -7, while SMAD1, SMAD5, and SMAD8 are targeted by the BMP branch after the recruitment of type I receptors ALK-1, -2, -3, or -6 (Figure 4) [33]. Once activated, these R-Smads bind to SMAD4, the only known co-Smad, and form trimers that translocate into the nucleus. The remaining SMAD6 and SMAD7 are classed as I-Smads, that bind to the R-Smads and inhibit the signaling cascade.

In the non-canonical branch (Figure 3, right), the cascade works through a Smad-independent manner via at least three signaling cascades, namely the extracellular signal-regulated kinase (ERK) (also known as mitogen-activated protein kinase (MAPK)), phosphatidylinositol-3 kinase (PI3K), and RhoA kinase cascades [34]. These three cascades can act independently or interact with each other to regulate gene transcription. In ERK signaling, for example (Figure 3, Ras-ERK), the cascade is initiated by a GTPase known as Ras, which is phosphorylated in response to the activation of the type I/II receptor complex formation. This results in a conformational change of Ras, allowing it to activate RAF, which in turn phosphorylates MEK and activates it. MEK finally phosphorylates ERK, also known as MAPK, which then directly activates or inhibits transcription factors such as *PAX6*, a key transcription factor essential for the development of the early brain and eye [35]. The kinase pathways involved in non-canonical signaling interact closely with each other, with Ras also activating the PI3K-Akt signaling pathway (Figure 3, PI3K-mTOR) [36]. The activated protein kinase Akt is involved in many different processes, depending on its downstream target. Frequently, Akt inactivates GSK-3 through phosphorylation [37].

### 2.2.2. TGF- $\beta$ /BMP Signaling: Neural and Retinal Development

In this section, we describe the role of TGF- $\beta$ /BMP signaling in neural and retinal development. Throughout development, TGF- $\beta$  and BMP signaling are involved in differentiation, proliferation and programmed cell death, which are discussed in this context below.

TGF- $\beta$  signaling has an important role in programmed cell death during retinal development. The analysis of developing chick retinas showed the presence of the type II receptor T $\beta$ RII, as well as the ligands TGF- $\beta$ 2 and TGF- $\beta$ 3 in the central retina and optic nerve head during an early period of programmed cell death [38]. Furthermore, T $\beta$ RII deletion in mice showed a significant increase in the apoptosis of retinal neurons during the development of the embryo, resulting in fewer retinal neurons and functional abnormalities [28]. The activation of the ERK and PI3K-Akt pathways through insulin also acts as a survival factor in the early chick embryonic retina to combat apoptosis, when progenitors and ganglion cells are developing [39]. Once the early retina has formed, TGF- $\beta$  signaling also affects the development and differentiation of specific cell types. Kim et al. (2005) showed that the binding of the ligand GDF11 to the ALK-4 and -5 receptors (Figure 4), controls the proliferation of retinal progenitor cells that express the early RGC-specific marker *ATOH7*, thereby limiting RGC development. GDF11 knockout mice showed significantly increased levels of RGCs, with around 50% more cells in the

ganglion cell layer than wild type mice. The same authors showed that GDF15 has the opposite effect to GDF11 and promotes RGC differentiation in mouse retinal progenitor cells by suppressing GDF11-induced SMAD2 phosphorylation [40]. This was subsequently confirmed in human embryonic stem cell models, where SMAD2 inhibition by SB431542, a synthetic inhibitor of the type I receptors ALK-4, -5, and -7, increased RGC differentiation. Finally, in human models, the addition of recombinant GDF11 significantly reduced the expression of the RGC marker *POU4F1*, which indicates that GDF11 negatively regulates RGC development [41].

BMP signaling is a vital part of the development of the neural crest. One of the earliest events in neural crest development is the formation of the neural plate border, which forms in an area of the neural plate with less BMP activity [42]. The neural plate eventually develops into the optic vesicles in the early stages of retinogenesis (Figure 1). This has also been shown in chick models, where the inhibition of BMP alongside TGF- $\beta$  affected neural tube dorsal–ventral patterning [43]. Building on this, dual SMAD inhibition has been successfully adapted to neuronal and retinal development from human stem cells [44–46]. BMP is involved in the early development of the eye, with murine models showing that BMP-2, -4, and -7 are highly present in the embryonic retina, before being downregulated in adult retinas. BMP4 especially has a significant role in this early period of development, as it stimulates progenitor cells to differentiate into retinal ganglion cells rather than other neural cells such as astrocytes [47]. BMP4 treatment has since been used regularly in retinal organoid cultures to induce retinal lineage development [48,49]. In zebrafish models, BMP signaling is necessary for the induction of photoreceptor differentiation through interaction with notch signaling [50]. Furthermore, the inhibition of BMP signaling in mice results in a reduction in the Müller glial cell-specific genes *Rlbp1* and *Glul*, showing the role BMP signaling plays in the development of retinal neurons [51]. In addition to roles in the differentiation of the retina, BMP signaling is involved in the development of other eye structures. BMP-7 null mutant mice were observed to have a range of eye defects, from abnormal lens development to the absence of the whole lens, retina and cornea [52]. Ras-ERK signaling (Figure 3, Ras-ERK) can also affect lens development. ERK signaling negatively regulates L-Maf, an important factor needed to promote the differentiation of lens cells from the neural retina [53]. GSK-3 plays an important role in neural and retinal development [54,55] and is also involved with a variety of other signaling pathways (Wnt, hedgehog, insulin and notch) [56–59]. Inhibited by Akt during non-canonical signaling, Marchena et al. also found that inhibition of GSK-3 by treatment with small molecule inhibitors led to retinal cell neuroprotection in a retinitis pigmentosa model [60].

### 2.3. Wnt Signaling

The Wnt signaling pathway is also highly conserved amongst species, and is responsible for regulating cell fate determination, cell migration and neural patterning. It operates through canonical (outlined in Figure 5) and non-canonical (not shown) signaling, similarly to the TGF- $\beta$ /BMP pathway. The canonical pathway is the most understood and revolves around the  $\beta$ -catenin protein. The non-canonical pathway is less understood and is mainly involved in tissue polarity and the regulation of intracellular calcium levels through either the non-canonical planar cell polarity (PCP) pathway or the non-canonical Wnt/calcium pathway. These pathways both work independently of  $\beta$ -catenin. Since relatively little is known about the non-canonical pathway, we focus here on the description of the canonical pathway below.

#### 2.3.1. Wnt Signaling: Mechanism of Action

In the absence of Wnt signaling, cells are in the so-called “OFF state” (Figure 5, left). The “OFF State” status of the cell results in the degradation of  $\beta$ -catenin and subsequent transcriptional repression. This occurs through the formation of a “destruction complex”, comprised of Axin, adenomatosis polyposis coli (APC), Casein kinase 1a (CK1a), and GSK-3 $\beta$ . The destruction complex phosphorylates  $\beta$ -catenin, which marks it for degradation

and becomes ubiquitinated [61]. The binding of Wnt to the cell membrane receptor results in the cell being in an “ON state” (Figure 5, right), which ultimately allows transcriptional activation. Initially, Wnt proteins bind to the transmembrane receptor Frizzled (Fz), which subsequently forms a complex with lipoprotein receptor-related proteins 5 and 6 (LRP5/6), triggering the recruitment of the phosphoprotein Dishevelled (Dsh). Dsh disrupts the destruction complex by translocating it to the membrane, where AXIN1 binds to LRP5/6 and the complex is phosphorylated and subsequently degraded. Once the destruction complex has been disassembled,  $\beta$ -catenin can accumulate and localize to the nucleus, where it acts as a coactivator of the T-cell factor/lymphoid enhancing factor (TCF/LEF) family of transcription factors, which are involved in cell fate decisions.

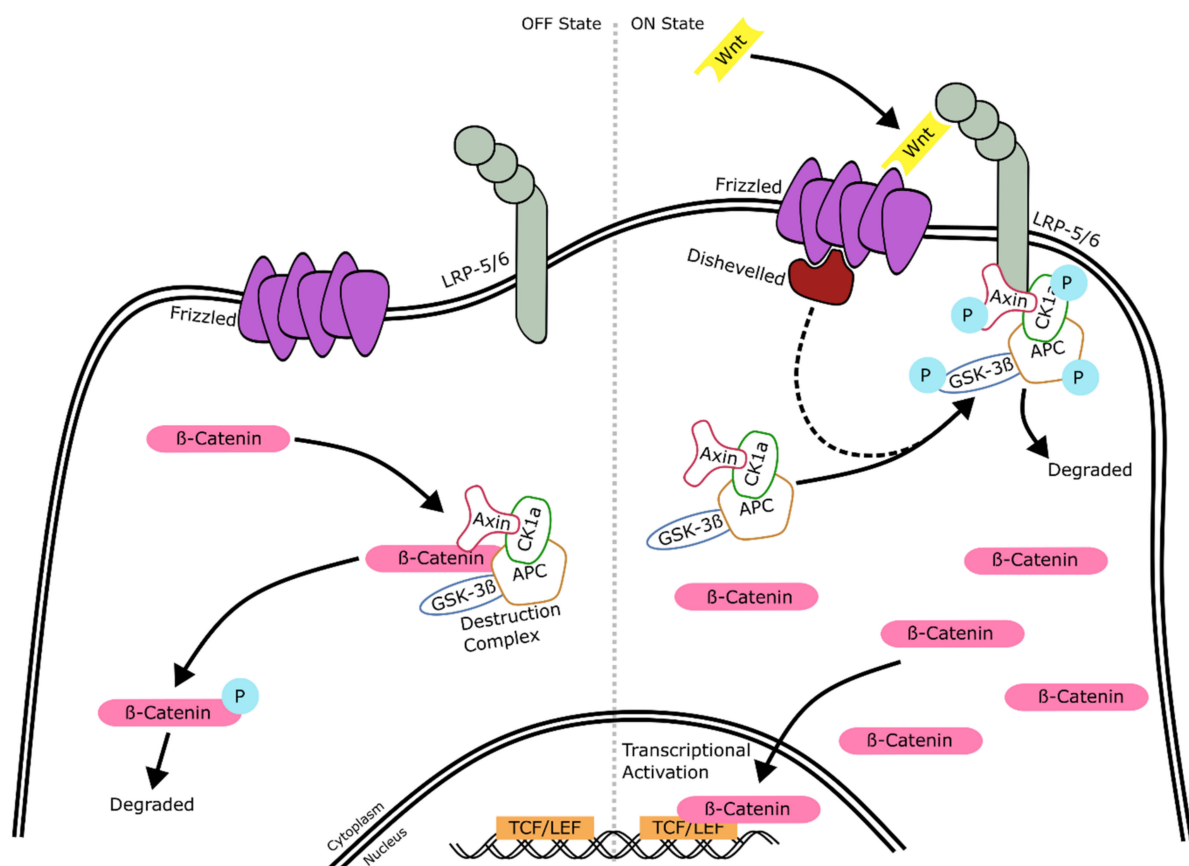


**Figure 5.** The canonical Wnt signaling pathway. **(Left)** Cells not activated by Wnt signaling exist in an “OFF state”. In the “OFF State” a so-called destruction complex is formed, comprised of Axin, CK1 $\alpha$ , APC and GSK-3 $\beta$ . The complex phosphorylates (P)  $\beta$ -Catenin, which leads to its degradation. **(Right)** Wnt binds to the cell membrane receptor Frizzled (Fz), which turns the cell into an “ON State”. Frizzled then forms a complex with LRP-5/-6, which results in the recruitment of Dishevelled (Dsh), a phosphoprotein. Dsh interacts with the destruction complex and translocates it to the membrane. Here, Axin binds to LRP-5/-6 and the destruction complex is degraded. This allows  $\beta$ -Catenin to accumulate in the cytoplasm and subsequently enter the nucleus, where it activates transcription of the TCF/LEF.

### 2.3.2. Wnt Signaling: Neural and Retinal Development

Wnt signaling has multiple essential roles in neural development and differentiation, including neural migration, the generation of the neural tube, axonal growth, and synapse formation [62–65]. In the eye, Wnt has been shown to play a key part in initial eye formation. In *Xenopus* models, the temporal and spatial expression of the Wnt signaling receptor Fz3 during development is restricted to the anterior neural plate, an anatomical precursor to the eye field. Fz3 is expressed throughout the developing optic vesicle, and affects the expression of *PAX6*, the master switch of eye development [66,67].

The importance of Wnt signaling in retinal development has been shown across species. In zebrafish, the activation of the Wnt pathway by the interaction of the ligand WNT8B and a Frizzled receptor inhibits the specification of the eye field [68]. Further research in murine models corroborated the hypothesis that WNT8B is a suppressor of early eye formation: WNT8B, usually expressed in the forebrain, expanded its expression into the optic pits in a conditional-knockout mouse model of *Six3* (a known early eye field marker), inhibiting the formation of neural retina [69]. This has since been shown in human stem cell models, where a knockdown of WNT8B restored neural retina formation in a *Pax6* knockout stem cell model [70]. Taken together, these data suggest that inhibitory WNT8B signaling is reversed by *Six3* expression, a known early eye field marker essential for the development of the neural retina. For specific retinal cell subtypes, Wnt signaling is active during injury, exerting neuroprotective effects. Activation by Wnt3a protected immortalized rat RGC-5 cells from cell death when cultured in elevated pressure conditions [71]. Similarly, Wnt signaling protected photoreceptors in an inherited retinal degeneration mouse model, increasing the pro-survival protein Stat3 [72]. Finally, after laser-induced injuries to mice retinas, the activation of Wnt signaling led to an increase in the proliferation of Müller glial cells [73]. Wnt inhibition is also often paired with the simultaneous inhibition of SMAD in human stem cell research, although it has also been used on its own as a way of directing cells to an eye field fate [74]. Nonetheless, the dual inhibition of Wnt and SMAD has been shown to direct the differentiation of stem cells efficiently into neural crest cells [75,76] as well as stimulate the genesis and differentiation of specific early-born neural retinal cells, such as cone photoreceptors and retinal ganglion cells, from the neuroectoderm [46,77].

Wnt signaling does not only play a role in the formation of the neural retina, but also has been implicated in the formation of the RPE. It is present in the dorsal section of the optic vesicle, which develops into the RPE [78]. Finally, Wnt signaling has a large role in the development of the lens and the initial lens epithelium. Although Wnt signaling is not necessary for lens fate determination, Wnt signaling is required for proper lens formation [79] and it is thought to play a role in the correct alignment of lens fiber cells [80].

#### 2.4. Notch Signaling

Notch signaling, presented in Figure 6, refers to an intercellular signaling cascade invoked by cell–cell interaction. Highly conserved amongst species, it is responsible for multiple cell differentiation processes, including neural development, cardiovascular formation, and pancreatic cell specification [81–83].

##### 2.4.1. Notch Signaling: Mechanism of Action

In general, notch signaling occurs through a multi-step process (Figure 6, from left to right). First, the ligands located in the ligand-containing cell membrane are activated by the ubiquitin–protein ligase Mib1. There are two families of notch ligands: Jagged (Jag1 and Jag2) and Delta-like ligands (Dll1, Dll3, Dll4) [84]. Next, this ligand binds to the notch transmembrane receptor on the target cell (four receptors are known: Notch1, Notch2, Notch3 or Notch4), where it forms a stable complex. After this interaction, the transmembrane receptor is cleaved on either side of the membrane of the target cell. The cleavage of the extracellular domain is known as S2 cleavage, and is initiated by the metalloprotease ADAM10 [85]. This cleavage triggers the notch intracellular domain (NICD) to be cleaved by  $\gamma$ -secretase, known as S3 cleavage. Finally, what remains of the extracellular ligand–receptor complex is endocytosed by the ligand-containing cell, while the cleaved intracellular domain of the receptor is transferred to the nucleus in the target cell. There, it forms a complex with recombinant binding protein j (Rbpj) and mastermind (Mam) that activates the transcription of several target genes, including *HES1* and *HES5* (described in detail below) [86].

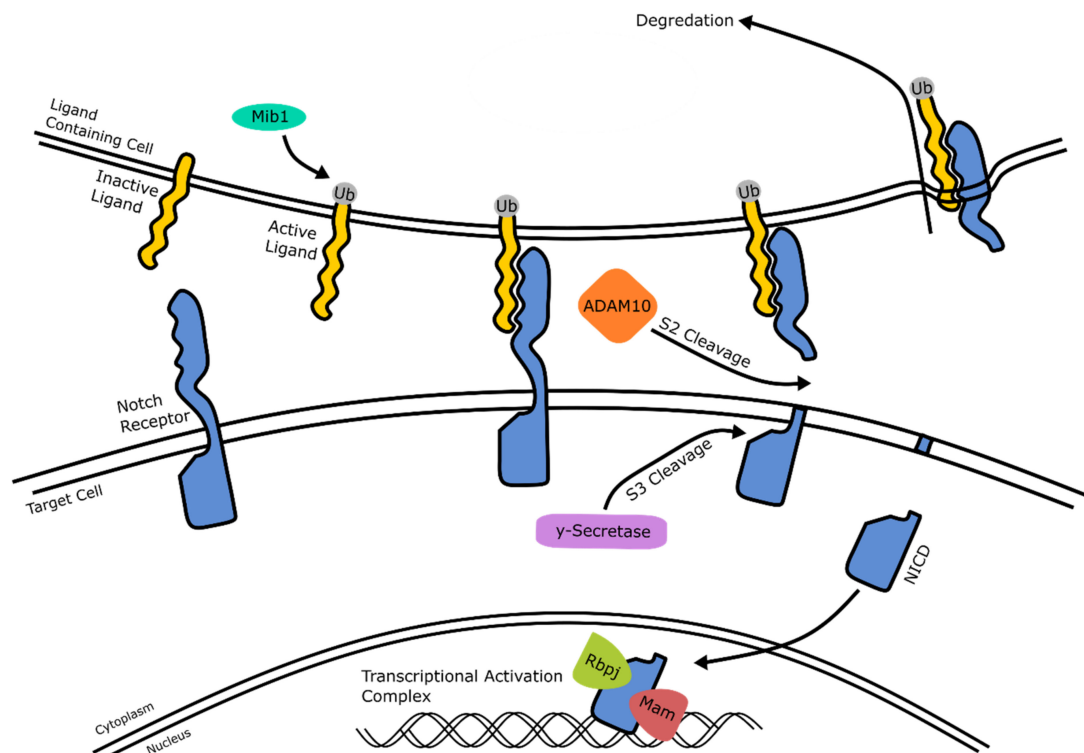


**Figure 6.** The notch signaling pathway. The multistep notch signaling pathway is presented from left to right in the figure. The first stage of notch signaling occurs in the ligand containing cell (**top**), where inactive ligands are ubiquitinated by Mib1 to become active. The ligands can then bind to a notch receptor present in the target cell membrane (**middle**). This receptor has an extracellular domain and an intracellular domain. The extracellular domain is cleaved by the metalloprotease ADAM10, before being endocytosed by the ligand containing cell. The intracellular domain in the target cell is then cleaved by  $\gamma$ -secretase and transported to the nucleus (**bottom**). Here, it forms a complex with Rbpj and Mam, activating transcription of target genes such as *HES1* and *HES5*.

#### 2.4.2. Notch Signaling: Neural and Retinal Development

In the developing central nervous system, notch plays an important role in the genesis, maintenance, and differentiation of neural progenitor cells. Chen et al. showed that notch inhibition leads to the accelerated differentiation of stem cells into the formation of neural rosettes by treating cultures with DAPT, a  $\gamma$ -secretase inhibitor [87]. Interestingly, these rosettes also possess Notch1, 2 and 3 receptors in their cell membrane, indicating that notch signaling has a role in maintaining neural cells in a progenitor state whilst inhibiting cell maturation [88].

Substantial experimental evidence points to notch signaling having a highly temporally defined role in the early formation of the eye. Indeed, Toonen et al. (2016) found that ADAM10 (Figure 6) conditional knockout mice showed an increased differentiation of early-born retinal neurons, which resulted in a highly disorganized retina lacking lamination [89]. Notch signaling affects the retinal progenitor cells in a similar fashion, with notch activation maintaining their progenitor state while inhibition leads to differentiation. However, continuous notch activation causes retinal progenitor cells to dedifferentiate and regain stem cell characteristics [90]. The knockdown of *Notch1* in early developmental stages in mice resulted in a smaller retina, likely due to the fewer numbers of retinal progenitor cells (RPCs). Furthermore, notch signaling is involved in the development of specific retinal neurons, such as ganglion cells, photoreceptors and Müller glial cells. Nelson et al. reported that there was a downregulation of notch signaling immediately preceding retinal ganglion cell development [91]. By following the expression of *Hes*, a family of well-known target genes of the notch signaling pathway that are found robustly in RPCs [92]; through reporter constructs, they found that while notch signaling is present in RPCs, it is not

active in developing ganglion cells. This has also been shown in chick models, where antisense oligonucleotides reduced notch expression. This resulted in increased RGC production in vitro, and even reinitiated RGC development in vivo in retinas where ganglion development had stopped [93]. In human stem cells, the decreased activity of notch via the  $\gamma$ -secretase inhibitor DAPT also induced neural rosettes to develop into functional retinal ganglion cells [94]. Jadhav et al. (2006) and Mizeracka et al. (2013) showed that decreased notch signaling at an early stage leads to enhanced cone photoreceptor production, whereas a later knockdown increases the numbers of rod photoreceptors [95,96]. In retinal explant cultures, Mochizuki et al. (2014) found that Müller glial cell markers, such as *RLBP1* and *HEY2*, are significantly upregulated in the presence of notch signaling. In contrast, the inhibition of notch signaling leads to a decrease in glia precursor cells and fewer differentiated Müller glial cells [97].

### 3. Agonists and Antagonists Involved in Regulating the Signaling Pathways of the Developing Retina

To manipulate the aforementioned pathways in order to improve retinal differentiation, they can be controlled with known small molecules, proteins or transcription factors that either activate (agonists) or inhibit (antagonists) them. Below, we describe, pathway by pathway, several commonly used (ant-) agonists that affect the activity of signaling pathways.

#### 3.1. Agonists and Antagonists of the Hedgehog Signaling Pathway

The regulation of the hedgehog signaling pathway with (ant-) agonists frequently revolves around the G protein-coupled receptor Smo (Figure 2). The main antagonist of Smo used in in vitro retinal models is cyclopamine. Cyclopamine is a naturally occurring steroidal alkaloid that targets Smo and has been used in in vitro models to induce the inhibition of hedgehog signaling at an early stage of development, facilitating retinal ganglion cell differentiation [98]. To complicate matters, the small molecule Smoothed Agonist (SAG) activates hedgehog signaling by binding to Smo itself, and therefore upregulates the activity of the Gli1/2 activation complex and subsequent target gene expression [99]. Thus, the addition of SAG into cultures at a late stage of development assists in the generation of retinal cells [100–102]. Finally, it is relevant to note here that hedgehog signaling can also be activated by the addition of recombinant Shh into cultures [103], although this is not common practice and, by convention, many groups prefer to use SAG.

#### 3.2. Agonists and Antagonists of the TGF- $\beta$ /BMP Signaling Pathway

In this section, we discuss the effect of small molecules on the activation or inhibition of TGF- $\beta$  and, subsequently, the BMP signaling pathways (Figure 3). The inhibition or activation of the TGF- $\beta$ /BMP signaling pathway is temporally controlled in in vitro retinal development, with inhibition within the first few days or activation in the second week of differentiation, promoting retinal development. The TGF- $\beta$  pathway is commonly inhibited early in development through treatment with either the small molecule SB431542, or a recombinant protein named COCO. SB431542 is a potent inhibitor of the TGF- $\beta$ , Activin and Nodal pathways (Figure 3). This antagonist exerts its effect by blocking the ALK-4, -5, and -7 receptors (Figure 4) [104]. SB431542, by itself or when combined with other inhibitors of the BMP pathway, efficiently accelerates the differentiation into the neuronal lineage [44,105,106]. SB431542 is typically added to cultures within the first seven days of cultures (Table 1). It improves the development of specific retinal cell types, such as photoreceptors, both in 2D cultures and 3D retinal organoid models [107–109]. COCO is part of the Dan family of TGF- $\beta$  antagonists [110], and is commonly used as an inhibitor of the BMP branch of the signaling pathway (Figure 3). However, Bates et al. showed in a *Xenopus* model that COCO also affects the TGF- $\beta$  side of the pathway by inhibiting Activin and Nodal signaling, therefore controlling germ layer specification [111,112]. Finally, COCO enhances the efficiency of photoreceptor differentiation [77], when used in combination with insulin growth factor 1 (IGF1). The prolonged treatment of COCO

avored cone differentiation over rods [113]. Taken together, this shows that, in the context of the TGF- $\beta$ /BMP signaling pathway, COCO has both agonistic and antagonistic properties [114]. It is, however, not commonly used in the protocols to generate retinal organoids, as small molecule inhibitors with the same or similar action are less expensive and can be more stable.

The cell signaling activity of the BMP pathway (Figure 3) can be affected by many readily available agonists and antagonists such as noggin, dorsomorphin, and BMP4. Noggin is a natural antagonist of the BMP signaling pathway. Once secreted, it binds to other BMP ligands, preventing them from binding to the receptors. Noggin inhibits at least BMP2, BMP4, BMP5, BMP6, BMP7, BMP13, and BMP14 [115], amongst other BMP ligands such as GDF-5 and GDF-6 [116,117]. High doses of noggin result in the specification of retinal and diencephalic regions at the expense of telencephalic regions in the developing *Xenopus* [118]. In human stem cell models, noggin has been routinely used to promote differentiation towards a photoreceptor fate [119,120]. However, in recent years, small molecule inhibitors, such as the BMP pathway antagonist dorsomorphin, have been favored over peptide antagonists such as noggin. In general, small molecule inhibitors are less expensive, have a higher penetrating capacity, and are more stable. Finally, dorsomorphin has also a more drastic effect on neural differentiation when compared to noggin [121,122].

Dorsomorphin was the first known small molecule inhibitor of the BMP pathway, and selectively inhibits the type I receptors ALK-2, -3, and -6 (Figure 4) in a dose-dependent manner. The inhibition of these receptors leads to downregulated gene transcription [123]. A derivative of dorsomorphin, named LDN193189, has a high affinity for ALK-2 and -3. Both dorsomorphin and LDN193189 efficiently block Smad-dependent and Smad-independent TGF- $\beta$  pathways and inhibit BMP signaling [124]. However, it appears that dorsomorphin is a non-specific inhibitor of BMP and could potentially inhibit other kinases in vivo as well [125]. LDN193189 is thought to be a 100-times more potent inhibitor of the BMP pathway than dorsomorphin [126], but it too affects, less specifically, several other kinases. In retinal differentiation, both these small molecules have been used in organoid models to increase the efficiency of retinal generation [127,128]. However, they are usually used in combination with SB431542 as part of a dual SMAD inhibition to inhibit both the TGF- $\beta$  and BMP sides of the pathway [107,108].

Retinal differentiation can be increased dramatically with the addition of an agonist, rather than an antagonist, of BMP signaling at a later time point. The addition of agonist BMP4 to retinal organoid cultures exposes the importance of timing in retinal development. Kuwahara et al. (2015) showed that treatment with BMP4 starting from day 6 onwards turned more than 95% of aggregates positive for RAX, a vital transcription factor essential for the development of the retina. Treatment with BMP4 starting from day 0, however, did not at all promote retinal or neural differentiation [127]. The timely addition of BMP4 between day 6 and 18 has since been adopted into many methods of generating retinal organoids [48,129–131].

### 3.3. Agonists and Antagonists of the Wnt Signaling Pathway

In this section, we describe the action of agonists and antagonists, such as CHIR99021 and IWR1e, on the activity of the Wnt signaling pathway. Wnt signaling, alongside TGF- $\beta$ /BMP, is one of the most commonly used pathways to regulate retinal development in in vitro retinal models. It also temporally controls retinal development, with inhibition in the first two weeks promoting retinal development. In contrast, activation during the third and fourth week of differentiation also increases retinal development. The activation or inhibition of this pathway can be regulated to a multitude of readily available small molecules and proteins. Chen et al. (2009) previously identified a large group of chemically related inhibitors, named Inhibitors of Wnt Response (IWRs) [132]. The IWR1-*endo* (IWR1e) inhibitor has been the most frequently used IWR in retinal research. IWR1e regulates Wnt activation by stabilizing Axin, one of the constituents of the aforementioned  $\beta$ -catenin destruction complex (Figure 5). In organoid models, IWR1e is commonly used

to promote the development of the retinal lineage and is most effectively added within the first 12 days of differentiation [74,133]. Similarly to IWRs, the small molecule XAV939 causes an accumulation of Axin in the cell, and decreases the amounts of  $\beta$ -catenin by promoting its degradation (Figure 5) [134], inhibiting Wnt signaling. Indeed, XAV939 treatment to early-stage stem cell-derived retinal cultures together with a BMP inhibitor resulted in an 84-fold increase in *PAX6* and 156-fold higher levels of *RAX* [135]. Yet another Wnt inhibitor used in retinal organoid development is the naturally occurring antagonist DKK1 protein, encoded by the *DKK1* gene. The protein has a high affinity to bind to LRP6 and prevents the formation of the Frizzled-LRP5/6 complex (Figure 5) [136]. This action subsequently prevents Dishevelled from interacting with the destruction complex, thus inhibiting Wnt signaling. Given their same mode of action, treatment with XAV939 or DKK1 in vitro is interchangeable, and both biomolecules efficiently direct stem cells towards retinal progenitor and retinal ganglion cells [137–139]. Most research groups inhibit Wnt signaling in the early stages of in vitro retinal development. However, it has also been activated at later time points in retinal organoid development with the help of the agonist CHIR99021, an extremely potent GSK-3 $\beta$  inhibitor. GSK-3 $\beta$  plays a vital role in the inhibition of Wnt signaling, as it is an essential part of the destruction complex that ultimately labels  $\beta$ -catenin for degradation. CHIR99021 has also been found to specifically promote the differentiation of retinal progenitor cells into retinal pigmented epithelium that exhibited increased pigment and better morphology than non-treated controls [140].

### 3.4. Agonists and Antagonists of the Notch Signaling Pathway

In in vitro retinal development, notch signaling (Figure 6) manipulation is predominantly used to promote photoreceptor differentiation and maturation through the action of the small molecule DAPT, which is added at later stages of retinal development. DAPT is a  $\gamma$ -secretase inhibitor and blocks the S3 cleavage of the notch intracellular domain. This means that the NICD cannot form the transcriptional activation complex needed to regulate target gene expression. DAPT treatment results in the upregulation of cone and photoreceptor-specific genes, such as *CRX*. DAPT addition induces a shift from dividing progenitor cells to post-mitotic photoreceptor precursor cells [141,142]. Reichmann et al. (2014) found that a short week-long treatment of DAPT is sufficient to accelerate photoreceptor differentiation. Using their specific protocol (Figure 7C), they reported that DAPT treatment induced cell cycle exit in the majority of retinal progenitor cells, with around 40% of cells positive for *CRX*, a photoreceptor precursor marker [143].

### 3.5. Agonists and Antagonists Used in Retinal Models That Regulate Additional Signaling Pathways

Many other small molecules, proteins or transcription factors are frequently used to regulate retinal development. In this section, we discuss the effects of the small molecule SU5402, IGF1, and various isoforms of fibroblast growth factor (FGF) on retinal development.

The small molecule SU5402 is a potent and selective inhibitor of the ERK pathway, effecting the non-canonical branch of the TGF- $\beta$ /BMP pathway (Figure 3). However, it is also heavily involved in the regulation of the fibroblast growth factor pathway (pathway not shown). When added on its own at early time points up until day 10 of differentiation, SU5402 treatment has led to a complete loss of *PAX6* and *RAX* expression, and consequently a loss of retinal fate [144]. In contrast, when added in combination with CHIR99021 at later stages of retinal development, SU5402 did promote retinal differentiation [145,146]. IGF1 has also been commonly added to retinal cultures over prolonged stages (Table 1) and plays a large role in both the development of the neural retina and long-term maturation of retinal ganglion cells [147,148]. Perhaps coincidentally, IGF1 is also one of the growth factors abundant in Matrigel that may accelerate retinal ganglion cell development in organoids models [149]. FGF signaling in retinal development is complex, as it depends on temporal and spatial signaling of a diverse group of FGF isoforms [144]. For example, FGF2 and FGF9 are constitutively expressed endogenously in the retina during development, and recombinant FGF2 can be added to cultures to favor the differentiation of the neural



retina [150]. FGF9 expression is increased in optic vesicle stages of development, and it has been used in disease models involving optic vesicle malformation to (partially) rescue the phenotype [3,151].

#### 4. Systematic Comparisons of Protocols and Supplements

##### 4.1. Directly Comparable Uses of Agonists and Antagonists in Retinal Organoid Models

In this section, we describe a literature-based review of predominate methods used for retinal organoid generation. In general, these methodologies can be separated based on protocol origin (Figure 7A–C) or the timing and concentrations of external supplements used (Table 1), which we describe consecutively below. Finally, we included the results of a series of pilot experiments by which we experimentally compare the role of several key (ant-) agonists during early retinal organoid development using one of these established methods. The reason for describing these methodologies is that protocols used to generate retinal organoids vary greatly in-between laboratories, with different groups tending to have their own favored method.

In general, embryoid bodies (EBs) can be generated in 3D floating culture, 3D Matrigel culture, or 2D adherent culture using simple reaggregation techniques or advanced microwell systems (Figure 8) [152,153]. The length of individual stages throughout the culture also varies between protocols and the progressive cell type-specific maturation depends on the focus of the protocol. Different methods of generating organoids also introduce a lot of variability that is protocol-dependent, such as the size and yield of organoids, and their ability to develop long-term lamination of the different cell layers. Protocols include many different small molecules or signaling factors, and nobody has systematically compared these “novel insights” in a reproducible manner using the same cell line and differentiation method. To understand which individual factors reported in the literature would work best to improve our previously published protocol, [149] with a 3D Matrigel-based start, we performed a systematic search of retinal organoid protocols. We made an inventory of which external factors were added at what time intervals in early retinal organoid development. We next chose the most commonly used conditions, compared them to our own (control) protocol and examined whether any differences in retinal organoid yield, morphology and gene expression were observed.

As cellular environments and development vary amongst species, we chose to concentrate solely on retinal organoids developed from human tissue. We identified 127 papers that generated retinal organoids (from 2011–2021) and reviewed their chosen methods. Although major upgrades and improvements have been published [152], we found that the majority of these methods could be traced back to three original major protocols [127,154,155] (Figure 7A,B). Nakano et al. (2012) used an initial Serum Free culture of Embryoid Body-like aggregates with Quick aggregation (SFEBq) method, with Rock Inhibitor (also known as Y-27632) and IWR1e present from day 0 to 12. Once an optic cup structure had started to form, they added SAG and CHIR99021 from day 15 to 18, before culturing for a longer term in standard medium with no more additions. Zhong et al. (2014) generated embryoid bodies using a 3D floating culture, with Blebbistatin present during the first day of culture (Table 1). No other factors are added other than taurine and retinoic acid, a pairing commonly used to enhance the long-term lamination of organoids. Finally, Kuwahara et al. (2015) also used an initial SFEBq culture to generate embryoid bodies, with Rock Inhibitor added from day 0 to 6. On day 6, BMP4 is added and gradually diluted with half medium changes up until day 18. Kuwahara et al. also examined the effects of other signal modulators on retinal development, including dorsomorphin, Wnt3a, IWR1e, SAG, cyclopamine, FGF2 and SU5402. However, they found BMP4 treatment to be most effective. Scientists are now exploiting the in vitro microenvironment of developing neuroepithelia through temporal manipulation with exogenous compounds to recapitulate the fetal microenvironment leading to enhanced retinal organoid differentiation. In addition, some groups have developed well-established protocols, which are isolated from the main cluster. For example, Goureau and coworkers used a 2D method of generating organoids

by expanding stem cells until self-forming neuroretinal-like structures appear. These were then cultured in a 3D environment, with the transient treatment of FGF2 between day 28 and 35 [156–158].

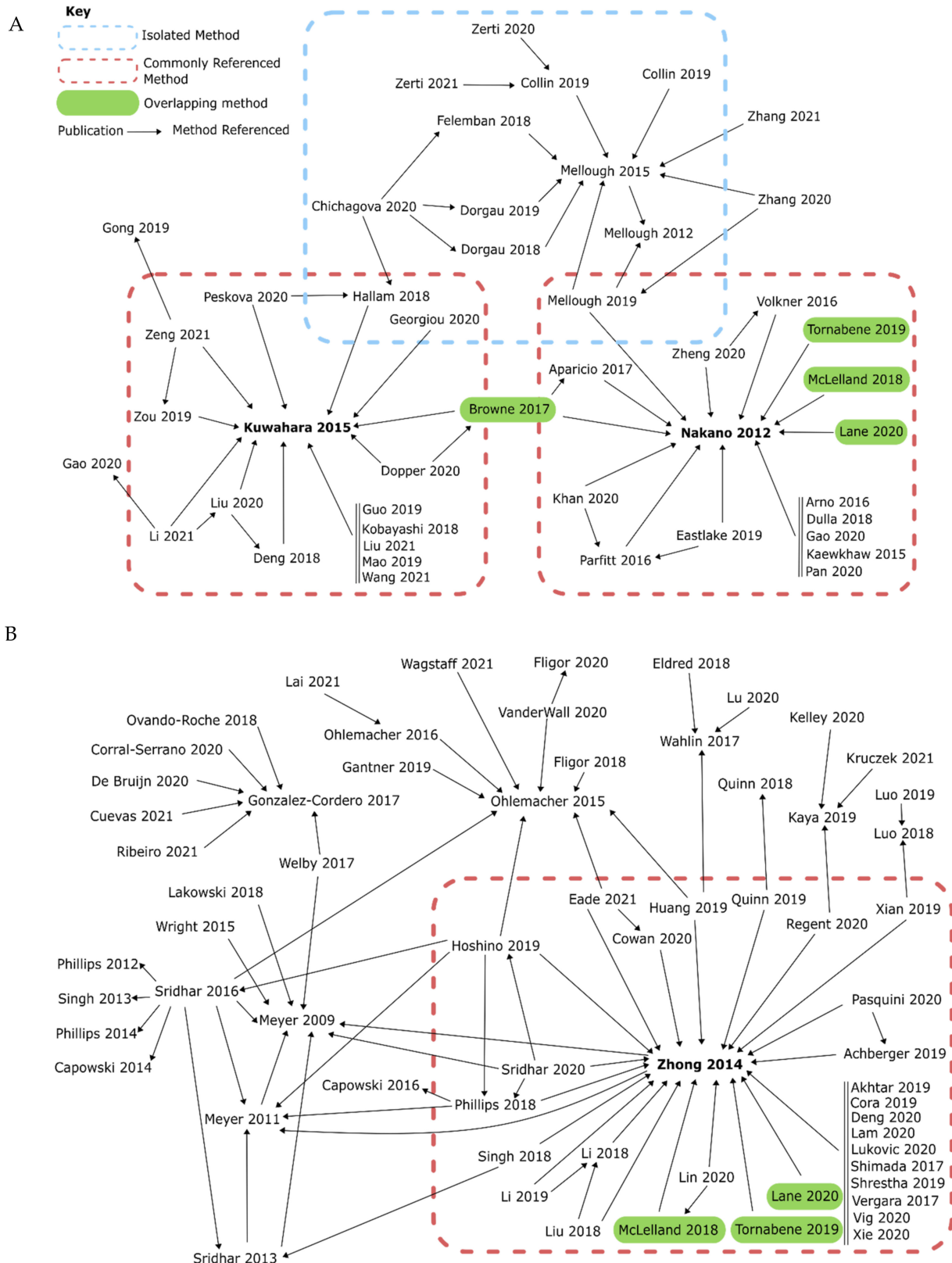
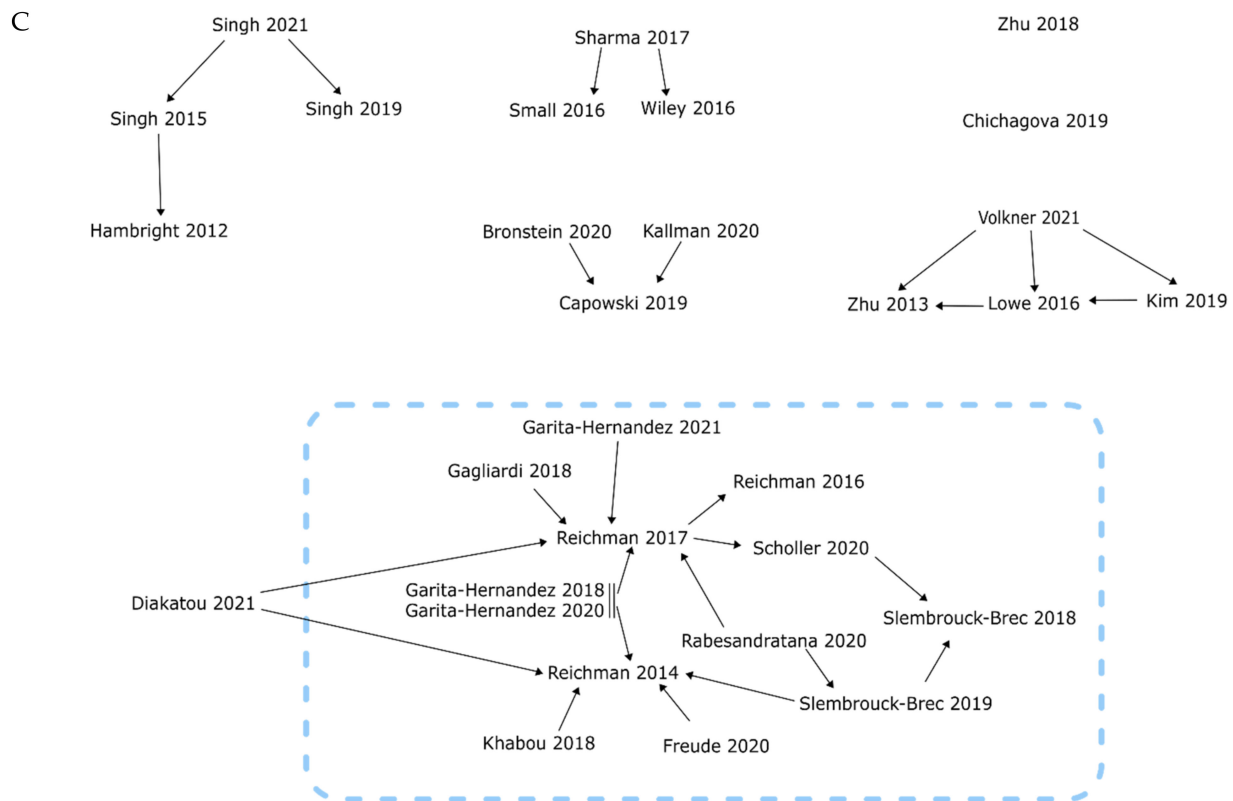


Figure 7. Cont.



**Figure 7.** The evolution of organoid protocols. (A–C) Our literature search revealed that a majority of retinal organoid protocols had developed from three major papers described in Section 4.1 (highlighted in red boxes) before being adapted to fit individual needs. We also found that some protocols were isolated in specific groups (highlighted in blue boxes) but were still well-established within that group. There were also a handful of “stand-alone” protocols that had been rarely used. Some more recent methods combine multiple protocols, shown by multiple arrows or highlighted in green. (A) We found that many manuscripts were based on the methods of Kuwahara et al. [127] and Nakano et al. [154], leading to a high frequency of protocols generating embryoid bodies using single cells. On the other hand, some protocols were used mainly by a single group (highlighted in blue). (B) Zhong et al. [155] was the most commonly referenced method of generating retinal organoids, building upon the previous work of Meyer et al. [135,144], and outlines how this protocol, a method with relatively few steps or additional supplements, has been used as a base for many models, being adapted as needed. (C) Alongside stand-alone protocols used solely by a single group (in blue), there were also a small number of manuscripts that did not relate to other methods. All papers included either produced retinal organoids, or were referenced as a method of producing retinal organoids [48,49,74,101,107–109,113,127,129–131,135,143–146,148–150,152,154–259].

Once we established which methods were previously used to generate retinal organoids, we systematically reviewed the steps of each protocol and indexed the external factors added to help the early development of the retinal lineage (Table 1), alongside other essentials, such as starting material and medium composition (Figure 8). We found that just over 40% of protocols use stem cell clumps in a suspension culture to generate embryoid bodies, as detailed in Zhong et al. [155] (Figure 8A). Around 35% of protocols use single cells to generate aggregates, which could be further sectioned into the type of plate used and the number of cells seeded per well. We found that the two most commonly used seeding densities and the most common plate type originated from two protocols: Nakano et al. [154], and Kuwahara et al. [127]. Nakano et al. generated aggregates using 9000 cells per well, and the popularity of the protocol is evident, with almost 30% of all single-cell aggregate methods using 9000 cells as their seeding density. Kuwahara et al. generated embryoid bodies using 12,000 cells per well, becoming the second most popular seeding density, with almost 25% of protocols using this amount. Both papers use V-bottom 96-well

plates, resulting in 60% of methods with a single-cell start using these for their initial seeding (Figure 8B).

Most protocols used a starting medium of either a Dulbecco's Modified Eagle Medium (DMEM)-based medium, a stem cell medium, or a defined ratio of the two (Figure 8C). We observed that approximately 30% of protocols used other types of media at the beginning of their cultures, such as Glasgow's Minimal Essential Medium (GMEM) or Iscove's Modified Dulbecco Medium (IMDM). Similar to the aforementioned seeding density or use of V-bottom plates, the use of GMEM or IMDM media could also be traced back to Nakano et al. and Kuwahara et al. No other methods incorporated either medium that were not based on the protocols of Nakano et al. or Kuwahara et al. (Figure S2). GMEM has been routinely used for mouse embryonic stem cell culture, and was present in previously published work from Nakano's lab generating optic tissue from murine stem cells [260]. IMDM is a highly enriched medium that is well suited to highly proliferating cultures. Given the rapid expansion of cells in the early stages of generating aggregates, IMDM could be a favorable choice for use during the earlier stages of differentiation. Interestingly, however, we found that the majority of methods that did not start with a DMEM-based medium during the early differentiation stages often opted to switch to a DMEM base during later culture stages. This meant that a DMEM-based medium was used at some point throughout culturing in almost 90% of methods (Figure 8C). We also found that 95% of protocols included N2 and B27 supplements, either separately or together during the cultures. N2 supplement is used extensively in neural cultures and is often added in the earlier stages of retinal organoid differentiation. We here referred to the stage where stem cells are being directed down an anterior neural fate. Obviously, a neural fate stimulating supplement, such as N2, will help this process. Heparin was also commonly used in the first 3 weeks of differentiation alongside N2 supplement, as not only does heparin promote the proliferation of stem cells [261], but it can also induce neuronal differentiation [262]. Furthermore, it has been shown that heparin promotes Wnt signaling, which could also affect the differentiation of early retinal organoids [263,264]. Interestingly, we observed that at really late stages of differentiation, B27 supplement was replaced with N2 supplement for the remaining culture time. The reason for this could be because N2 supplement helps in the survival of post mitotic neurons. B27 supplement is used primarily to support the long-term viability of neuronal cells, and as such is commonly added during long-term culturing, after the initial differentiation into the neural lineage.

As we were concentrating on the initial development of the retina, we did not take into account supplements added for long-term development, such as taurine or retinoic acid [48,149,177,226]. Some factors influencing early development, such as Rock Inhibitor or Blebbistatin, were often used in cultures and were method independent. These can be used interchangeably and were mostly used in the first few days of cultures to initiate differentiation, reduce apoptosis and improve EB formation. However, Rock Inhibitor was frequently present for an extended time up to day 18, and is therefore also likely to affect the Rho-kinase section of the TGF- $\beta$  non-canonical pathway outlined in Figure 3.

We also found that a selection of factors were added throughout development, whereas other additions were restricted to certain time points. For example, IWR1e, an inhibitor of the Wnt signaling pathway (Figure 5), was never added after day 14. In contrast, CHIR99021, a Wnt activator, was always added between days 14 and 24. This shows us that in stem cell-derived organoid models, the Wnt pathway needs to be regulated at specific early stages of retinal differentiation to initiate the proper development of the retinal lineage. In all the protocols reviewed, the BMP4 protein, simulating the BMP pathway (Figure 3), was always added before day 18, which hallmarks the beginning of developmental change from anterior neural fate to retinal fate. Note that, at this time point, neurospheres are still developing their anterior neural identity and have not yet developed into organoids. This reveals the essential role of the BMP pathway in the initial stages of development of neurospheres. The inhibition of BMP signaling was uncommon, with just 8 out of 131 protocols using noggin, dorsomorphin or LDN193189 inhibition for this

purpose. Several other external factors, such as SU5402 or SAG, were frequently added in-between 12 to 24 days of early retinal organoid development, which is the time interval where many protocols transition from an anterior neural lineage to a full retinal lineage. Since SU5402 and SAG affect the FGF (not shown) and hedgehog (Figure 2) signaling pathways, respectively; their pathways appear to be essential for this transition in vivo, and studies have shown in chick explant models that SU5402 suppresses the differentiation of the early-born retinal ganglion cells [265]. DAPT, the  $\gamma$ -secretase inhibitor involved in notch signaling (Figure 6), is routinely added to improve photoreceptor differentiation and maturation [186,230,248]. In vitro, it was never added in the first 4 weeks of cultures, reinforcing that role of preparing the retina for late-born retinal neurons.

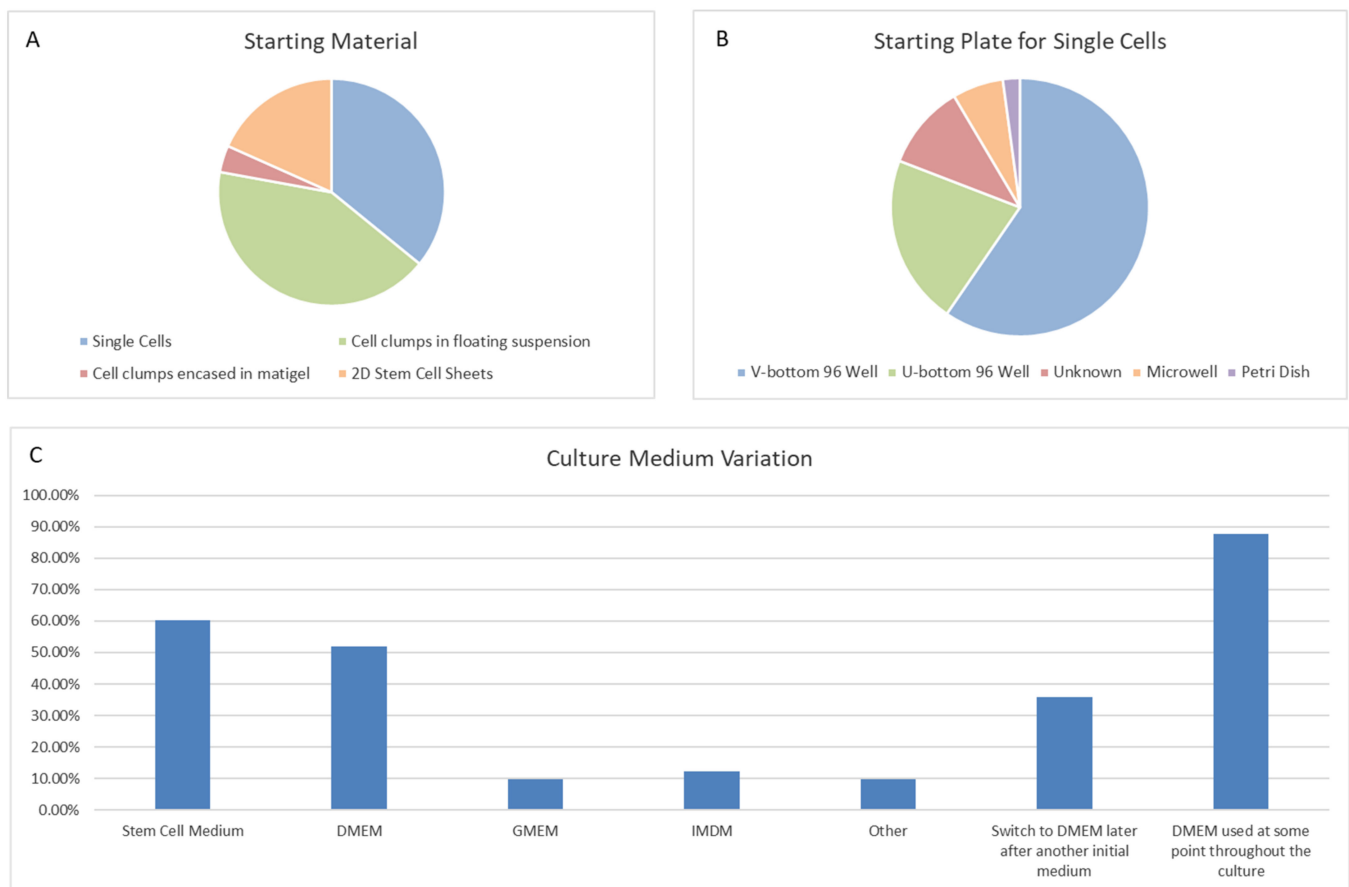


**Figure 8.** A breakdown of organoid techniques used. (A) Analysis of organoid protocols revealed that the most popular method of generating retinal organoids was starting with stem cell clumps in suspension, followed closely by single-cell aggregation. (B) For single-cell aggregation starts, the majority of methods used 96-well plates, with V-bottom plates being the most popular. (C) Different protocols use a variety of different media to start their differentiations, either alone or in combination. We found that starting with stem cell medium and/or DMEM was the most popular choice. Interestingly, although other protocols did start with other media such as GMEM or IMDM, we found that for long-term culturing, they switched to DMEM, meaning the overall number of protocols that use DMEM at some point in the differentiation is extremely high.

Other than temporal differences, we also observed that a range of concentrations was utilized for these aforementioned exogenous supplements. To complicate matters, some factors were kept at one constant concentration throughout methods used (SAG, FGF2), while for others (CHIR99021, SU5402), a whole range of concentrations were used, between 3  $\mu$ M–3 mM and 2.5  $\mu$ M–3 mM, respectively (Table 1). Interestingly, a number of frequently used supplement concentrations and/or timings related to individual groups or protocols, such as Blebbistatin, IWR1e or FGF2. Blebbistatin added from day 0 to 1

originated from Zhong et al. [155], which in part explains the popularity of these conditions. Similarly, IWR1e added at 3  $\mu$ M from day 0 to 12 originated from the method of Nakano et al. [154], which has also been a heavily used method. In contrast, FGF2 supplements are routinely added almost solely by the group of Olivier Goureau [156] (Figure S2). Finally, we found that the dual SMAD inhibition of the TGF- $\beta$  and BMP pathways by SB431542 and LDN193189 was an exclusive pairing and always used together.

**Table 1.** Summary of the additions used to promote retinal differentiation in organoid protocols and their frequency, concentration, and time interval of use. Analysis of the literature uncovered many supplements that are added to regulate signaling pathways throughout the development of retinal organoids. We decided to use the conditions and concentrations highlighted with an asterisk (\*) and test their effect on retinal differentiation in our organoid protocol, representing the more popular time points or concentrations used for a range of conditions affecting different signaling pathways. For further explanation of the individual additions used, see text.

	Description	Concentration	Length of Addition	Reference
BDNF	Activator of TGF- $\beta$ and BMP signaling through PI3K and ERK signaling cascades	20 ng/mL	Day 63 onwards	Singh '19 [235]
bFGF	FGF signaling ligand	10 ng/mL	Day 14 onwards	Singh '15 [234], Singh '19 [235], Singh '21 [236]
		5 $\mu$ M	Day 0–1	Lu '20 [211]
Blebbistatin	Inhibitor of NMII-ATPase, downstream of Rock inhibition	10 $\mu$ M	Day 0–1	Achberger '19 [159], Akhtar '19 [160], Cora '19 [165], Deng '20 [170], Lane '20 [202], Li '19 [203], Luo '18 [214], Luo '19 [213], Quinn '18 [226], Quinn '19 [225], Tornabene '19 [240], Vergara '17 [242], Vig '20 [243], Xian '19 [250], Xie '20 [251], Zhong '14 [155]
		10 mM	Day 0–1	Li '18 [204], Lin '20 [206], Liu '18 [209]
		50 ng/mL	Day 6–15	VanderWall '20 [241]
			Day 6–18	Mao '19 [215]
		55 ng/mL	Day 6–15	Döpfer '20 [108]
			Day 6–20	Khan '20 [196]
		100 ng/mL	Day 0–10	Meyer '09 [144]
		0.05 $\mu$ g/ $\mu$ L	Day 5–20	Hoshino '19 [189]
		0.5 $\mu$ g/ $\mu$ L	Day 6–12	Sridhar '20 [237]
BMP4	BMP signaling ligand		Day 6–15	Bronstein '20 [130], Capowski '19 [49], Kallman '20 [192]
			Day 6–16	Fligor '20 [131]
		1.5 nM	Day 6–18	Browne '17 [107], Deng '18 [169], Guo '19 [188], Hallam '18 [145], Kobayashi '18 [129], Kuwahara '15 [127], Li '21 [205], Liu '20 [208], Liu '21 [207], Phillips '18 [224], Wang '21 [246], Zeng '21 [252], Zou '19 [259]
		2.2 nM	Day 6–18	Peskova '20 [223]
		2.25 nM	Day 6–18	Chichagova '20 [48], Georgiou '20 [146]

Table 1. Cont.

Description	Concentration	Length of Addition	Reference	
CHIR99021	3 $\mu$ M	Day 15–18	Aparicio '17 [74], Arno '16 [161], Browne '17 [107], Lane '20 [202], Nakano '12 [154], Pan '20 [113], Parfitt '16 [221], Zheng '20 [257]	
		Day 15–21	Döpfer '20 [108]	
		Day 18–24 *	Guo '19 [188], Hallam '18 [145]	
	4 $\mu$ M	Day 18–24	Georgiou '20 [146]	
		10 $\mu$ M	Unknown	Luo '18 [214], Luo '19 [213]
	3 mM	Day 14–17	Wiley '16 [248]	
		Day 15–18	Sharma '17 [230]	
Day 18–21		Kobayashi '18 [129]		
COCO	30 $\mu$ M	Day 0–12	Pan '20 [113]	
		Day 0–30	Pan '20 [113]	
DAPT	10 $\mu$ M	Day 28–35	Khabou '18 [195]	
		Day 28–42 *	Eldred '18 [177], Lu '20 [211], Zerti '20 [253]	
		Day 29–42	Shrestha '19 [232]	
		Day 29–45	Wahlin '17 [245]	
		Day 42–49	Garita-Hernandez '20 [186], Garita-Hernandez '21 [184]	
		Day 44–50	Garita-Hernandez '18 [185]	
		Day 60–72	Zerti '20 [253]	
	Day 90–102	Zerti '20 [253]		
10 mM	Day 30–40	Sharma '17 [230], Wiley '16 [248]		
DKK-1	10 ng/mL	Day 0–7	Zhu '18 [109]	
		Day 18–21	Singh '15 [234]	
	20 ng/mL	Day 28–35	Singh '19 [235], Singh '21 [236]	
	100 ng/mL	Day 2–4	Meyer '11 [135]	
		Unknown	Luo '18 [214], Luo '19 [213]	
Dorsomorphin	BMP inhibitor targeting ALK-2, -3, and -6 inhibition	100 ng/mL	Day 2–4	Meyer '11 [135]
EC23	Synthetic retinoid	0.3 $\mu$ M	Day 18–41	Völkner '16 [101]
			Day 25–120	Völkner '21 [244]
FGF2	FGF signaling ligand	10 ng/mL	Day 14–21	Khabou '18 [195], Reichman '14 [143]
			Day 21–28	Reichman '14 [143]
			Day 28–35	Diakatou '21 [171], Freude '20 [180], Gagliardi '18 [181], Garita-Hernandez '18 [185], Garita-Hernandez '20 [186], Garita-Hernandez '21 [184], Rabesandratana '20 [158], Reichman '14 [143], Reichman '17 [156], Scholler '20 [229], Slembrouck-Brec '18 [157], Slembrouck-Brec '19 [150]

Table 1. Cont.

Description		Concentration	Length of Addition	Reference
FGF9	FGF signaling ligand	10 ng/mL	Day 21 onwards	Singh '15 [234]
			Day 35 onwards	Singh '19 [235], Singh '21 [236]
IGF1	Interacts with insulin receptors to regulate downstream signaling pathways such as Akt and ERK	5 ng/mL	Day 0–35	Chichagova '19 [162], Chichagova '20 [48]
			Day 0–37 *	Collin '19 [163], Collin '19 [164], Dorgau '18 [173], Dorgau '19 [172], Felemban '18 [178], Mellough '15 [148], Mellough '19 [217], Zhang '20 [255], Zhang '21 [256]
			Day 2–29	Zerti '20 [253]
			Day 0–7	Zhu '18 [109]
		10 ng/mL	Day 18–21	Singh '15 [234]
			Day 30 onwards	Zerti '20 [253]
			Day 35 onwards	Chichagova '19 [162], Chichagova '20 [48]
			Day 37–90	Collin '19 [163], Collin '19 [164], Dorgau '18 [173], Dorgau '19 [172], Felemban '18 [178], Mellough '15 [148], Mellough '19 [217], Zhang '20 [255], Zhang '21 [256]
			Day 42–200	Kaya '19 [193], Kelley '20 [194], Kruczek '21 [198]
			Day 20–30	Regent '20 [227]
20 ng/mL	Day 21/28 onwards	Kaya '19 [193], Kelley '20 [194], Kruczek '21 [198]		
	Day 28–35	Singh '19 [235], Singh '21 [236]		
	Day 35 onwards	Regent '20 [227]		
	Day 0–12	Sharma '17 [230], Wiley '16 [248]		
IWR1e	Inhibitor of Wnt signaling through stabilization of AXIN	3 nM	Day 0–7	Zhu '18 [109]
			Day 0–6	Döpfer '20 [108]
		3 µM	Day 1–6	Eldred '18 [177], Wahlin '17 [245]
			Day 1–8	Lu '20 [211]
			Day 0–12 *	Arno '16 [161], Eastlake '19 [176], Gao '20 [183], Kaewkhaw '15 [191], Lane '20 [202], Nakano '12 [154], Pan '20 [113], Parfitt '16 [221], Völkner '16 [101], Zheng '20 [257]
			Day 0–18	Browne '17 [107]
			Day 2–12	Aparicio '17 [74], Browne '17 [107]
			Day 2–14	Dulla '18 [174]
		3 mM	Day 2–20	Khan '20 [196]
		LDN193189	Inhibitor of BMP signaling through inhibition of ALK-2, -3, and -6 receptors	100 nM
Day 0–7*	Zhu '18 [109]			
3 µM	Day 0–6			Browne '17 [107]



Table 1. Cont.

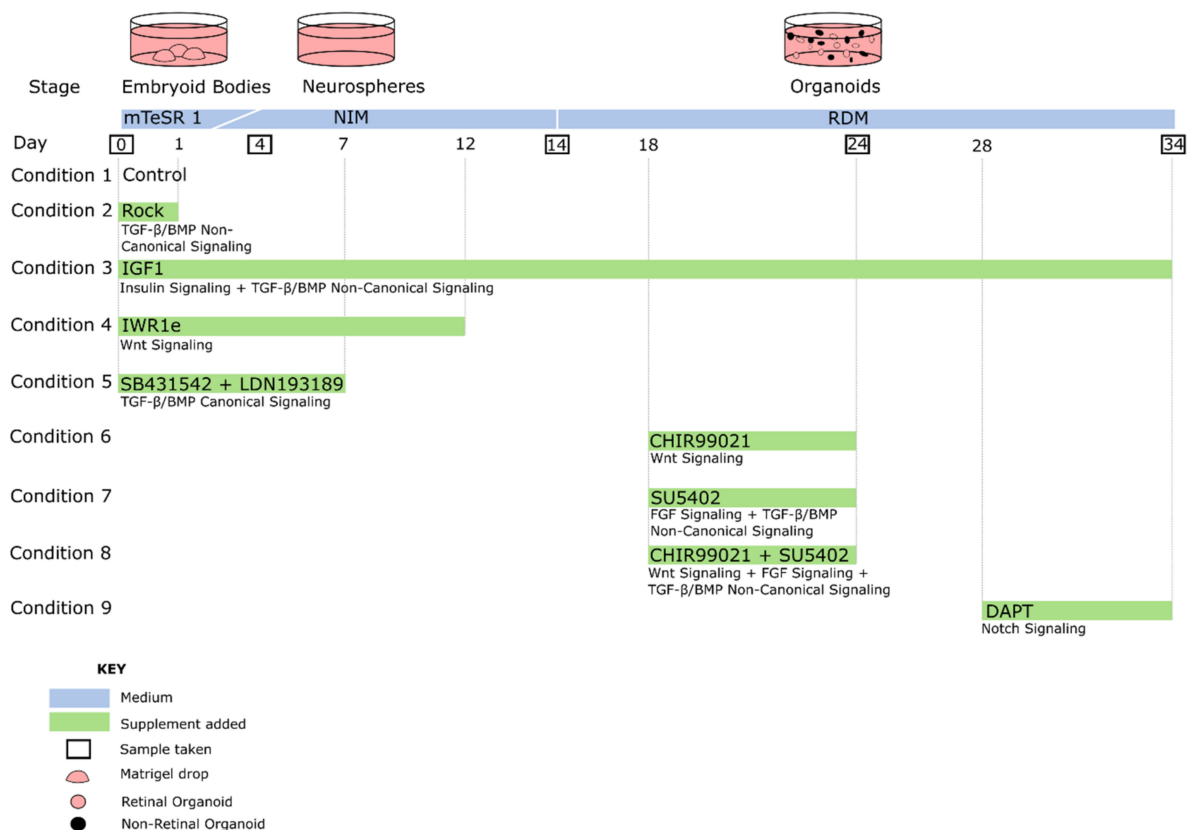
Description		Concentration	Length of Addition	Reference
Noggin	TGF- $\beta$ signaling ligand	10 ng/mL	Day 0–7	Zhu '18 [109]
		100 ng/mL	Day 0 onwards	Singh '15 [234], Singh '19 [235], Singh '21 [236]
			Day 2–4	Meyer '11 [135]
			Day 0–1*	Achberger '19 [159], Aparicio '17 [74], Browne '17 [107], Cora '19 [165], Cowan '20 [152], Lai '21 [199], Lam '20 [201], Shrestha '19 [232], Zerti '20 [253], Zerti '21 [254]
Rock Inhibitor (Y-27632)	Inhibitor of Rock	10 $\mu$ M	Day 0–2	Collin '19 [163], Collin '19 [164], Dorgau '18 [173], Dorgau '19 [172], Felemban '18 [178], Georgiou '20 [146], Hallam '18 [145]
			Day 0–14	Dulla '18 [174]
			Day 24–25	Achberger '19 [159], Cora '19 [165]
			Day 0–1	Döpfer '20 [108], Kaya '19 [193], Kelley '20 [194], Kruczek '21 [198], Regent '20 [227], Zheng '20 [257]
		20 $\mu$ M	Day 0–4	Kaewkhaw '15 [191]
			Day 0–6	Deng '18 [169], Guo '19 [188], Kobayashi '18 [129], Kuwahara '15 [127], Wang '21 [246], Zeng '21 [252], Zou '19 [259]
			Day 0–12	Eastlake '19 [176], Gao '20 [183], Lane '20 [202], Nakano '12 [154], Pan '20 [113], Völkner '16 [101]
			Day 0–18	Li '21 [205], Liu '20 [208], Liu '21 [207], Parfitt '16 [221]
			Day 0–20	Khan '20 [196]
			10 mM	Day 0–1
20 mM	Day 0–12	Sharma '17 [230], Wiley '16 [248]		
SAG	Hedgehog pathway activator through activation of Smo	100 nM	Day 8–16	Eldred '18 [177]
			Day 10–18	Lu '20 [211]
			Day 12–18	Eastlake '19 [176], Gao '20 [183], Kaewkhaw '15 [191], Völkner '16 [101], Wahlin '17 [245]
			Day 12–20	Khan '20 [196]
			Day 14–17	Wiley '16 [248]
			Day 14–20	Dulla '18 [174]
			Day 15–18	Aparicio '17 [74], Arno '16 [161], Browne '17 [107], Lane '20 [202], Nakano '12 [154], Pan '20 [113], Parfitt '16 [221], Sharma '17 [230], Zheng '20 [257]
SB431542	Inhibitor of TGF- $\beta$ signaling through inhibition of ALK-4, -5, and -7 receptors	3 $\mu$ M	Day 0–6	Browne '17 [107]
		10 $\mu$ M	Day 0–6	Döpfer '20 [108]
			Day 0–7*	Zhu '18 [109]

Table 1. Cont.

Description		Concentration	Length of Addition	Reference
SU5402	Inhibitor of FGF signaling through inhibition of fibroblast growth fact receptor 1 (FGFR-1)	2.5 $\mu$ M	Day 18–24	Chichagova '20 [48], Georgiou '20 [146]
		5 $\mu$ M	Day 15–21	Döpfer '20 [108]
			Day 18–24*	Guo '19 [188], Hallam '18 [145]
		10 $\mu$ M	Day 0–10	Meyer '09 [144]
		3 mM	Day 16–40	Meyer '09 [144]
Wnt3a	Wnt signaling activator	100 ng/mL	Day 0–10	Meyer '09 [144]
XAV939	Wnt signaling inhibitor through stabilizing AXIN	100 ng/mL	Day 2–4	Meyer '11 [135]

#### 4.2. Comparison of Specific Signaling Pathway Modulators and Their Effect on Retinal Organoid Differentiation

After collating the results of the literature search, we selected a range of conditions that were representative of the methods we examined and performed a pilot experiment using our previously published protocol [149] (outlined in Figure 9). We chose conditions that spanned retinal development, from initial time points when embryoid bodies and neurospheres form (day 0–14), to later stages when 3D organoids start to form and mature (day 14 onwards). We observed retinal organoid development by brightfield microscopy, and took samples at day 0, 4, 14, 24 and 34 to measure the expression of key retinal developmental genes such as *PAX6*, *RAX* and *VSX2*.



**Figure 9.** Experimental outline of pilot. A collection of frequently used agonists and antagonists for different signaling pathways reviewed in this article were systematically tested for their efficiency at directing retinal development. Adapting

our previously published protocol [149], stem cell clumps were embedded in 3D Matrigel drops for 4 days, transitioning from mTeSR1 medium to neural induction medium (NIM). At day 4, they were removed from the gel and plated in a 2D environment for a further 10 days to allow the embryoid bodies to enter the anterior neural fate. Once neurospheres had formed, they were scraped off and cultured 3D in a floating environment in retinal differentiation medium (RDM) to form organoids. Condition 1 was the control condition, with no supplements added. Condition 2 consisted of treatment with Rock Inhibitor from day 0 to 1 only. Condition 3 included a continuous treatment of IGF1 from day 0 to 34. Condition 4 consisted of IWR1e treatment from day 0 to 12. Condition 5 included a double treatment of SB431542 and LDN193189 from day 0 to 7. Conditions 6–8 all included treatments from day 18 to 24 consisting of CHIR99021, SU5402, and CHIR99021 + SU5402, respectively. Finally, condition 9 consisted of treatment with DAPT from day 28 to 34. All culture conditions were kept until day 34, and samples were taken at day 0, 4, 14, 24 and 34 for analysis. (Pilot study:  $n = 1$  for all conditions).

#### 4.2.1. Regulation of Signaling Pathways by External Factors Affecting Retinal Development

To make an inventory of the effect that (ant-) agonists have on the key signaling pathways (Figures 2–6) in retinal organoid development, we tested a range of conditions spanning the early and late regulation of these pathways in a proof-of-concept experiment (Figure 9). In separate cultures, we added supplements affecting early retinal development (between days 0 and 12) (Figure 9), including Rock Inhibitor, IGF1, IWR1e and the combination of SB431542/LDN193189. Similarly, we treated cultures with supplements affecting the later stages of development (between days 18 and 34, Figure 9), by adding CHIR99021, SU5402, the combination CHIR99021/SU5402 and, finally, DAPT. All conditions were systematically and simultaneously evaluated by microscopy and RT-PCR, as described below.

In the embryoid body stage from day 0 to 4, we did not observe significant developmental differences between culture additions and the control. All conditions (control, Rock Inhibitor, IGF1, IWR1e, SB431542/LDN193189, CHIR99021, SU5402, CHIR99021/SU5402, DAPT) produced healthy EBs (Figure 10A). It is important to note that in CHIR99021, SU5402, CHIR99021/SU5402 and DAPT conditions, the EB stage (day 0–4) is the same as the control conditions, due to these additions being added at later time points, as depicted in Figure 9. In contrast, during the second stage of development, from day 4 to 14 when the EBs are plated in a 2D environment (Figure 9), a number of changes were observed in the IWR1e, Rock Inhibitor, and SB431542 + LDN193189-treated cells compared to the control (Figure 10B). The addition of IWR1e inhibited the outgrowth of the neurospheres, with the epithelial outgrowth barely leaving the neural center of the neurosphere after 10 days. There was also increased cell death in this condition, defined by brightfield microscopy, when compared to the control, also seen in SB431542 + LDN193189-treated cells. Rock Inhibitor-treated cells displayed two types of epithelial outgrowth, with distinct borders forming between the two, which no other condition exhibited. All the remaining conditions (IGF1, CHIR99021, SU5402, CHIR99021 + SU5402, and DAPT) developed comparably to the control during the neurosphere stage (Supplementary Figure S1).

Organoids generally develop into a retinal or non-retinal fate between days 20 and 25, at which point they should be separated from each other. In our test, the yield of retinal organoids was measured with brightfield microscopy during this final stage at day 25 (Table 2), and varied greatly between various culture conditions tested. We found that some conditions behaved similarly to the control: the treatment of SU5402 or DAPT had no apparent effect on retinal organoid yield (Table 2), whilst some supplements added during the initial phase of development, from day 0 to 12, harmed the yield of retinal organoids. IWR1e-treated cells did not form retinal organoids, and only formed around half the number of total (retinal and non-retinal) organoids compared to the control (Table 2). The surviving organoids were also significantly smaller, most likely the result of the increased cell death observed during the 2D stage (Figure 10C). Rock Inhibitor and SB431542/LDN193189-treated cultures had similar numbers of total organoids compared to the control, but with fewer retinal organoids, resulting in a lower yield. IGF1 was added

throughout the culture time, and had a positive effect on retinal development, with almost double the yield of retinal organoids by day 25. The treatment with CHIR99021 boosted retinal organoid yield five-fold, whilst also generating more than double the total amount of organoids compared to the control (Table 2). Organoids made by CHIR99021 treatment showed characteristic golden laminated structures that were present throughout longer-term culturing. Initial data from our laboratory suggest long-term retinal development is not affected by CHIR99021 treatment (Wagstaff et al., unpublished). Adding SU5402 in combination with CHIR99021 only negatively added to the outcome, with a retinal yield only 2.5-fold higher than the control, whilst adding SU5402 alone had no apparent effect compared to the control (Table 2, Figure S1).

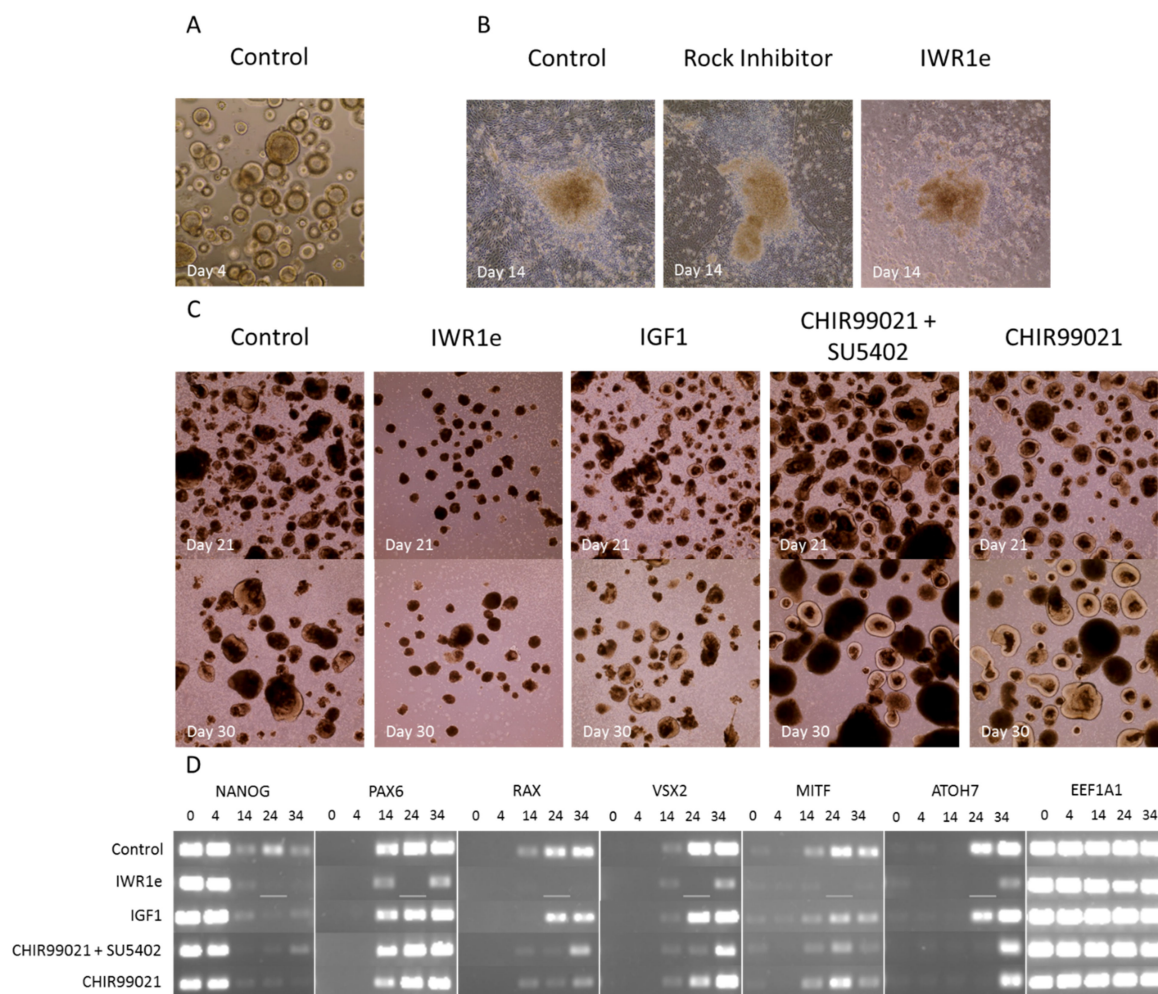


**Figure 10.** Changes in retinal development through microscopy and gene expression assay. (A) All conditions developed comparable embryoid bodies to the control up to day 4. (B) Throughout the next 2D stage of generating neurospheres (day 4–14), changes between conditions were observed. Rock Inhibitor-treated cells had two distinct types of epithelial outgrowth, with a border separating them, whereas IWR1e-treated cells resulted in poor epithelial outgrowth and an increase in cell death. (C) Only IWR1e, IGF1, CHIR99021 + SU5402, and CHIR99021 treatments showed significant changes in retinal organoid yield compared to the control. IWR1e treatment severely impact retinal organoid yield and the overall organoid size. Continuous IGF1 treatment resulted in almost double the number of retinal organoids compared to the control. CHIR99021/SU5402 double treatment increased retinal organoid yield 2.5-fold; however, individual CHIR99021 treatment gave the best yield with a 5-fold increase. (D) The differences between conditions were also largely reflected in the gene expression of key developmental markers such as *PAX6*, *RAX* and *VSX2*, as well as cell-specific markers such as *MITF* and *ATOH7*. Differences of retinal development genes were observed between conditions over time (Day 0, 4, 14, 24, 34). Unfortunately, IWR1e treatment resulted in poor organoid yields and subsequently, there was less RNA available for day 24, as represented by the *EEF1A1* reference gene sample.

**Table 2.** Retinal organoid yields. Cultures were analyzed on day 25, and both retinal and non-retinal organoids were manually counted for each condition through brightfield microscopy images. The yield of retinal organoids compared to the total amount of organoids was then calculated for each condition either focusing on the early-stage regulation (Rock Inhibitor, IWR1e, IGF1, SB431542/LDN193189) or late-stage regulation (CHIR99021, SU5402, CHIR99021/SU5402, DAPT) of signaling pathways.

Condition	Number of Retinal Organoids	Number of Non-Retinal Organoids	Yield of Retinal Organoids <sup>1</sup>
Control	9	80	10.1%
Rock Inhibitor	3	114	2.6%
IGF1	17	78	17.9%
IWR1e	0	42	0.0%
SB431542 + LDN193189	1	106	0.9%
CHIR99021	105	99	51.5%
SU5402	10	118	7.8%
CHIR99021 + SU5402	56	175	24.2%
DAPT	10	112	8.2%

<sup>1</sup> *n* = 1 for quantification of retinal organoid yields.

#### 4.2.2. Variable Retinal Development Confirmed by Gene Expression Changes of Key Markers

We took organoid samples at pivotal times throughout development: day 0, day 4, day 14, day 24, and day 34. These coincided with the end of the embryoid body stage (day 4), the end of the neurosphere stage (day 14), and the period when retinal organoids start to develop separately from the non-retinal organoids (day 24). We analyzed the RNA from the samples by RT-PCR for the presence and changes in gene expression of crucial retinal genes (Figure 10D). In the developing retinal organoid control [149], the stem cell marker *NANOG* was highly expressed on days 0 and 4, before decreasing on days 14, 24, and 34. The early retinal markers *PAX6* and *RAX* and the optic cup marker *VSX2* were all present from day 14 onwards, with *VSX2* expression increasing between day 14 and 24. The RPE-specific marker *MITF* was expressed throughout development, peaking at day 24. Finally, the retinal ganglion cell marker *ATOH7* was highly expressed from day 24 onwards. In line with the results of retinal organoid yields, treatment with SU5402 or DAPT did not appear to change the expression of key retinal developmental genes compared to the control. Interestingly, all conditions resulted in lower levels of the stem cell marker *NANOG* when compared to the control in days 14 to 34, suggesting an improved transition from a stem cell state to differentiation into the neural lineage.

As described above, the addition of IWR1e produced the lowest retinal organoid yield (Table 2), and this is reflected in its gene expression (Figure 10D). IWR1e treatment leads to a complete loss of *RAX* throughout the culture, and a decrease in expression of the retinal lineage markers *PAX6* and *VSX2*. The RPE-specific marker *MITF* expression was present, and the ganglion-specific *ATOH7* was severely reduced, with a lowered expression at day 24 and a large decrease at day 34. Treatment with Rock Inhibitor or SB431542/LDN193189 had no apparent effect on retinal gene expression, even though retinal organoid yield was decreased. IGF1 treatment resulted in a delay of *RAX* expression, with *RAX* only present from day 24 onwards. However, the expression of other markers, upon prolonged IGF1 treatment, remained unchanged throughout development compared to the control. Prolonged IGF1 treatment appeared to slightly increase the yield of retinal organoids (Table 2). The condition with the best retinal yield, CHIR99021 treatment, unexpectedly exhibited a slight decrease in *RAX* expression, although *PAX6* and *VSX2* expression was comparable to the control. Furthermore, there was a delay in the expression of *ATOH7*, with *ATOH7* being absent until day 34. This was mirrored in CHIR99021 and SU5402

double treatment, where *ATOH7* was not expressed until day 34, alongside an apparent decrease in *VSX2* expression (Figure 10D).

#### 4.3. Comparison of Cell Type-Specific Expression during Retinal Organoid Development

As presented above, the many different methods used to generate retinal organoids gives rise to increased variability between cultures, making methods hard to compare. Techniques such as RNA-seq allow us to quantify the amount of cell type-specific RNA present in cultures, which gives us an idea of cell types present in the diverse organoid stages, and the gene expression similarities and differences between protocols. We can also estimate how representative these datasets are for human retinal development. Datasets have been generated from multiple stem cell lines used to make retinal organoids and fetal retinal cultures [8,191,197]. We analyzed these three datasets for the expression of relevant cell type-specific markers, and aligned them both to the RT-PCR data presented in this manuscript, and the RNA-seq data from our control retinal organoid differentiation protocol [149]. At this point, it is important to note that due to the different methods and analysis used, these data cannot be directly compared, but can act only as an indication of the cell types present and when they appear. For reason of comparison (cells in their full physiological context), we focused on expression studies of whole retinal organoids.

We initially compared the RT-PCR data from this manuscript with RNA-seq data we previously published generating retinal organoids from H1 embryonic stem cells. In general, we found that the appearance of retinal genes in the control condition in our pilot experiment described in this manuscript matched the control retinal organoid differentiation RNA-seq data we previously published (Figure 11A): *NANOG* was present on days 0 and 4 before losing its expression. *PAX6* was the first neural developmental gene to be expressed, followed by the retinal marker *RAX*, with *VSX2* being expressed last. *MITF* expression seemed to peak at day 25 before decreasing, as seen in our pilot control condition. *ATOH7* was expressed from day 25 onwards. Dataset GSE119274 [197], presented in Figure 11B, originated from a study that also used the embryonic stem cell line H1 to generate retinal organoids, taking samples from day 15, 1 month, 3 months, 6.5 months and 9 months in culture. We observed that *PAX6* is also the first retinal developmental marker to appear in this method, peaking after 1 month of culture, with *RAX* and *VSX2* being similarly expressed at this time point, similarly to our RT-PCR and RNA-seq data. We also observed a significant increase in the expression of *ATOH7* between 15 days and 1 month of culture, mirroring our RT-PCR analysis of *ATOH7* in our cultures. Another group, Kaewkhaw et al. (2015), cultured organoids and generated the dataset GSE67645 [191]. Their RNA-seq for the relevant data is presented in Figure 11C. These authors generated retinal organoids using another embryonic stem cell line, H9, and analyzed samples taken throughout the culture at days 0, 37, 47, 67 and 90. They showed higher levels of *PAX6*, *RAX* and *VSX2* expression at day 37 compared to the cell-specific marker *MITF*, something we also observed in our cultures. Similarly, the expression of *ATOH7* increased significantly between day 0 and 37, in line with our findings. Finally, we analyzed the transcriptomic dataset GSE104827 [8] of the developing fetal human retina (presented here in Figure 11D). Extensive data from samples were available throughout development (day 52 or 54, 53, 57, 67, 80, 94, 94 (second sample), 105, 107, 115, 125, 132, 136). Ideally, in vitro retinal development should be as close to fetal expression as possible. However, it is often difficult to compare these due to the hugely different environments and timelines. The most striking difference was the large increase in total expression when compared to the data of our retinal organoids (Figure 11A), with some genes expressed 100-fold more. Although it was difficult to compare all of the different organoid datasets with the fetal retina, we did observe some interesting similarities. In dataset GSE104827, *PAX6* expression was at its highest after around 50 days of development, before decreasing over time to day 136. In our retinal organoid RNAseq data, we also observed a peak in *PAX6* expression after around 60 days of development, before decreasing over the course of the differentiation to day 160. The fetal expression of *RAX* slightly increased and decreased

throughout development, but remained somewhat constant between day 52 and 136. This was mirrored in our organoid development, varying slightly but keeping relatively stable over time. Interestingly, we observed that *VSX2* expression in fetal retina increased over time from day 53 to 136, whereas in all three organoid datasets, *VSX2* expression was at its peak within the first month of development, before decreasing over time during the culture. Finally, we found that although *ATOH7* expression in the fetal retina did mirror the expression found in our dataset, the peak of expression was shifted to an earlier time point. In our RNAseq dataset, *ATOH7* expression increased gradually until day 63, where it peaked before decreasing over time. However, in the fetal retina, *ATOH7* expression peaked by day 53, and by day 67 was already reduced by around half, decreasing further throughout development. When comparing these similarities in gene expression, it is important to consider the relative timeline, as retinal organoid maturation and fetal eye maturation do not occur within the same timeframe. Taken together, these data highlight important similarities and differences between in vitro and in vivo retinal development.

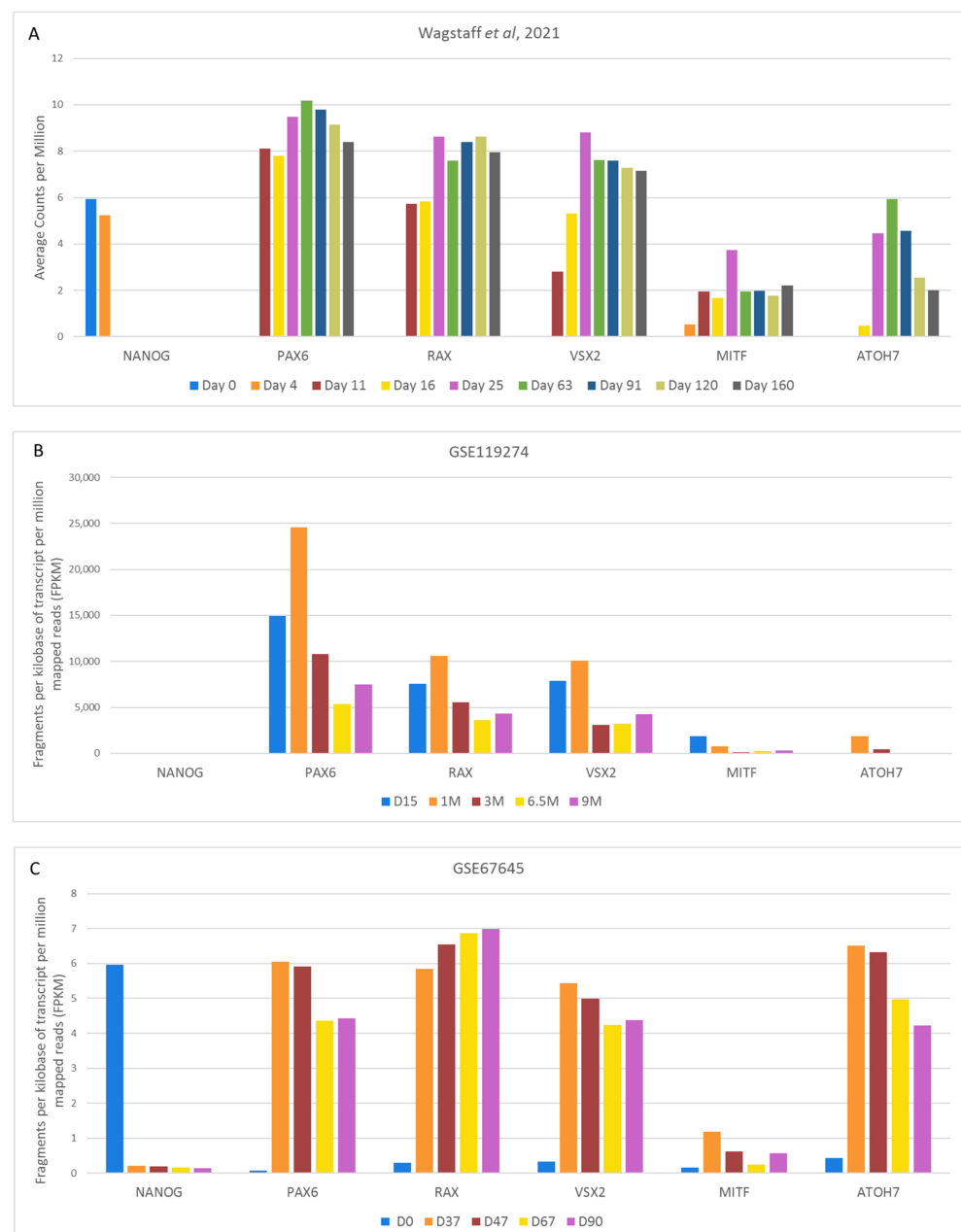
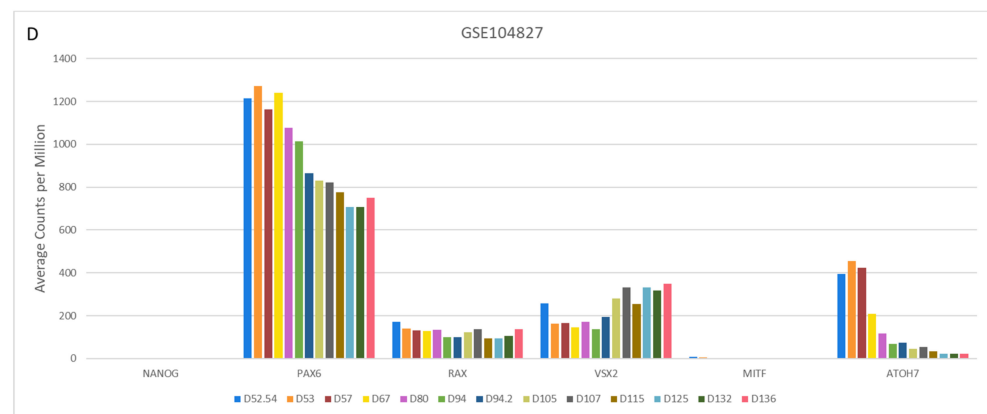


Figure 11. Cont.



**Figure 11.** RNA-seq analysis of differing methods of in vitro retinal development, in addition to in vivo fetal retinal development. We compared the gene expression of our pilot experiment to RNA-seq analysis of different retinal organoid differentiations and fetal retina samples. (A) Our previously published protocol using H1 embryonic stem cells shared similar gene expression with our pilot experiment shown in this manuscript over the course of the first 34 days. (B) A different method of generating retinal organoids using the H1 embryonic stem cell line also showed expression of key retinal genes increasing over the first month, comparably to our pilot experiment and RNA-seq. (C) Retinal organoids generated from a different embryonic stem cell line (H9) showed variable expression levels of key genes when compared to A and B. Some genes, such as *RAX*, increased over time in line with other RNA-seqs; however, other genes, such as *VSX2*, unexpectedly decreased over time. (D) RNA-seq of fetal retina presented surprising results. After being expressed by day 10, *PAX6* and *RAX* both decreased until day 69, before significantly increasing along with *VSX2*. This was not shown in RNA-seqs of retinal organoids, where *PAX6* and *RAX* expression slowly increased throughout earlier time points, not decreased.

## 5. Discussion and Conclusions

Since the introduction of retinal organoid technology, there has been a need to emulate in vivo retinal development as closely as possible in vitro. To achieve this, research has been increasingly focused on the temporal identification of mapping the molecular changes that cells undergo during retinal development. This has culminated in numerous protocols that vary greatly in their method and as such, are difficult to compare. This review systematically, and for the first time, explores the many different methods that are used to generate retinal organoids. It includes an inventory and comparison of the origin, signaling pathways and (ant-) agonists used in the literature. Furthermore, we systematically tested a range of additions reviewed here using our own protocol [149] to corroborate the possible effect they had on organoid development.

Our review shows that a significant proportion of current methods originate from three main protocols [127,154,155]. Using these as a base, researchers have continuously improved methods to influence in vitro development by regulating important signaling pathways present throughout in vivo embryonic development. These pathways include the TGF- $\beta$ /BMP, hedgehog, Wnt and notch signaling pathways. By manipulating these signaling pathways, using (ant-)agonists (IWR1e, BMP4, CHIR99021), researchers aim to establish a more reliable and reproducible way of generating organoids that perfectly mimic the in vivo situation. We systematically looked at a number of conditions that further contribute to the improvement and consistency of the existing protocols. In experimental conditions, we observed that a lot of the most commonly used additions, such as IWR1e, SB431542/LDN193189, and SU5402, did not positively affect retinal development in our protocol except for CHIR99021 treatment, which significantly improved retinal organoid yield. However, it is important to note here that our pilot experiments reported here, do not conclude that the commonly used additions such as IWR1e have no effect in other methods of generating retinal organoids and/or animal models of retinal development.



It is also important to note that we present preliminary findings in a pilot experiment about the effects these different signaling molecules have on retinal organoid development. For more definitive conclusions, extensive further studies are needed. The large variation between protocol methods, coupled with the increasing variability between different cell lines means that further experiments should be carried out to optimize culture conditions.

### *5.1. The Use of Different Protocols Gives Rise to Variable and Difficult to Compare Cultures*

The majority of the established methods of generating retinal organoids arise from three core protocols, with different (ant-)agonists being used. Embryoid bodies are often created in vastly different environments, including SFEBq [154], free floating EB formation [155], and a 3D Matrigel suspension [149]. In SFEBq cultures, stem cells are dissociated to single cells and quickly re-aggregated in low adhesion 96-well plates with a defined number of cells per well. In free floating EB formation, stem cells are dissociated into small clumps and cultured in suspension, where they aggregate to form EBs. Three-dimensional Matrigel suspension also dissociates stem cells into small clumps, before embedding them in Matrigel drops (Figure 9), where they form EBs. These conditions are also continuously being optimized and innovated, from controlling embryoid body size by counting the number of starting cells, to generating microwell systems that can result in hundreds of similar EBs [152]. This variation in method can affect the efficiency of external factors on your culture, as we observed.

IWR1e and IGF1 are two of the most commonly used external factors added to retinal organoids cultures (Table 1). However, it is important to note that some supplements that are regularly added may come from a single well-replicated protocol and might not be as effective throughout all methodologies. For instance, over two-thirds of the times IWR1e is used, it is added between day 0 and 12 at a concentration of 3  $\mu$ M, showing a consistently positive effect on retinal development. This concentration and timeline come from Nakano et al. (2012), one of the most popular methods to use by multiple different groups. Therefore, although the use of IWR1e is widespread and popular, it can be traced back to a specific protocol. In our protocol, however, using IWR1e between day 0 and 12 at 3  $\mu$ M resulted in a complete loss of retinal identity based on brightfield microscopy and RT-PCR, as well as fewer organoids overall. IGF1, on the other hand, has been added at multiple time points throughout organoid development at various concentrations, depending on the protocol used. In our hands, it had a positive effect, increasing the yield of retinal organoids. The results we observed for the IWR1e treatment are drastically different to other methods, which could, in turn, be explained by our method of choice. To generate our embryoid bodies, we use a 3D Matrigel encasement method, described previously [149]. Matrigel is well known for being a semi-defined substrate full of extracellular proteins and factors. The presence of these proteins in the initial culture could not only affect native cell–cell interactions and signaling in the control conditions, but also could exert a conflicting effect on the initial embryonic signaling to some external factors. These drastic differences show how, just as retinal yields can be cell-line-dependent, small molecule effects are not only time- and concentration-dependent, but also method-dependent, and should be adapted to individual protocols.

### *5.2. Healthy Early Development of Embryoid Bodies Is Not a Guarantee for Healthy Organoids*

One of the most important steps of generating proper retinal organoids as a reliable model, with long-term lamination and all retinal cell types present and matured, is to have good starting material. Organoids generated from imperfect stem cells or embryoid bodies tend to lose their retinal identity throughout development. They usually also affect the surrounding organoids and thus, the entire culture. The importance of initial EB development has been previously shown by systematically testing mechanical, enzymatic and dissociation–reaggregation methods of generating embryoid bodies from stem cells in parallel [148]. Using these methods, the EBs were cultured either in the presence or absence of Rock Inhibitor for the first 48 h. Although Rock Inhibitor aided embryoid body

formation, there was no impact on early retinal specific gene expression. Interestingly, we also observed no significant changes in retinal yield or gene expression in the Rock Inhibitor-treated and control retinal organoid cultures.

In line with this, we did not observe any negative effects during the initial stage of embryoid body formation (day 0 to 4) for any of our conditions tested, with all cultures comparable to the control (Figure 10). In contrast, during the second stage of development characterized by the formation of neurospheres (day 4 to 14), we observed reduced neuroepithelial outgrowth in cultures treated by IWR1e, and increased cell death in both IWR1e-treated and SB431542/LDN193189 double-treated cells. These both resulted in cultures with very few retinal organoids, with a significantly reduced size.

### 5.3. One Pathway, One Agonist/Antagonist?

The analysis and comparison of different protocols showed that there are most likely multiple supplements that affected the same pathway. Are all of these different factors needed, or are some redundant? This, again, depends on the model that is being used. As we have shown, the inhibition of the Wnt pathway at an early stage in development by either DKK1 or IWR1e is commonly used to increase retinal organoid yield (Table 1). Both supplements are usually added within the first two weeks of development but inhibit Wnt signaling through different substrates of the Wnt signaling pathway. DKK1 affects the upstream binding of *Frizzled* to LRP5/6, preventing the formation of the *Frizzled*–LRP5/6 complex on the cell surface; IWR1e inhibition occurs downstream by stabilizing Axin, part of the destruction complex within the cell (Figure 5). Interestingly, mutations in *Drosophila Frizzled* cause defects in the polarity of the fly eye [266]. In murine models, *Frizzled* knockouts cause increased cell death, incomplete closure of the ventral fissure, and late-onset progressive retinal degeneration [267]. Therefore, when exploring the effect of the upstream *Frizzled* mutations in retinal organoid development, the possible upstream DKK1-mediated effect should be taken into account.

In addition to the aforementioned multiple Wnt inhibitors, we also observed that multiple activators of the Wnt pathway (Figure 5) have been used in retinal organoid protocols. For example, Wnt3a and CHIR99021 (Table 1) both activate Wnt signaling. However, similarly to DKK1 and IWR1e, they effect different parts of the pathway. Wnt3a acts upstream, and is added as a recombinant protein, acting as a ligand that binds to *Frizzled* and activates Wnt signaling. In contrast, CHIR99021 acts downstream, and is a GSK-3 $\beta$  inhibitor that activates Wnt signaling from inside the cell.

A number of other supplements affect one single pathway in slightly different ways. For example, in the BMP pathway (Figure 3) the antagonist noggin acts slightly more upstream than dorsomorphin: noggin binds to specific ligands in a competitive manner, preventing them from binding to cell surface receptors. Dorsomorphin, on the other hand, inhibits the receptors themselves. The action can be very specific and subtle. For example, dorsomorphin inhibits ALK-2, -3, and -6 receptors, whereas its derivative, LDN193189, only inhibits ALK-2 and -3 receptors. However, to complicate matters, LDN193189 is significantly more potent than dorsomorphin, allowing researchers to gain a similar affect with smaller concentrations of LDN193189 than dorsomorphin. A final example of signaling complexity is the IGF1 treatment: IGF1 affects the MAP kinase and PI3 kinase pathways, which are a part of the non-canonical branch of the TGF- $\beta$ /BMP signaling pathway (Figure 3). However, IGF1 does not act through the traditional TGF- $\beta$ /BMP receptors, as it binds to the insulin-like growth factor 1 receptor (IGF1R), allowing for an alternative way of regulating the TGF- $\beta$ /BMP signaling pathway.

### 5.4. Does the Synergistic Addition of Multiple Factors Result in an Additive Effect, or Is It Not Necessary?

We noticed in the literature that a subset of factors were commonly added together to target a single pathway simultaneously, or influence multiple pathways. For example, dual SMAD inhibition by SB431542 and LDN193189 is used to regulate both the branches of the TGF- $\beta$ /BMP signaling pathway, and we found that they were added exclusively together in

retinal organoid protocols [107,108] (Table 1). The suppression of TGF- $\beta$  and BMP signaling has also been achieved by SB431542 and dorsomorphin treatment and is used in vitro and in vivo to direct cells into the neural and retinal fates [105,268,269]. Yet, other factors such as CHIR99021 and SU5402, affecting the Wnt and FGF pathways, respectively, were either used together or individually in different differentiation methods. To investigate the potential effect of the dual inhibition of these factors, we experimentally tested CHIR99021 and SU5402 additions individually, as well as together (Figure 9). We found that CHIR99021 treatment positively influenced retinal organoid development in our protocol, whereas SU5402 treatment did not (Table 2, Figure S1). In the dual treatment, the positive effects of CHIR99021 were less pronounced, with fewer retinal organoids developing and a decrease in the expression of the optic cup marker *VSX2* compared to the individual CHIR99021 treatment. This suggests that in our protocol, SU5402 does not increase the development of retinal cell fate and obstructs the effect of CHIR99021 treatment.

It is important to note that in the overwhelming majority of protocols, more than one (ant-) agonist is used. The number of combinations of different supplements is very large and as such, not every condition can be tested. We broke these conditions down into their separate factors and tested a range of the most commonly used methods, but this does not take into account the synergistic effect that multiple treatments could have. For example, we found that Wnt inhibition during early development had an extremely negative effect on retinal gene expression and organoid yield. However, in protocols that use IWR1e, additional treatment with SAG immediately follows this, which activates hedgehog signaling [113,191,240], something that did not happen during our “individual” conditions. Furthermore, we observed that SU5402 has no significant effect on the development of retinal development in our protocol. However, in other protocols, SU5402 treatment is sometimes preceded by the addition of BMP4 at an earlier time point [48,129,188]. This could explain the differences we see using these additions in our and other organoid development protocols.

### 5.5. Research Implications and Future Perspectives

Here, we presented a review, that is, to our knowledge, the first systematic overview on methods used to generate retinal organoids, focusing on the external treatments used to influence the activity of specific pathways that lead to improved retinal organoid development. We aimed to provide an insight into how researchers are continuously improving their methods to best mimic in vivo development through the regulation of these vital signaling pathways. Although we are still lacking major knowledge in the field of retinal development, constantly evolving methods and techniques such as single-cell RNA-seq are allowing us to map the molecular route that cells take more clearly than ever before. Recent publications presenting single-cell RNA-seq analysis of retinal organoids and human retinas allow us to visualize retinal development in great detail [152]. This, in turn, allows us to recreate the in vivo environment more and more precisely. While we show here an in-depth analysis of treatments used in organoid development, we only provide the most important snapshot of the experimental conditions researchers frequently use. Many combinations are used in conjunction with one another, and these should be addressed in the future to reduce variability between protocols and increase comparability. This review presents a solid base, showing the many additions that are used in retinal organoids protocols, what pathway these work through and how that pathway affects retinal development, that can be built upon in future studies.

## 6. Materials and Methods

### 6.1. Protocol Search

We searched the literature in a comprehensive manner to include all protocols used to generate retinal organoids, which was undertaken using the NCBI publication database PubMed. Searches up to and including 8 May 2021 for the terms “Retinal Organoid” and “Retinal” AND “Organoid” identified 449 and 103 results, respectively. We removed

duplicate literature entries, and we screened and excluded manuscripts based on the following predefined criteria: (1) that the authors should generate their own retinal organoids, and (2) that these organoids should be made from human stem cell tissue (hESC or hiPSC). Further, the papers should be (3) readily available in original articles and (4) published in English. For example, this meant that papers generating organoids from primary retinal tissue, or papers analyzing publicly available organoid transcriptomes, were discarded. No additional criteria were used in order to include as many methods as possible. In order to check whether we did not miss any articles, after the initial screen, we inspected referenced papers from the selected publication set, and possible relevant remaining articles were included in the final analysis. In total, we identified 127 manuscripts, using 131 methods.

### 6.2. Organoid Generation

Organoids were generated as previously described [149], with one minor change. Briefly, H1 ESCs (WiCell, Madison, WI, USA) were dissociated into smaller clumps (around 100  $\mu\text{m}$  in diameter) using 0.5 mM EDTA in PBS, embedded in Matrigel (Corning, Corning, NY, USA) and plated with 3ml of an mTeSR1 and neural induction medium (NIM) mixture (3:1 ratio). NIM consisted of DMEM/F12 (-L-Glutamine) (1:1), N2 supplement, non-essential amino acids, heparin (2  $\mu\text{g}/\text{mL}$ ), PenStrep and GlutaMAX. The day of embedment was annotated as day 0, with the medium being changed on day 1, (1:1 ratio), day 2 (1:3 ratio) and day 3 (full NIM). After four days of differentiation, large organized embryoid bodies were formed, which were taken out of the Matrigel with cell recovery solution (Corning, Corning, NY, USA). The whole EBs were then plated on 6-well plates coated with hESC-qualified Matrigel (Corning, Corning, NY, USA), and were incubated for a further 10 days, with NIM media changes every other day. On day 11, the neural centers were carefully dislodged and transferred to a 60 mm dish containing retinal differentiation medium (RDM). RDM consisted of DMEM/F12 (-L-Glutamine) (3:1), B27 supplement, non-essential amino acids, PenStrep and GlutaMAX. Retinal organoids were kept in culture up until day 34, changing RDM medium every other day. For experiments containing supplements ( $n = 1$ ), they were added with every medium change unless stated otherwise as follows: Rock Inhibitor (10  $\mu\text{M}$ —SelleckChem, Houston, TX, USA) from day 0 to 1, IGF1 (5 ng/mL—ThermoFisher, Waltham, MA, USA) from day 0 onwards, IWR1e (3  $\mu\text{M}$ —Merck Millipore, Burlington, MA, USA) from day 0 to 12, SB431542 (10  $\mu\text{M}$ —Sigma, St. Louis, MO, USA) + LDN193189 (100 nM—SelleckChem, Houston, TX, USA) from day 0 to 7, CHIR99021 (3  $\mu\text{M}$ —Merck Millipore, Burlington, MA, USA) from day 18 to 24, SU5402 (5  $\mu\text{M}$ —StemCell Technologies, Vancouver, BC, Canada) from day 18 to 24, CHIR99021 + SU5402 double treatment from day 18 to 24, and DAPT (10 mM—Sigma, St. Louis, MO, USA), from day 28 onwards. Supplements were reconstituted according to the manufacturer's instructions. Carriers were tested previously for adverse effects, of which none were found.

### 6.3. RT-PCR and sqPCR

To generate a snapshot overview of gene expression between the different conditions used, the presence and gene expression of markers of retina specific cell types in the whole organoids was measured. Total RNA was extracted from 5 to 6 organoids per sample using the Qiagen RNeasy Mini kit with a DNase step according to the manufacturer's instructions. cDNA was generated using Superscript III (Invitrogen, Waltham, MA, USA), and sq-PCR was performed with HOT FIREpol DNA Polymerase (Solis Biodyne, Tartu, Estonia). Input RNA of 50 ng was used for all samples other than IWR1e day 24, where less had to be used due to poor sample yield. Gene expression was compared to the reference gene *EEF1A*. sq-PCR primer sequences can be found in Supplementary Table S1.

### 6.4. RNA-Seq Analysis

To compare relative expression of key marker genes of retinal development in our studies with other (published) datasets, we acquired published RNA-seq datasets from

GEO (<https://www.ncbi.nlm.nih.gov/geo>). In-depth descriptions of different RNA-seq methods can be found in each publication [8,149,191,197].

**Supplementary Materials:** The following are available online at <https://www.mdpi.com/article/10.3390/ijms22137081/s1>. Table S1. A list of primer sets used for RT-PCR analysis. Figure S1. Brightfield images of all conditions throughout development. Figure S2. Venn diagrams showing the specificity and exclusivity of certain methods and additions.

**Author Contributions:** Conceptualization, P.E.W.; methodology, P.E.W.; data curation, P.E.W., A.L.M.A.t.A.; writing—original draft preparation, P.E.W.; writing—review and editing, P.E.W., A.H.B., C.J.F.B., P.M.J.Q., A.L.M.A.t.A., A.A.B.; visualization, P.E.W.; funding acquisition, P.E.W., P.M.J.Q., A.A.B. All authors have read and agreed to the published version of the manuscript.

**Funding:** This research was carried out under the Marie Skłodowska-Curie Horizon 2020 Innovative Training Networks program, Project ID 675033 and by Uitzicht grant number 2020-19 (ANVVB, LSBS, Oogfonds, Stichting Beheer Het Schild). PMJQ is the current recipient of a Curing Retinal Blindness Foundation (CRBF) grant and a Knights Templar Eye Foundation (KTEF) Career Starter grant.

**Institutional Review Board Statement:** The study was conducted according to the guidelines of the Declaration of Helsinki, and approved by the Ethics Committee of Amsterdam UMC (protocol code NL45478, approved 27 September 2017).

**Data Availability Statement:** All data generated or analyzed during this study are included in this published article (and its Supplementary Materials files).

**Acknowledgments:** P.E.W. would like to thank Reinier Bakker, Jacoline ten Brink, Mark Buijs and Isa Van der Veen for their support and advice, and all other members of the Bergen group. P.M.J.Q. would like to thank his team members at JCVC.

**Conflicts of Interest:** The authors declare no conflict of interest.

## References

1. Wu, Y.; Peng, S.; Finnell, R.H.; Zheng, Y. Organoids as a new model system to study neural tube defects. *FASEB J.* **2021**, *35*, e21545. [[CrossRef](#)] [[PubMed](#)]
2. Quinn, P.M.; Wijnholds, J. Retinogenesis of the human fetal retina: An apical polarity perspective. *Genes* **2019**, *10*, 987. [[CrossRef](#)] [[PubMed](#)]
3. O'Hara-Wright, M.; Gonzalez-Cordero, A. Retinal organoids: A window into human retinal development. *Development* **2020**, *147*, dev189746. [[CrossRef](#)] [[PubMed](#)]
4. Lachke, S.; Maas, R.L. Building the developmental oculome: Systems biology in vertebrate eye development and disease. *Wiley Interdiscip. Rev. Syst. Biol. Med.* **2010**, *2*, 305–323. [[CrossRef](#)]
5. Bryan, C.D.; Casey, M.A.; Pfeiffer, R.L.; Jones, B.W.; Kwan, K.M. Optic cup morphogenesis requires neural crest-mediated basement membrane assembly. *Development* **2020**, *147*, dev181420. [[CrossRef](#)] [[PubMed](#)]
6. Gage, P.J.; Rhoades, W.; Prucka, S.K.; Hjalt, T. Fate maps of neural crest and mesoderm in the mammalian eye. *Investig. Ophthalmol. Vis. Sci.* **2005**, *46*, 4200–4208. [[CrossRef](#)] [[PubMed](#)]
7. Aavani, T.; Tachibana, N.; Wallace, V.; Biernaskie, J.; Schuurmans, C. Temporal profiling of photoreceptor lineage gene expression during murine retinal development. *Gene Expr. Patterns* **2017**, *23–24*, 32–44. [[CrossRef](#)] [[PubMed](#)]
8. Hoshino, A.; Ratnapriya, R.; Brooks, M.J.; Chaitankar, V.; Wilken, M.S.; Zhang, C.; Starostik, M.R.; Gieser, L.; La Torre, A.; Nishio, M.; et al. Molecular anatomy of the developing human retina. *Dev. Cell* **2017**, *43*, 763–779.e4. [[CrossRef](#)]
9. Centanin, L.; Wittbrodt, J. Retinal neurogenesis. *Development* **2014**, *141*, 241–244. [[CrossRef](#)]
10. Mustafi, D.; Engel, A.H.; Palczewski, K. Structure of cone photoreceptors. *Prog. Retin. Eye Res.* **2009**, *28*, 289–302. [[CrossRef](#)]
11. Stenkamp, D.L. Development of the vertebrate eye and retina. *Prog. Mol. Biol. Transl. Sci.* **2015**, *134*, 397–414. [[CrossRef](#)]
12. Machold, R.; Fishell, G. Hedgehog patterns midbrain ARChitecture. *Trends Neurosci.* **2002**, *25*, 10–11. [[CrossRef](#)]
13. Roelink, H.; Augsburger, A.; Heemskerk, J.; Korzh, V.; Norlin, S.; I Altaba, A.R.; Tanabe, Y.; Placzek, M.; Edlund, T.; Jessell, T.; et al. Floor plate and motor neuron induction by vhh-1, a vertebrate homolog of hedgehog expressed by the notochord. *Cell* **1994**, *76*, 761–775. [[CrossRef](#)]
14. Ingham, P.W. Hedgehog signaling in animal development: Paradigms and principles. *Genes Dev.* **2001**, *15*, 3059–3087. [[CrossRef](#)]
15. Choy, S.W.; Cheng, S.H. Hedgehog signaling. *Vitam. Horm.* **2012**, *88*, 1–23. [[CrossRef](#)]
16. E Gallardo, V.; Bovolenta, P. Positive and negative regulation of Shh signalling in vertebrate retinal development. *F1000Research* **2018**, *7*, 1934. [[CrossRef](#)]
17. Cavodeassi, F.; Creuzet, S.; Etchevers, H.C. The hedgehog pathway and ocular developmental anomalies. *Qual. Life Res.* **2019**, *138*, 917–936. [[CrossRef](#)]

18. Rahnama, F.; Shimokawa, T.; Lauth, M.; Finta, C.; Kogerman, P.; Teglund, S.; Toftgård, R.; Zaphiropoulos, P.G. Inhibition of GLI1 gene activation by Patched1. *Biochem. J.* **2006**, *394*, 19–26. [[CrossRef](#)]
19. Chiang, C.; Litingtung, Y.; Lee, E.; Young, K.E.; Corden, J.L.; Westphal, H.; Beachy, P.A. Cyclopia and defective axial patterning in mice lacking Sonic hedgehog gene function. *Nat. Cell Biol.* **1996**, *383*, 407–413. [[CrossRef](#)]
20. Neumann, C.J. Patterning of the Zebrafish retina by a wave of Sonic hedgehog activity. *Science* **2000**, *289*, 2137–2139. [[CrossRef](#)]
21. Russell, C. The roles of hedgehogs and fibroblast growth factors in eye development and retinal cell rescue. *Vis. Res.* **2003**, *43*, 899–912. [[CrossRef](#)]
22. Zhao, L.; Zevallos, S.E.; Rizzoti, K.; Jeong, Y.; Lovell-Badge, R.; Epstein, D.J. Disruption of SoxB1-dependent Sonic hedgehog expression in the hypothalamus causes septo-optic dysplasia. *Dev. Cell* **2012**, *22*, 585–596. [[CrossRef](#)] [[PubMed](#)]
23. Trousse, F.; Martí, E.; Gruss, P.; Torres, M.; Bovolenta, P. Control of retinal ganglion cell axon growth: A new role for Sonic hedgehog. *Development* **2001**, *128*, 3927–3936. [[CrossRef](#)] [[PubMed](#)]
24. Dakubo, G.D.; Mazerolle, C.; Furimsky, M.; Yu, C.; St-Jacques, B.; McMahon, A.P.; Wallace, V.A. Indian hedgehog signaling from endothelial cells is required for sclera and retinal pigment epithelium development in the mouse eye. *Dev. Biol.* **2008**, *320*, 242–255. [[CrossRef](#)]
25. Stenkamp, D.L.; Frey, R.A.; Prabhudesai, S.N.; Raymond, P. Function for hedgehog genes in Zebrafish retinal development. *Dev. Biol.* **2000**, *220*, 238–252. [[CrossRef](#)]
26. Kerr, C.L.; Huang, J.; Williams, T.; West-Mays, J.A. Activation of the hedgehog signaling pathway in the developing lens stimulates EctopicFoxE3 expression and disruption in fiber cell differentiation. *Investig. Ophthalmol. Vis. Sci.* **2012**, *53*, 3316–3330. [[CrossRef](#)]
27. Hata, A.; Chen, Y.-G. TGF- $\beta$  signaling from receptors to smads. *Cold Spring Harb. Perspect. Biol.* **2016**, *8*, a022061. [[CrossRef](#)]
28. Braunger, B.M.; Pielmeier, S.; Demmer, C.; Landstorfer, V.; Kawall, D.; Abramov, N.; Leibinger, M.; Kleiter, I.; Fischer, D.; Jäggle, H.; et al. TGF- signaling protects retinal neurons from programmed cell death during the development of the mammalian eye. *J. Neurosci.* **2013**, *33*, 14246–14258. [[CrossRef](#)]
29. Nickel, J.; Mueller, T.D. Specification of BMP signaling. *Cells* **2019**, *8*, 1579. [[CrossRef](#)]
30. Murali, D.; Kawaguchi-Niida, M.; Deng, C.-X.; Furuta, Y. Smad4 is required predominantly in the developmental processes dependent on the BMP branch of the TGF- $\beta$  signaling system in the embryonic mouse retina. *Investig. Ophthalmol. Vis. Sci.* **2011**, *52*, 2930–2937. [[CrossRef](#)]
31. Heldin, C.-H.; Moustakas, A. Signaling receptors for TGF- $\beta$  family members. *Cold Spring Harb. Perspect. Biol.* **2016**, *8*, a022053. [[CrossRef](#)]
32. Byfield, S.D.; Major, C.; Laping, N.J.; Roberts, A.B. SB-505124 is a selective inhibitor of transforming growth factor- $\beta$  Type I receptors ALK4, ALK5, and ALK7. *Mol. Pharmacol.* **2004**, *65*, 744–752. [[CrossRef](#)]
33. Wharton, K.; Derynck, R. TGF family signaling: Novel insights in development and disease. *Development* **2009**, *136*, 3691–3697. [[CrossRef](#)]
34. Zhang, Y.E. Non-Smad signaling pathways of the TGF- $\beta$  family. *Cold Spring Harb. Perspect. Biol.* **2016**, *9*, a022129. [[CrossRef](#)]
35. Nishina, S.; Kohsaka, S.; Yamaguchi, Y.; Handa, H.; Kawakami, A.; Fujisawa, H.; Azuma, N. PAX6 expression in the developing human eye. *Br. J. Ophthalmol.* **1999**, *83*, 723–727. [[CrossRef](#)]
36. Castellano, E.; Downward, J. RAS interaction with PI3K: More than just another effector pathway. *Genes Cancer* **2011**, *2*, 261–274. [[CrossRef](#)]
37. Duda, P.; Akula, S.M.; Abrams, S.L.; Steelman, L.S.; Martelli, A.M.; Cocco, L.; Ratti, S.; Candido, S.; Libra, M.; Montalto, G.; et al. Targeting GSK3 and associated signaling pathways involved in cancer. *Cells* **2020**, *9*, 1110. [[CrossRef](#)]
38. Dünker, N.; Schuster, N.; Kriegelstein, K. TGF-beta modulates programmed cell death in the retina of the developing chick embryo. *Development* **2001**, *128*, 1933–1942. [[CrossRef](#)]
39. Chavarría, T.; Valenciano, A.I.; Mayordomo, R.; Egea, J.; Comella, J.X.; Hallböök, F.; De Pablo, F.; De La Rosa, E.J. Differential, age-dependent MEK-ERK and PI3K-Akt activation by insulin acting as a survival factor during embryonic retinal development. *Dev. Neurobiol.* **2007**, *67*, 1777–1788. [[CrossRef](#)]
40. Kim, J.; Wu, H.-H.; Lander, A.D.; Lyons, K.M.; Matzuk, M.M.; Calof, A.L. GDF11 Controls the timing of progenitor cell competence in developing retina. *Science* **2005**, *308*, 1927–1930. [[CrossRef](#)]
41. Chang, K.-C.; Sun, C.; Cameron, E.G.; Madaan, A.; Wu, S.; Xia, X.; Zhang, X.; Tenerelli, K.; Nahmou, M.; Knasel, C.M.; et al. Opposing effects of growth and differentiation factors in cell-fate specification. *Curr. Biol.* **2019**, *29*, 1963–1975.e5. [[CrossRef](#)]
42. Schille, C.; Schambony, A. Signaling pathways and tissue interactions in neural plate border formation. *Neurogenesis* **2017**, *4*, e1292783. [[CrossRef](#)]
43. Chesnutt, C.; Burrus, L.W.; Brown, A.M.; Niswander, L. Coordinate regulation of neural tube patterning and proliferation by TGF $\beta$  and WNT activity. *Dev. Biol.* **2004**, *274*, 334–347. [[CrossRef](#)]
44. Chambers, S.M.; Fasano, C.A.; Papapetrou, E.P.; Tomishima, M.; Sadelain, M.; Studer, L. Highly efficient neural conversion of human ES and iPS cells by dual inhibition of SMAD signaling. *Nat. Biotechnol.* **2009**, *27*, 275–280. [[CrossRef](#)]
45. Ishikawa, M.; Aoyama, T.; Shibata, S.; Sone, T.; Miyoshi, H.; Watanabe, H.; Nakamura, M.; Morota, S.; Uchino, H.; Yoo, A.S.; et al. miRNA-Based rapid differentiation of purified neurons from hPSCs advances towards quick screening for neuronal disease phenotypes In Vitro. *Cells* **2020**, *9*, 532. [[CrossRef](#)] [[PubMed](#)]

46. Chavali, V.R.M.; Haider, N.; Rath, S.; Vratasha, V.; Alapati, T.; He, J.; Gill, K.; Nikonov, R.; Duong, T.T.; McDougald, D.S.; et al. Dual SMAD inhibition and Wnt inhibition enable efficient and reproducible differentiations of induced pluripotent stem cells into retinal ganglion cells. *Sci. Rep.* **2020**, *10*, 11828. [[CrossRef](#)] [[PubMed](#)]
47. Du, Y.; Xiao, Q.; Yip, H.K. Regulation of retinal progenitor cell differentiation by bone morphogenetic protein 4 is mediated by the Smad/Id cascade. *Investig. Ophthalmol. Vis. Sci.* **2010**, *51*, 3764–3773. [[CrossRef](#)] [[PubMed](#)]
48. Chichagova, V.; Hilgen, G.; Ghareeb, A.; Georgiou, M.; Carter, M.; Sernagor, E.; Lako, M.; Armstrong, L. Human iPSC differentiation to retinal organoids in response to IGF1 and BMP4 activation is line- and method-dependent. *Stem Cells* **2019**, *38*, 195–201. [[CrossRef](#)] [[PubMed](#)]
49. Capowski, E.E.; Samimi, K.; Mayerl, S.J.; Phillips, M.J.; Pinilla, I.; Howden, S.E.; Saha, J.; Jansen, A.D.; Edwards, K.L.; Jager, L.D.; et al. Reproducibility and staging of 3D human retinal organoids across multiple pluripotent stem cell lines. *Development* **2019**, *146*, dev171686. [[CrossRef](#)]
50. Quillien, A.; Blanco-Sanchez, B.; Halluin, C.; Moore, J.C.; Lawson, N.; Blader, P.; Cau, E. BMP signaling orchestrates photoreceptor specification in the zebrafish pineal gland in collaboration with Notch. *Development* **2011**, *138*, 2293–2302. [[CrossRef](#)]
51. Ueki, Y.; Wilken, M.S.; Cox, K.E.; Chipman, L.; Bermingham-McDonogh, O.; Reh, T.A. A transient wave of BMP signaling in the retina is necessary for Müller glial differentiation. *Development* **2015**, *142*, 533–543. [[CrossRef](#)]
52. Luo, G.; Hofmann, C.; Bronckers, A.; Sohocki, M.; Bradley, A.; Karsenty, G. BMP-7 is an inducer of nephrogenesis, and is also required for eye development and skeletal patterning. *Genes Dev.* **1995**, *9*, 2808–2820. [[CrossRef](#)]
53. Ochi, H.; Ogino, H.; Kageyama, Y.; Yasuda, K. The stability of the lens-specific Maf protein is regulated by Fibroblast Growth Factor (FGF)/ERK signaling in lens fiber differentiation. *J. Biol. Chem.* **2003**, *278*, 537–544. [[CrossRef](#)]
54. Pachenari, N.; Kiani, S.; Javan, M. Inhibition of glycogen synthase kinase 3 increased subventricular zone stem cells proliferation. *Biomed. Pharmacother.* **2017**, *93*, 1074–1082. [[CrossRef](#)]
55. Kisseleff, E.; Vigouroux, R.J.; Hottin, C.; Lourdel, S.; Shah, P.; Chédotal, A.; Perron, M.; Swaroop, A.; Roger, J.E. Glycogen Synthase Kinase 3 regulates the genesis of the rare displaced ganglion cell retinal subtype. *bioRxiv* **2021**. [[CrossRef](#)]
56. Huang, J.; Guo, X.; Li, W.; Zhang, H. Activation of Wnt/ $\beta$ -catenin signalling via GSK3 inhibitors direct differentiation of human adipose stem cells into functional hepatocytes. *Sci. Rep.* **2017**, *7*, 40716. [[CrossRef](#)]
57. Aikin, R.A.; Ayers, K.L.; Théron, P.P. The role of kinases in the Hedgehog signalling pathway. *EMBO Rep.* **2008**, *9*, 330–336. [[CrossRef](#)]
58. Kaidanovich-Beilin, O.; Woodgett, J.R. GSK-3: Functional insights from cell biology and animal models. *Front. Mol. Neurosci.* **2011**, *4*, 40. [[CrossRef](#)]
59. Ekim, W.-Y.; Snider, W.D. Functions of GSK-3 signaling in development of the nervous system. *Front. Mol. Neurosci.* **2011**, *4*, 44. [[CrossRef](#)]
60. Marchena, M.; Villarejo-Zori, B.; Zaldivar-Diez, J.; Palomo, V.; Gil, C.; Sánchez, C.H.; Martínez, A.; De La Rosa, E.J. Small molecules targeting glycogen synthase kinase 3 as potential drug candidates for the treatment of retinitis pigmentosa. *J. Enzym. Inhib. Med. Chem.* **2017**, *32*, 522–526. [[CrossRef](#)]
61. Moon, R.T. The promise and perils of Wnt signaling through beta-Catenin. *Science* **2002**, *296*, 1644–1646. [[CrossRef](#)]
62. Clark, C.E.; Nourse, C.C.; Cooper, H.M. The tangled web of non-canonical Wnt signalling in neural migration. *Neurosignals* **2012**, *20*, 202–220. [[CrossRef](#)]
63. Cerpa, W.; Gambrell, A.; Inestrosa, N.C.; Barria, A. Regulation of NMDA-receptor synaptic transmission by Wnt signaling. *J. Neurosci.* **2011**, *31*, 9466–9471. [[CrossRef](#)]
64. Ciani, L.; Salinas, P.C. WNTs in the vertebrate nervous system: From patterning to neuronal connectivity. *Nat. Rev. Neurosci.* **2005**, *6*, 351–362. [[CrossRef](#)]
65. Carter, M.; Chen, X.; Slowinska, B.; Minnerath, S.; Glickstein, S.; Shi, L.; Campagne, F.; Weinstein, H.; Ross, M.E. Crooked tail (Cd) model of human folate-responsive neural tube defects is mutated in Wnt coreceptor lipoprotein receptor-related protein 6. *Proc. Natl. Acad. Sci. USA* **2005**, *102*, 12843–12848. [[CrossRef](#)]
66. Shi, D.-L.; Goisset, C.; Boucaut, J.-C. Expression of Xfz3, a Xenopus frizzled family member, is restricted to the early nervous system. *Mech. Dev.* **1998**, *70*, 35–47. [[CrossRef](#)]
67. Rasmussen, J.T.; Deardorff, M.A.; Tan, C.; Rao, M.S.; Klein, P.S.; Vetter, M.L. Regulation of eye development by frizzled signaling in Xenopus. *Proc. Natl. Acad. Sci. USA* **2001**, *98*, 3861–3866. [[CrossRef](#)] [[PubMed](#)]
68. Cavodeassi, F.; Carreira-Barbosa, F.; Young, R.M.; Concha, M.L.; Allende, M.L.; Houart, C.; Tada, M.; Wilson, S.W. Early stages of Zebrafish eye formation require the coordinated activity of Wnt11, Fz5, and the Wnt/ $\beta$ -Catenin pathway. *Neuron* **2005**, *47*, 43–56. [[CrossRef](#)]
69. Liu, W.; Lagutin, O.; Swindell, E.; Jamrich, M.; Oliver, G. Neuroretina specification in mouse embryos requires Six3-mediated suppression of Wnt8b in the anterior neural plate. *J. Clin. Investig.* **2010**, *120*, 3568–3577. [[CrossRef](#)]
70. Tao, Y.; Cao, J.; Li, M.; Hoffmann, B.; Xu, K.; Chen, J.; Lu, X.; Guo, F.; Li, X.; Phillips, M.J.; et al. PAX 6D instructs neural retinal specification from human embryonic stem cell-derived neuroectoderm. *EMBO Rep.* **2020**, *21*, e50000. [[CrossRef](#)] [[PubMed](#)]
71. Fragoso, M.A.; Yi, H.; Nakamura, R.E.I.; Hackam, A.S. The Wnt signaling pathway protects retinal ganglion Cell 5 (RGC-5) cells from elevated pressure. *Cell. Mol. Neurobiol.* **2010**, *31*, 163–173. [[CrossRef](#)]

72. Patel, A.K.; Surapaneni, K.; Yi, H.; Nakamura, R.E.I.; Karli, S.Z.; Syeda, S.; Lee, T.; Hackam, A.S. Activation of Wnt/ $\beta$ -catenin signaling in Muller glia protects photoreceptors in a mouse model of inherited retinal degeneration. *Neuropharmacology* **2015**, *91*, 1–12. [[CrossRef](#)]
73. Liu, B.; Hunter, D.J.; Rooker, S.; Chan, A.; Paulus, Y.; Leucht, P.; Nusse, Y.; Nomoto, H.; Helms, J.A. Wnt signaling promotes Müller cell proliferation and survival after injury. *Investig. Ophthalmol. Vis. Sci.* **2013**, *54*, 444–453. [[CrossRef](#)]
74. Aparicio, J.; Hopp, H.; Choi, A.; Comar, J.M.; Liao, V.; Harutyunyan, N.; Lee, T. Temporal expression of CD184(CXCR4) and CD171(LICAM) identifies distinct early developmental stages of human retinal ganglion cells in embryonic stem cell derived retina. *Exp. Eye Res.* **2017**, *154*, 177–189. [[CrossRef](#)]
75. Menendez, L.; Yatskievych, T.A.; Antin, P.; Dalton, S. Wnt signaling and a Smad pathway blockade direct the differentiation of human pluripotent stem cells to multipotent neural crest cells. *Proc. Natl. Acad. Sci. USA* **2011**, *108*, 19240–19245. [[CrossRef](#)]
76. Chambers, S.M.; Mica, Y.; Lee, G.; Studer, L.; Tomishima, M.J. Dual-SMAD inhibition/WNT activation-based methods to induce neural crest and derivatives from human pluripotent stem cells. *Methods Mol. Biol.* **2013**, *1307*, 329–343. [[CrossRef](#)]
77. Zhou, S.; Flamier, A.; Abdouh, M.; Tétreault, N.; Barabino, A.; Wadhwa, S.; Bernier, G. Differentiation of human embryonic stem cells into cone photoreceptors through simultaneous inhibition of BMP, TGF $\beta$  and Wnt signaling. *Development* **2015**, *142*, 3294–3306. [[CrossRef](#)]
78. Hägglund, A.-C.; Berghard, A.; Carlsson, L. Canonical Wnt/ $\beta$ -Catenin signalling is essential for optic cup formation. *PLoS ONE* **2013**, *8*, e81158. [[CrossRef](#)]
79. Fujimura, N. WNT/ $\beta$ -Catenin signaling in vertebrate eye development. *Front. Cell Dev. Biol.* **2016**, *4*, 138. [[CrossRef](#)]
80. Sugiyama, Y.; Lovicu, F.J.; McAvoy, J.W. Planar cell polarity in the mammalian eye lens. *Organogenesis* **2011**, *7*, 191–201. [[CrossRef](#)]
81. Aguirre, A.; Rubio, M.E.; Gallo, V. Notch and EGFR pathway interaction regulates neural stem cell number and self-renewal. *Nat. Cell Biol.* **2010**, *467*, 323–327. [[CrossRef](#)] [[PubMed](#)]
82. Grego-Bessa, J.; Luna-Zurita, L.; del Monte, G.; Bolós, V.; Melgar, P.; Arandilla, A.; Garratt, A.; Zang, H.; Mukoyama, Y.-S.; Chen, H.; et al. Notch signaling is essential for ventricular chamber development. *Dev. Cell* **2007**, *12*, 415–429. [[CrossRef](#)] [[PubMed](#)]
83. Murtaugh, L.C.; Stanger, B.Z.; Kwan, K.M.; Melton, D.A. Notch signaling controls multiple steps of pancreatic differentiation. *Proc. Natl. Acad. Sci. USA* **2003**, *100*, 14920–14925. [[CrossRef](#)]
84. Stupnikov, M.R.; Yang, Y.; Mori, M.; Lu, J.; Cardoso, W.V. Jagged and Delta-like ligands control distinct events during airway progenitor cell differentiation. *eLife* **2019**, *8*, e50487. [[CrossRef](#)]
85. Van Tetering, G.; van Diest, P.; Verlaan, I.; van der Wall, E.; Kopan, R.; Vooijs, M. Metalloprotease ADAM10 is required for notch1 site 2 cleavage. *J. Biol. Chem.* **2009**, *284*, 31018–31027. [[CrossRef](#)]
86. Mills, E.A.; Goldman, D. The regulation of notch signaling in retinal development and regeneration. *Curr. Pathobiol. Rep.* **2017**, *5*, 323–331. [[CrossRef](#)]
87. Chen, C.-Y.; Liao, W.; Lou, Y.-L.; Li, Q.; Hu, B.; Wang, Y.; Deng, Z.-F. Inhibition of Notch signaling facilitates the differentiation of human-induced pluripotent stem cells into neural stem cells. *Mol. Cell. Biochem.* **2014**, *395*, 291–298. [[CrossRef](#)]
88. Banda, E.; McKinsey, A.; Germain, N.; Carter, J.; Anderson, N.C.; Grabel, L. Cell polarity and neurogenesis in embryonic stem cell-derived neural rosettes. *Stem Cells Dev.* **2015**, *24*, 1022–1033. [[CrossRef](#)]
89. Toonen, J.A.; Ronchetti, A.; Sidjanin, D.J. A Disintegrin and metalloproteinase10 (ADAM10) regulates NOTCH signaling during early retinal development. *PLoS ONE* **2016**, *11*, e0156184. [[CrossRef](#)]
90. Jadhav, A.P.; Cho, S.-H.; Cepko, C.L. Notch activity permits retinal cells to progress through multiple progenitor states and acquire a stem cell property. *Proc. Natl. Acad. Sci. USA* **2006**, *103*, 18998–19003. [[CrossRef](#)]
91. Nelson, B.R.; Gumuscu, B.; Hartman, B.H.; Reh, T.A. Notch activity is downregulated just prior to retinal ganglion cell differentiation. *Dev. Neurosci.* **2006**, *28*, 128–141. [[CrossRef](#)]
92. Riesenberger, A.N.; Conley, K.W.; Le, T.T.; Brown, N.L. Separate and coincident expression of Hes1 and Hes5 in the developing mouse eye. *Dev. Dyn.* **2018**, *247*, 212–221. [[CrossRef](#)]
93. Silva, A.O.; Ercole, C.E.; McLoon, S.C. Regulation of ganglion cell production by notch signaling during retinal development. *J. Neurobiol.* **2003**, *54*, 511–524. [[CrossRef](#)]
94. Riazifar, H.; Jia, Y.; Chen, J.; Lynch, G.; Huang, T. Chemically induced specification of retinal ganglion cells from human embryonic and induced pluripotent stem cells. *Stem Cells Transl. Med.* **2014**, *3*, 424–432. [[CrossRef](#)]
95. Jadhav, A.P.; Mason, H.A.; Cepko, C.L. Notch 1 inhibits photoreceptor production in the developing mammalian retina. *Development* **2006**, *133*, 913–923. [[CrossRef](#)]
96. Mizeracka, K.; Trimarchi, J.; Stadler, M.B.; Cepko, C.L. Analysis of gene expression in wild-type and Notch1 mutant retinal cells by single cell profiling. *Dev. Dyn.* **2013**, *242*, 1147–1159. [[CrossRef](#)]
97. Mochizuki, Y.; Iida, A.; Lyons, E.; Kageyama, R.; Nakauchi, H.; Murakami, A.; Watanabe, S. Use of cell type-specific transcriptome to identify genes specifically involved in Müller glia differentiation during retinal development. *Dev. Neurobiol.* **2013**, *74*, 426–437. [[CrossRef](#)]
98. Teotia, P.; Chopra, D.A.; Dravid, S.M.; Van Hook, M.J.; Qiu, F.; Morrison, J.; Rizzino, A.; Ahmad, I. Generation of functional human retinal ganglion cells with target specificity from pluripotent stem cells by chemically defined recapitulation of developmental mechanism. *Stem Cells* **2017**, *35*, 572–585. [[CrossRef](#)]
99. Stanton, B.Z.; Peng, L.F. Small-molecule modulators of the Sonic Hedgehog signaling pathway. *Mol. Biosyst.* **2010**, *6*, 44–54. [[CrossRef](#)]



100. Gao, L.; Chen, X.; Zeng, Y.; Li, Q.; Zou, T.; Chen, S.; Wu, Q.; Fu, C.; Xu, H.; Yin, Z.Q. Intermittent high oxygen influences the formation of neural retinal tissue from human embryonic stem cells. *Sci. Rep.* **2016**, *6*, 29944. [[CrossRef](#)]
101. Völkner, M.; Zschätzsch, M.; Rostovskaya, M.; Overall, R.; Busskamp, V.; Anastassiadis, K.; Karl, M.O. Retinal organoids from pluripotent stem cells efficiently recapitulate retinogenesis. *Stem Cell Rep.* **2016**, *6*, 525–538. [[CrossRef](#)] [[PubMed](#)]
102. Worthington, K.S.; Wiley, L.A.; Kaalberg, E.E.; Collins, M.M.; Mullins, R.F.; Stone, E.M.; Tucker, B.A. Two-photon polymerization for production of human iPSC-derived retinal cell grafts. *Acta Biomater.* **2017**, *55*, 385–395. [[CrossRef](#)] [[PubMed](#)]
103. Ng, T.K.; Yung, J.S.Y.; Choy, K.W.; Cao, D.; Leung, C.K.S.; Cheung, H.S.; Pang, C.P. Transdifferentiation of periodontal ligament-derived stem cells into retinal ganglion-like cells and its microRNA signature. *Sci. Rep.* **2015**, *5*, 16429. [[CrossRef](#)] [[PubMed](#)]
104. Inman, G.; Nicolás, F.J.; Callahan, J.F.; Harling, J.D.; Gaster, L.M.; Reith, A.D.; Laping, N.J.; Hill, C. SB-431542 is a potent and specific inhibitor of transforming growth factor- $\beta$  superfamily Type I activin receptor-like Kinase (ALK) receptors ALK4, ALK5, and ALK7. *Mol. Pharmacol.* **2002**, *62*, 65–74. [[CrossRef](#)]
105. Madhu, V.; Dighe, A.S.; Cui, Q.; Deal, D.N. Dual inhibition of activin/Nodal/TGF- $\beta$  and BMP signaling pathways by SB431542 and dorsomorphin induces neuronal differentiation of human adipose derived stem cells. *Stem Cells Int.* **2016**, *2016*, 1035374. [[CrossRef](#)]
106. Qi, Y.; Zhang, X.-J.; Renier, N.; Wu, Z.; Atkin, T.; Sun, Z.; Ozair, M.Z.; Tchieu, J.; Zimmer, B.; Fattahi, F.; et al. Combined small-molecule inhibition accelerates the derivation of functional cortical neurons from human pluripotent stem cells. *Nat. Biotechnol.* **2017**, *35*, 154–163. [[CrossRef](#)]
107. Browne, A.W.; Arnesano, C.; Harutyunyan, N.; Khuu, T.; Martinez, J.C.; Pollack, H.A.; Koos, D.S.; Lee, T.C.; Fraser, S.E.; Moats, R.A.; et al. Structural and functional characterization of human stem-cell-derived retinal organoids by live imaging. *Investig. Ophthalmol. Vis. Sci.* **2017**, *58*, 3311–3318. [[CrossRef](#)]
108. Döpfer, H.; Menges, J.; Bozet, M.; Brenzel, A.; Lohmann, D.; Steenpass, L.; Kanber, D. Differentiation protocol for 3D retinal organoids, immunostaining and signal quantitation. *Curr. Protoc. Stem Cell Biol.* **2020**, *55*, e120. [[CrossRef](#)]
109. Zhu, J.; Reynolds, J.; Garcia, T.; Cifuentes, H.; Chew, S.; Zeng, X.; Lamba, D.A. Generation of transplantable retinal photoreceptors from a current good manufacturing practice-manufactured human induced pluripotent stem cell line. *Stem Cells Transl. Med.* **2017**, *7*, 210–219. [[CrossRef](#)]
110. Popovic, N.; Hooker, E.; Barabino, A.; Flamier, A.; Provost, F.; Buscarlet, M.; Bernier, G.; Larrivière, B. COCO/DAND5 inhibits developmental and pathological ocular angiogenesis. *EMBO Mol. Med.* **2021**, *13*, e12005. [[CrossRef](#)]
111. Bates, T.J.D.; Vonica, A.; Heasman, J.; Brivanlou, A.H.; Bell, E. Coco regulates dorsoventral specification of germ layers via inhibition of TGF $\beta$  signalling. *Development* **2013**, *140*, 4177–4181. [[CrossRef](#)]
112. Schweickert, A.; Vick, P.; Getwan, M.; Weber, T.; Schneider, I.; Eberhardt, M.; Beyer, T.; Pachur, A.; Blum, M. The nodal inhibitor coco is a critical target of leftward flow in *Xenopus*. *Curr. Biol.* **2010**, *20*, 738–743. [[CrossRef](#)]
113. Pan, D.; Xia, X.-X.; Zhou, H.; Jin, S.-Q.; Lu, Y.-Y.; Liu, H.; Gao, M.-L.; Jin, Z.-B. COCO enhances the efficiency of photoreceptor precursor differentiation in early human embryonic stem cell-derived retinal organoids. *Stem Cell Res. Ther.* **2020**, *11*, 366. [[CrossRef](#)]
114. Deglincerti, A.; Haremaki, T.; Warmflash, A.; Sorre, B.; Brivanlou, A.H. Coco is a dual-activity modulator of TGF- $\beta$  signaling. *Development* **2015**, *142*, 2678–2685. [[CrossRef](#)]
115. Blázquez-Medela, A.M.; Jumabay, M.; Boström, K.I. Beyond the bone: Bone morphogenetic protein signaling in adipose tissue. *Obes. Rev.* **2019**, *20*, 648–658. [[CrossRef](#)]
116. Merino, R.; Macias, D.; Gañan, Y.; Economides, A.; Wang, X.; Wu, Q.; Stahl, N.; Sampath, K.; Varona, P.; Hurler, J.M. Expression and function of Gdf-5 during digit skeletogenesis in the embryonic chick leg bud. *Dev. Biol.* **1999**, *206*, 33–45. [[CrossRef](#)]
117. Chang, C.; Hemmati-Brivanlou, A. *Xenopus* GDF6, a new antagonist of noggin and a partner of BMPs. *Development* **1999**, *126*, 3347–3357. [[CrossRef](#)]
118. Messina, A.; Lan, L.; Incitti, T.; Bozza, A.; Andreazzoli, M.; Vignali, R.; Cremisi, F.; Bozzi, Y.; Casarosa, S. Noggin-Mediated retinal induction reveals a novel interplay between bone morphogenetic protein inhibition, transforming growth factor  $\beta$ , and Sonic hedgehog signaling. *Stem Cells* **2015**, *33*, 2496–2508. [[CrossRef](#)]
119. Lamba, D.A.; McUsic, A.; Hirata, R.K.; Wang, P.-R.; Russell, D.; Reh, T.A. Generation, purification and transplantation of photoreceptors derived from human induced pluripotent stem cells. *PLoS ONE* **2010**, *5*, e8763. [[CrossRef](#)]
120. Tucker, B.A.; Mullins, R.F.; Streb, L.M.; Anfinson, K.; Eyestone, M.E.; Kaalberg, E.; Riker, M.J.; Drack, A.V.; Braun, T.A.; Stone, E.M. Patient-specific iPSC-derived photoreceptor precursor cells as a means to investigate retinitis pigmentosa. *eLife* **2013**, *2*, e00824. [[CrossRef](#)]
121. Kim, D.-S.; Lee, J.S.; Leem, J.W.; Huh, Y.J.; Kim, J.Y.; Kim, H.-S.; Park, I.-H.; Daley, G.Q.; Hwang, D.-Y.; Kim, N.-W. Robust enhancement of neural differentiation from human ES and iPS cells regardless of their innate difference in differentiation propensity. *Stem Cell Rep.* **2010**, *6*, 270–281. [[CrossRef](#)] [[PubMed](#)]
122. Morizane, A.; Doi, D.; Kikuchi, T.; Nishimura, K.; Takahashi, J. Small-molecule inhibitors of bone morphogenetic protein and activin/nodal signals promote highly efficient neural induction from human pluripotent stem cells. *J. Neurosci. Res.* **2011**, *89*, 117–126. [[CrossRef](#)] [[PubMed](#)]
123. Yu, P.B.; Hong, C.C.; Sachidanandan, C.; Babitt, J.L.; Deng, D.Y.; A Hoyng, S.; Lin, H.Y.; Bloch, K.D.; Peterson, R.T. Dorsomorphin inhibits BMP signals required for embryogenesis and iron metabolism. *Nat. Chem. Biol.* **2008**, *4*, 33–41. [[CrossRef](#)] [[PubMed](#)]

124. Boergemann, J.; Kopf, J.; Yu, P.; Knaus, P. Dorsomorphin and LDN-193189 inhibit BMP-mediated Smad, p38 and Akt signalling in C2C12 cells. *Int. J. Biochem. Cell Biol.* **2010**, *42*, 1802–1807. [[CrossRef](#)] [[PubMed](#)]
125. Vogt, J.; Traynor, R.; Sapkota, G.P. The specificities of small molecule inhibitors of the TGF $\beta$  and BMP pathways. *Cell. Signal.* **2011**, *23*, 1831–1842. [[CrossRef](#)]
126. Cuny, G.D.; Yu, P.B.; Laha, J.K.; Xing, X.; Liu, J.-F.; Lai, C.S.; Deng, D.Y.; Sachidanandan, C.; Bloch, K.D.; Peterson, R.T. Structure–activity relationship study of bone morphogenetic protein (BMP) signaling inhibitors. *Bioorganic Med. Chem. Lett.* **2008**, *18*, 4388–4392. [[CrossRef](#)]
127. Kuwahara, A.; Ozone, C.; Nakano, T.; Saito, K.; Eiraku, M.; Sasai, Y. Generation of a ciliary margin-like stem cell niche from self-organizing human retinal tissue. *Nat. Commun.* **2015**, *6*, 6286. [[CrossRef](#)]
128. Sluch, V.M.; Chamling, X.; Liu, M.M.; Berlinicke, C.A.; Cheng, J.; Mitchell, K.L.; Welsbie, D.S.; Zack, D.J. Enhanced stem cell differentiation and immunopurification of genome engineered human retinal ganglion cells. *Stem Cells Transl. Med.* **2017**, *6*, 1972–1986. [[CrossRef](#)]
129. Kobayashi, W.; Onishi, A.; Tu, H.-Y.; Takihara, Y.; Matsumura, M.; Tsujimoto, K.; Inatani, M.; Nakazawa, T.; Takahashi, M. Culture systems of dissociated mouse and human pluripotent stem cell–derived retinal ganglion cells purified by two-step immunopanning. *Investig. Ophthalmol. Vis. Sci.* **2018**, *59*, 776–787. [[CrossRef](#)]
130. Bronstein, R.; Capowski, E.E.; Mehrotra, S.; Jansen, A.D.; Navarro-Gomez, D.; Maher, M.; Place, E.; Sangermano, R.; Bujakowska, K.M.; Gamm, D.M.; et al. A combined RNA-seq and whole genome sequencing approach for identification of non-coding pathogenic variants in single families. *Hum. Mol. Genet.* **2020**, *29*, 967–979. [[CrossRef](#)]
131. Fligor, C.M.; Huang, K.-C.; Lavekar, S.S.; VanderWall, K.B.; Meyer, J.S. Differentiation of retinal organoids from human pluripotent stem cells. *Methods Cell Biol.* **2020**, *159*, 279–302. [[CrossRef](#)]
132. Chen, B.; Dodge, M.E.; Tang, W.; Lu, J.; Ma, Z.; Fan, C.-W.; Wei, S.; Hao, W.; Kilgore, J.; Williams, N.S.; et al. Small molecule–mediated disruption of Wnt-dependent signaling in tissue regeneration and cancer. *Nat. Chem. Biol.* **2009**, *5*, 100–107. [[CrossRef](#)]
133. Kegeles, E.; Perepelkina, T.; Baranov, P. Semi-Automated approach for retinal tissue differentiation. *Transl. Vis. Sci. Technol.* **2020**, *9*, 24. [[CrossRef](#)]
134. Sakata, T.; Chen, J.K. Chemical ‘Jekyll and Hyde’s: Small-molecule inhibitors of developmental signaling pathways. *Chem. Soc. Rev.* **2011**, *40*, 4318–4331. [[CrossRef](#)]
135. Meyer, J.S.; Howden, S.E.; Wallace, K.A.; Verhoeven, A.D.; Wright, L.S.; Capowski, E.E.; Pinilla, I.; Martin, J.M.; Tian, S.; Stewart, R.; et al. Optic vesicle-like structures derived from human pluripotent stem cells facilitate a customized approach to retinal disease treatment. *STEM CELLS* **2011**, *29*, 1206–1218. [[CrossRef](#)]
136. Semenov, M.V.; Tamai, K.; Brott, B.K.; Kühl, M.; Sokol, S.; He, X. Head inducer Dickkopf-1 is a ligand for Wnt coreceptor LRP6. *Curr. Biol.* **2001**, *11*, 951–961. [[CrossRef](#)]
137. Deng, F.; Chen, M.; Liu, Y.; Hu, H.; Xiong, Y.; Xu, C.; Liu, Y.; Li, K.; Zhuang, J.; Ge, J. Stage-specific differentiation of iPSCs toward retinal ganglion cell lineage. *Mol. Vis.* **2016**, *22*, 536–547.
138. Gill, K.P.; Hung, S.; Sharov, A.; Lo, C.Y.; Needham, K.; Lidgerwood, G.E.; Jackson, S.; Crombie, D.E.; Nayagam, B.; Cook, A.L.; et al. Enriched retinal ganglion cells derived from human embryonic stem cells. *Sci. Rep.* **2016**, *6*, 30552. [[CrossRef](#)]
139. Shao, J.; Zhou, P.-Y.; Peng, G.-H. Experimental study of the biological properties of human embryonic stem cell–derived retinal progenitor cells. *Sci. Rep.* **2017**, *7*, 42363. [[CrossRef](#)]
140. Leach, L.L.; Buchholz, D.E.; Nadar, V.P.; Lowenstein, S.E.; Clegg, D.O. Canonical/ $\beta$ -Catenin Wnt pathway activation improves retinal pigmented epithelium derivation from human embryonic stem cells. *Investig. Ophthalmol. Vis. Sci.* **2015**, *56*, 1002–1013. [[CrossRef](#)]
141. Nelson, B.R.; Hartman, B.H.; Georgi, S.A.; Lan, M.S.; Reh, T.A. Transient inactivation of Notch signaling synchronizes differentiation of neural progenitor cells. *Dev. Biol.* **2007**, *304*, 479–498. [[CrossRef](#)]
142. Kruczek, K.; Cordero, A.G.; Goh, D.; Naeem, A.; Jonikas, M.; Blackford, S.; Kloc, M.; Duran, Y.; Georgiadis, A.; Sampson, R.; et al. Differentiation and transplantation of embryonic stem cell-derived cone photoreceptors into a mouse model of end-stage retinal degeneration. *Stem Cell Rep.* **2017**, *8*, 1659–1674. [[CrossRef](#)]
143. Reichman, S.; Terray, A.; Slembrouck, A.; Nanteau, C.; Orioux, G.; Habeler, W.; Nandrot, E.F.; Sahel, J.; Monville, C.; Goureau, O. From confluent human iPS cells to self-forming neural retina and retinal pigmented epithelium. *Proc. Natl. Acad. Sci. USA* **2014**, *111*, 8518–8523. [[CrossRef](#)]
144. Meyer, J.; Shearer, R.L.; Capowski, E.E.; Wright, L.S.; Wallace, K.A.; McMillan, E.L.; Zhang, S.-C.; Gamm, D.M. Modeling early retinal development with human embryonic and induced pluripotent stem cells. *Proc. Natl. Acad. Sci. USA* **2009**, *106*, 16698–16703. [[CrossRef](#)] [[PubMed](#)]
145. Hallam, D.; Hilgen, G.; Dorgau, B.; Zhu, L.; Yu, M.; Bojic, S.; Hewitt, P.; Schmitt, M.; Uteng, M.; Kustermann, S.; et al. Human-Induced pluripotent stem cells generate light responsive retinal organoids with variable and nutrient-dependent efficiency. *Stem Cells* **2018**, *36*, 1535–1551. [[CrossRef](#)] [[PubMed](#)]
146. Georgiou, M.; Chichagova, V.; Hilgen, G.; Dorgau, B.; Sernagor, E.; Armstrong, L.; Lako, M. Room temperature shipment does not affect the biological activity of pluripotent stem cell-derived retinal organoids. *PLoS ONE* **2020**, *15*, e0233860. [[CrossRef](#)]
147. Lamba, D.A.; Karl, M.; Ware, C.B.; Reh, T.A. Efficient generation of retinal progenitor cells from human embryonic stem cells. *Proc. Natl. Acad. Sci. USA* **2006**, *103*, 12769–12774. [[CrossRef](#)]

148. Mellough, C.; Collin, J.; Khazim, M.; White, K.; Sernagor, E.; Steel, D.; Lako, M. IGF-1 signaling plays an important role in the formation of three-dimensional laminated neural retina and other ocular structures from human embryonic stem cells. *Stem Cells* **2015**, *33*, 2416–2430. [[CrossRef](#)]
149. Wagstaff, P.E.; Asbroek, A.L.M.A.T.; Brink, J.B.T.; Jansonius, N.M.; Bergen, A.A.B. An alternative approach to produce versatile retinal organoids with accelerated ganglion cell development. *Sci. Rep.* **2021**, *11*, 1101. [[CrossRef](#)]
150. Slembrouck-Brec, A.; Rodrigues, A.; Rabesandratana, O.; Gagliardi, G.; Nanteau, C.; Fouquet, S.; Thuret, G.; Reichman, S.; Orieux, G.; Goureau, O. Reprogramming of adult retinal Müller glial cells into human-induced pluripotent stem cells as an efficient source of retinal cells. *Stem Cells Int.* **2019**, *2019*, 7858796. [[CrossRef](#)] [[PubMed](#)]
151. Gamm, D.M.; Clark, E.; Capowski, E.E.; Singh, R. The role of FGF9 in the production of neural retina and RPE in a pluripotent stem cell model of early human retinal development. *Am. J. Ophthalmol.* **2019**, *206*, 113–131. [[CrossRef](#)]
152. Cameron Cowan, A.S.; Renner, M.; De Gennaro, M.; Roma, G.; Nigsch, F.; Roska Correspondence, B.; Cowan, C.S.; Gross-Scherf, B.; Goldblum, D.; Hou, Y.; et al. Cell types of the human retina and its organoids at single-cell resolution. *Cell* **2020**, *182*, 1623–1640.e34. [[CrossRef](#)]
153. Tso, A.; Ragi, S.D.; Costa, B.L.D.; Fehnel, A.; Li, Y.; Quinn, P.M.J. Molecular and therapeutic strategies for Retinitis Pigmentosa: Generation of Human iPSC-Derived Retinal Organoids for Assessment of AAV-Mediated Gene Delivery. In: Walker, J.M., ed. *Methods Mol. Biol.* **2021**, in press.
154. Nakano, T.; Ando, S.; Takata, N.; Kawada, M.; Muguruma, K.; Sekiguchi, K.; Saito, K.; Yonemura, S.; Eiraku, M.; Sasai, Y. Self-formation of optic cups and storable stratified neural retina from human ESCs. *Cell Stem Cell* **2012**, *10*, 771–785. [[CrossRef](#)]
155. Zhong, X.; Gutierrez, C.; Xue, T.; Hampton, C.; Vergara, M.N.; Cao, L.-H.; Peters, A.; Park, T.S.; Zambidis, E.T.; Meyer, J.; et al. Generation of three-dimensional retinal tissue with functional photoreceptors from human iPSCs. *Nat. Commun.* **2014**, *5*, 4047. [[CrossRef](#)]
156. Reichman, S.; Slembrouck, A.; Gagliardi, G.; Chaffiol, A.; Terray, A.; Nanteau, C.; Potey, A.; Belle, M.; Rabesandratana, O.; Duebel, J.; et al. Generation of storable retinal organoids and retinal pigmented epithelium from adherent human iPSCs in xeno-free and feeder-free conditions. *Stem Cells* **2017**, *35*, 1176–1188. [[CrossRef](#)]
157. Slembrouck-Brec, A.; Nanteau, C.; Sahel, J.-A.; Goureau, O.; Reichman, S. Defined xeno-free and feeder-free culture conditions for the generation of human iPSC-derived retinal cell models. *J. Vis. Exp.* **2018**, *139*, e57795. [[CrossRef](#)]
158. Rabesandratana, O.; Chaffiol, A.; Mialot, A.; Slembrouck-Brec, A.; Joffrois, C.; Nanteau, C.; Rodrigues, A.; Gagliardi, G.; Reichman, S.; Sahel, J.-A.; et al. Generation of a transplantable population of human iPSC-derived retinal ganglion cells. *Front. Cell Dev. Biol.* **2020**, *8*, 585675. [[CrossRef](#)]
159. Achberger, K.; Probst, C.; Haderspeck, J.; Bolz, S.; Rogal, J.; Chuchuy, J.; Nikolova, M.; Cora, V.; Antkowiak, L.; Haq, W.; et al. Merging organoid and organ-on-a-chip technology to generate complex multi-layer tissue models in a human retina-on-a-chip platform. *eLife* **2019**, *8*, e46188. [[CrossRef](#)]
160. Akhtar, T.; Xie, H.; Khan, M.I.; Zhao, H.; Bao, J.; Zhang, M.; Xue, T. Accelerated photoreceptor differentiation of hiPSC-derived retinal organoids by contact co-culture with retinal pigment epithelium. *Stem Cell Res.* **2019**, *39*, 101491. [[CrossRef](#)]
161. Arno, G.; Agrawal, S.A.; Eblimit, A.; Bellingham, J.; Xu, M.; Wang, F.; Chakarova, C.; Parfitt, D.A.; Lane, A.; Burgoyne, T.; et al. Mutations in REEP6 cause autosomal-recessive retinitis pigmentosa. *Am. J. Hum. Genet.* **2016**, *99*, 1305–1315. [[CrossRef](#)] [[PubMed](#)]
162. Chichagova, V.; Dorgau, B.; Felemban, M.; Georgiou, M.; Armstrong, L.; Lako, M. Differentiation of retinal organoids from human pluripotent stem cells. *Curr. Protoc. Stem Cell Biol.* **2019**, *50*, e95. [[CrossRef](#)] [[PubMed](#)]
163. Collin, J.; Queen, R.; Zerti, D.; Dorgau, B.; Hussain, R.; Coxhead, J.; Cockell, S.; Lako, M. Deconstructing retinal organoids: Single cell RNA-Seq reveals the cellular components of human pluripotent stem cell-derived retina. *Stem Cells* **2019**, *37*, 593–598. [[CrossRef](#)] [[PubMed](#)]
164. Collin, J.; Zerti, D.; Queen, R.; Santos-Ferreira, T.; Bauer, R.; Coxhead, J.; Hussain, R.; Steel, D.; Mellough, C.; Ader, M.; et al. CRX expression in pluripotent stem cell-derived photoreceptors marks a transplantable subpopulation of early cones. *Stem Cells* **2019**, *37*, 609–622. [[CrossRef](#)]
165. Cora, V.; Haderspeck, J.; Antkowiak, L.; Mattheus, U.; Neckel, P.H.; Mack, A.F.; Bolz, S.; Ueffing, M.; Pashkovskaia, N.; Achberger, K.; et al. A cleared view on retinal organoids. *Cells* **2019**, *8*, 391. [[CrossRef](#)]
166. Corral-Serrano, J.C.; Lamers, I.J.C.; Van Reeuwijk, J.; Duijkers, L.; Hoogendoorn, A.D.M.; Yildirim, A.; Argyrou, N.; Ruigrok, R.A.A.; Letteboer, S.J.F.; Butcher, R.; et al. PCARE and WASF3 regulate ciliary F-actin assembly that is required for the initiation of photoreceptor outer segment disk formation. *Proc. Natl. Acad. Sci. USA* **2020**, *117*, 9922–9931. [[CrossRef](#)]
167. Cuevas, E.; Holder, D.L.; AlShehri, A.H.; Tréguier, J.; Lakowski, J.; Sowden, J.C. NRL<sup>-/-</sup> gene edited human embryonic stem cells generate rod-deficient retinal organoids enriched in S-cone-like photoreceptors. *Stem Cells* **2021**, *39*, 414–428. [[CrossRef](#)]
168. De Bruijn, S.E.; Fiorentino, A.; Ottaviani, D.; Fanucchi, S.; Melo, U.S.; Corral-Serrano, J.C.; Mulders, T.; Georgiou, M.; Rivolta, C.; Pontikos, N.; et al. Structural variants create new topological-associated domains and ectopic retinal enhancer-gene contact in dominant retinitis pigmentosa. *Am. J. Hum. Genet.* **2020**, *107*, 802–814. [[CrossRef](#)]
169. Deng, W.-L.; Gao, M.-L.; Lei, X.-L.; Lv, J.-N.; Zhao, H.; He, K.-W.; Xia, X.-X.; Li, L.-Y.; Chen, Y.-C.; Li, Y.-P.; et al. Gene correction reverses ciliopathy and photoreceptor loss in iPSC-derived retinal organoids from retinitis pigmentosa patients. *Stem Cell Rep.* **2018**, *10*, 1267–1281. [[CrossRef](#)]
170. Deng, X.; Iwagawa, T.; Fukushima, M.; Watanabe, S. Characterization of human-induced pluripotent stem cells carrying homozygous RB1 gene deletion. *Genes Cells* **2020**, *25*, 510–517. [[CrossRef](#)]

171. Diakatou, M.; Dubois, G.; Erkilic, N.; Sanjurjo-Soriano, C.; Meunier, I.; Kalatzis, V. Allele-Specific knockout by CRISPR/Cas to treat autosomal dominant retinitis pigmentosa caused by the G56R mutation in NR2E3. *Int. J. Mol. Sci.* **2021**, *22*, 2607. [[CrossRef](#)]
172. Dorgau, B.; Felemban, M.; Hilgen, G.; Kiening, M.; Zerti, D.; Hunt, N.C.; Doherty, M.; Whitfield, P.; Hallam, D.; White, K.; et al. Decellularised extracellular matrix-derived peptides from neural retina and retinal pigment epithelium enhance the expression of synaptic markers and light responsiveness of human pluripotent stem cell derived retinal organoids. *Biomaterials* **2019**, *199*, 63–75. [[CrossRef](#)]
173. Dorgau, B.; Felemban, M.; Sharpe, A.; Bauer, R.; Hallam, D.; Steel, D.H.; Lindsay, S.; Mellough, C.; Lako, M. Laminin  $\gamma$ 3 plays an important role in retinal lamination, photoreceptor organisation and ganglion cell differentiation. *Cell Death Dis.* **2018**, *9*, 615. [[CrossRef](#)]
174. Dulla, K.; Aguila, M.; Lane, A.; Jovanovic, K.; Parfitt, D.A.; Schulken, I.; Chan, H.L.; Schmidt, I.; Beumer, W.; Vorthoren, L.; et al. Splice-Modulating oligonucleotide QR-110 restores CEP290 mRNA and function in human c.2991+1655A>G LCA10 models. *Mol. Ther. Nucleic Acids* **2018**, *12*, 730–740. [[CrossRef](#)]
175. Eade, K.; Giles, S.; Harkins-Perry, S.; Friedlander, M. Toxicity screens in human retinal organoids for pharmaceutical discovery. *J. Vis. Exp.* **2021**, *169*, e62269. [[CrossRef](#)]
176. Eastlake, K.; Wang, W.; Jayaram, H.; Murray-Dunning, C.; Carr, A.-J.; Ramsden, C.M.; Vugler, A.; Gore, K.; Clemo, N.; Stewart, M.; et al. Phenotypic and functional characterization of Müller glia isolated from induced pluripotent stem cell-derived retinal organoids: Improvement of retinal ganglion cell function upon transplantation. *Stem Cells Transl. Med.* **2019**, *8*, 775–784. [[CrossRef](#)]
177. Eldred, K.C.; Hadyniak, S.E.; Hussey, K.A.; Brennerman, B.; Zhang, P.-W.; Chamling, X.; Sluch, V.M.; Welsbie, D.S.; Hattar, S.; Taylor, J.; et al. Thyroid hormone signaling specifies cone subtypes in human retinal organoids. *Science* **2018**, *362*, eaau6348. [[CrossRef](#)]
178. Felemban, M.; Dorgau, B.; Hunt, N.C.; Hallam, D.; Zerti, D.; Bauer, R.; Ding, Y.; Collin, J.; Steel, D.; Krasnogor, N.; et al. Extracellular matrix component expression in human pluripotent stem cell-derived retinal organoids recapitulates retinogenesis in vivo and reveals an important role for IMPG1 and CD44 in the development of photoreceptors and interphotoreceptor matrix. *Acta Biomater.* **2018**, *74*, 207–221. [[CrossRef](#)]
179. Fligor, C.M.; Langer, K.B.; Sridhar, A.; Ren, Y.; Shields, P.K.; Edler, M.C.; Ohlemacher, S.K.; Sluch, V.M.; Zack, D.J.; Zhang, C.; et al. Three-Dimensional retinal organoids facilitate the investigation of retinal ganglion cell development, organization and neurite outgrowth from human pluripotent stem cells. *Sci. Rep.* **2018**, *8*, 14520. [[CrossRef](#)]
180. Freude, K.K.; Saruhanian, S.; McCauley, A.; Paterson, C.; Odette, M.; Oostenink, A.; Hyttel, P.; Gillies, M.; Haukedal, H.; Kolko, M. Enrichment of retinal ganglion and Müller glia progenitors from retinal organoids derived from human induced pluripotent stem cells—Possibilities and current limitations. *World J. Stem Cells* **2020**, *12*, 1171–1183. [[CrossRef](#)]
181. Gagliardi, G.; BEN M'Barek, K.; Chaffiol, A.; Slembrouck-Brec, A.; Conart, J.-B.; Nanteau, C.; Rabesandratana, O.; Sahel, J.-A.; Duebel, J.; Orioux, G.; et al. Characterization and transplantation of CD73-positive photoreceptors isolated from human iPSC-derived retinal organoids. *Stem Cell Rep.* **2018**, *11*, 665–680. [[CrossRef](#)]
182. Gantner, M.L.; Eade, K.; Wallace, M.; Handzlik, M.K.; Fallon, R.; Trombley, J.; Bonelli, R.; Giles, S.; Harkins-Perry, S.; Heeren, T.; et al. Serine and lipid metabolism in macular disease and peripheral neuropathy. *N. Engl. J. Med.* **2019**, *381*, 1422–1433. [[CrossRef](#)]
183. Gao, M.-L.; Lei, X.-L.; Han, F.; He, K.-W.; Jin, S.-Q.; Zhang, Y.-Y.; Jin, Z.-B. Patient-Specific retinal organoids recapitulate disease features of late-onset retinitis pigmentosa. *Front. Cell Dev. Biol.* **2020**, *8*, 128. [[CrossRef](#)]
184. Garita-Hernandez, M.; Chaffiol, A.; Guibbal, L.; Routet, F.; Khabou, H.; Riancho, L.; Toualbi, L.; Picaud, S.; Sahel, J.-A.; Goureau, O.; et al. Control of microbial opsin expression in stem cell derived cones for improved outcomes in cell therapy. *Front. Cell. Neurosci.* **2021**, *15*, 648210. [[CrossRef](#)] [[PubMed](#)]
185. Garita-Hernandez, M.; Guibbal, L.; Toualbi, L.; Routet, F.; Chaffiol, A.; Winckler, C.; Harinquet, M.; Robert, C.; Fouquet, S.; Bellow, S.; et al. Optogenetic light sensors in human retinal organoids. *Front. Neurosci.* **2018**, *12*, 789. [[CrossRef](#)]
186. Garita-Hernandez, M.; Routet, F.; Guibbal, L.; Khabou, H.; Toualbi, L.; Riancho, L.; Reichman, S.; Duebel, J.; Sahel, J.-A.; Goureau, O.; et al. AAV-Mediated gene delivery to 3D retinal organoids derived from human induced pluripotent stem cells. *Int. J. Mol. Sci.* **2020**, *21*, 994. [[CrossRef](#)] [[PubMed](#)]
187. Cordero, A.G.; Kruczek, K.; Naeem, A.; Fernando, M.; Kloc, M.; Ribeiro, J.F.C.; Goh, D.; Duran, Y.; Blackford, S.; Abelleira-Hervas, L.; et al. Recapitulation of human retinal development from human pluripotent stem cells generates transplantable populations of cone photoreceptors. *Stem Cell Rep.* **2017**, *9*, 820–837. [[CrossRef](#)] [[PubMed](#)]
188. Guo, Y.; Wang, P.; Ma, J.H.; Cui, Z.; Yu, Q.; Liu, S.; Xue, Y.; Zhu, D.; Cao, J.; Li, Z.; et al. Modeling retinitis pigmentosa: Retinal organoids generated from the iPSCs of a patient with the USH2A mutation show early developmental abnormalities. *Front. Cell. Neurosci.* **2019**, *13*, 361. [[CrossRef](#)]
189. Hoshino, A.; Horvath, S.; Sridhar, A.; Chitsazan, A.; Reh, T.A. Synchrony and asynchrony between an epigenetic clock and developmental timing. *Sci. Rep.* **2019**, *9*, 3770. [[CrossRef](#)]
190. Huang, K.-C.; Wang, M.-L.; Chen, S.-J.; Kuo, J.-C.; Wang, W.-J.; Nguyen, P.N.N.; Wahlin, K.J.; Lu, J.-F.; Tran, A.A.; Shi, M.; et al. Morphological and molecular defects in human three-dimensional retinal organoid model of X-linked juvenile retinoschisis. *Stem Cell Rep.* **2019**, *13*, 906–923. [[CrossRef](#)]
191. Kaewkhaw, R.; Kaya, K.D.; Brooks, M.; Homma, K.; Zou, J.; Chaitankar, V.; Rao, M.; Swaroop, A. Transcriptome dynamics of developing photoreceptors in three-dimensional retina cultures recapitulates temporal sequence of human cone and rod differentiation revealing cell surface markers and gene networks. *Stem Cells* **2015**, *33*, 3504–3518. [[CrossRef](#)]

192. Kallman, A.; Capowski, E.E.; Wang, J.; Kaushik, A.M.; Jansen, A.D.; Edwards, K.L.; Chen, L.; Berlinicke, C.A.; Phillips, M.J.; Pierce, E.A.; et al. Investigating cone photoreceptor development using patient-derived NRL null retinal organoids. *Commun. Biol.* **2020**, *3*, 82. [[CrossRef](#)]
193. Kaya, K.D.; Chen, H.Y.; Brooks, M.J.; Kelley, R.A.; Shimada, H.; Nagashima, K.; De Val, N.; Drinnan, C.T.; Gieser, L.; Kruczek, K.; et al. Transcriptome-based molecular staging of human stem cell-derived retinal organoids uncovers accelerated photoreceptor differentiation by 9-cis retinal. *Mol. Vis.* **2019**, *25*, 663–678.
194. Kelley, R.A.; Chen, H.Y.; Swaroop, A.; Li, T. Accelerated development of rod photoreceptors in retinal organoids derived from human pluripotent stem cells by supplementation with 9-cis retinal. *STAR Protoc.* **2020**, *1*, 100033. [[CrossRef](#)]
195. Khabou, H.; Garita-Hernandez, M.; Chaffiol, A.; Reichman, S.; Jaillard, C.; Brazhnikova, E.; Bertin, S.; Forster, V.; Desrosiers, M.; Winckler, C.; et al. Noninvasive gene delivery to foveal cones for vision restoration. *JCI Insight* **2018**, *3*, e96029. [[CrossRef](#)]
196. Khan, M.; Arno, G.; Fakin, A.; Parfitt, D.A.; Dhooze, P.P.; Albert, S.; Bax, N.M.; Duijkers, L.; Niblock, M.; Hau, K.L.; et al. Detailed phenotyping and therapeutic strategies for intronic ABCA4 variants in stargardt disease. *Mol. Ther. Nucleic Acids* **2020**, *21*, 412–427. [[CrossRef](#)]
197. Kim, S.; Lowe, A.; Dharmat, R.; Lee, S.; Owen, L.A.; Wang, J.; Shakoor, A.; Li, Y.; Morgan, D.J.; Hejazi, A.A.; et al. Generation, transcriptome profiling, and functional validation of cone-rich human retinal organoids. *Proc. Natl. Acad. Sci. USA* **2019**, *116*, 10824–10833. [[CrossRef](#)]
198. Kruczek, K.; Qu, Z.; Gentry, J.; Fadl, B.R.; Gieser, L.; Hiriyanna, S.; Batz, Z.; Samant, M.; Samanta, A.; Chu, C.J.; et al. Gene therapy of dominant CRX-leber congenital amaurosis using patient stem cell-derived retinal organoids. *Stem Cell Rep.* **2021**, *16*, 252–263. [[CrossRef](#)]
199. Lai, H.I.A.M.; Chou, S.-J.; Chien, Y.; Tsai, P.-H.; Chien, C.-S.; Hsu, C.-C.; Jheng, Y.-C.; Wang, M.-L.; Chiou, S.-H.; Chou, Y.-B.; et al. Expression of endogenous angiotensin-converting enzyme 2 in human induced pluripotent stem cell-derived retinal organoids. *Int. J. Mol. Sci.* **2021**, *22*, 1320. [[CrossRef](#)]
200. Lakowski, J.; Welby, E.; Budinger, D.; Di Marco, F.; Di Foggia, V.; Bainbridge, J.W.; Wallace, K.; Gamm, D.M.; Ali, R.R.; Sowden, J.C. Isolation of human photoreceptor precursors via a cell surface marker panel from stem cell-derived retinal organoids and fetal retinae. *Stem Cells* **2018**, *36*, 709–722. [[CrossRef](#)]
201. Lam, P.T.; Gutierrez, C.; Del Rio-Tsonis, K.; Robinson, M.L. Generation of a retina reporter hiPSC line to label progenitor, ganglion, and photoreceptor cell types. *Transl. Vis. Sci. Technol.* **2020**, *9*, 21. [[CrossRef](#)]
202. Lane, A.; Jovanovic, K.; Shortall, C.; Ottaviani, D.; Panes, A.B.; Schwarz, N.; Guarascio, R.; Hayes, M.J.; Palfi, A.; Chadderton, N.; et al. Modeling and rescue of RP2 retinitis pigmentosa using iPSC-derived retinal organoids. *Stem Cell Rep.* **2020**, *15*, 67–79. [[CrossRef](#)]
203. Li, G.; Gao, G.; Wang, P.; Song, X.; Xu, P.; Xie, B.; Zhou, T.; Pan, G.; Peng, F.; Zhang, Q.; et al. Generation and characterization of induced pluripotent stem cells and retinal organoids from a Leber’s congenital amaurosis patient with novel RPE65 mutations. *Front. Mol. Neurosci.* **2019**, *12*, 212. [[CrossRef](#)] [[PubMed](#)]
204. Li, G.; Xie, B.; He, L.; Zhou, T.; Gao, G.; Liu, S.; Pan, G.; Ge, J.; Peng, F.; Zhong, X. Generation of retinal organoids with mature rods and cones from urine-derived human induced pluripotent stem cells. *Stem Cells Int.* **2018**, *2018*, 4968658. [[CrossRef](#)] [[PubMed](#)]
205. Li, Y.-P.; Deng, W.-L.; Jin, Z.-B. Modeling retinitis pigmentosa through patient-derived retinal organoids. *STAR Protoc.* **2021**, *2*, 100438. [[CrossRef](#)] [[PubMed](#)]
206. Lin, B.; McLelland, B.T.; Aramant, R.B.; Thomas, B.B.; Nistor, G.; Keirstead, H.S.; Seiler, M.J. Retina organoid transplants develop photoreceptors and improve visual function in RCS rats With RPE dysfunction. *Investig. Ophthalmol. Vis. Sci.* **2020**, *61*, 34. [[CrossRef](#)] [[PubMed](#)]
207. Liu, H.; Hua, Z.-Q.; Jin, Z.-B. Modeling human retinoblastoma using embryonic stem cell-derived retinal organoids. *STAR Protoc.* **2021**, *2*, 100444. [[CrossRef](#)]
208. Liu, H.; Zhang, Y.; Zhang, Y.-Y.; Li, Y.-P.; Hua, Z.-Q.; Zhang, C.-J.; Wu, K.-C.; Yu, F.; Zhang, Y.; Su, J.; et al. Human embryonic stem cell-derived organoid retinoblastoma reveals a cancerous origin. *Proc. Natl. Acad. Sci. USA* **2020**, *117*, 33628–33638. [[CrossRef](#)]
209. Liu, S.; Xie, B.; Song, X.; Zheng, D.; He, L.; Li, G.; Gao, G.; Peng, F.; Yu, M.; Ge, J.; et al. Self-Formation of RPE spheroids facilitates enrichment and expansion of hiPSC-derived RPE generated on retinal organoid induction platform. *Investig. Ophthalmol. Vis. Sci.* **2018**, *59*, 5659–5669. [[CrossRef](#)]
210. Lowe, A.; Harris, R.; Bhansali, P.; Cvekl, A.; Liu, W. Intercellular adhesion-dependent cell survival and rock-regulated actomyosin-driven forces mediate self-formation of a retinal organoid. *Stem Cell Rep.* **2016**, *6*, 743–756. [[CrossRef](#)]
211. Lu, Y.; Shiao, F.; Yi, W.; Lu, S.; Wu, Q.; Pearson, J.D.; Kallman, A.; Zhong, S.; Hoang, T.; Zuo, Z.; et al. Single-Cell analysis of human retina identifies evolutionarily conserved and species-specific mechanisms controlling development. *Dev. Cell* **2020**, *53*, 473–491.e9. [[CrossRef](#)]
212. Lukovic, D.; Castro, A.A.; Kaya, K.D.; Munezero, D.; Gieser, L.; Davó-Martínez, C.; Corton, M.; Cuenca, N.; Swaroop, A.; Ramamurthy, V.; et al. Retinal organoids derived from hiPSCs of an AIPL1-LCA patient maintain cytoarchitecture despite reduced levels of mutant AIPL1. *Sci. Rep.* **2020**, *10*, 5426. [[CrossRef](#)]
213. Luo, Z.; Xu, C.; Li, K.; Xian, B.; Liu, Y.; Li, K.; Liu, Y.; Rong, H.; Tang, M.; Hu, D.; et al. Islet1 and Brn3 expression pattern study in human retina and hiPSC-derived retinal organoid. *Stem Cells Int.* **2019**, *2019*, 8786396. [[CrossRef](#)]
214. Luo, Z.; Zhong, X.; Li, K.; Xie, B.; Liu, Y.; Ye, M.; Li, K.; Xu, C.; Ge, J. An optimized system for effective derivation of three-dimensional retinal tissue via Wnt signaling regulation. *Stem Cells* **2018**, *36*, 1709–1722. [[CrossRef](#)]

215. Mao, X.; An, Q.; Xi, H.; Yang, X.-J.; Zhang, X.; Yuan, S.; Wang, J.; Hu, Y.; Liu, Q.; Fan, G. Single-Cell RNA sequencing of hESC-derived 3D retinal organoids reveals novel genes regulating RPC commitment in early human retinogenesis. *Stem Cell Rep.* **2019**, *13*, 747–760. [[CrossRef](#)]
216. McLelland, B.T.; Lin, B.; Mathur, A.; Aramant, R.B.; Thomas, B.B.; Nistor, G.; Keirstead, H.S.; Seiler, M.J. Transplanted hESC-derived retina organoid sheets differentiate, integrate, and improve visual function in retinal degenerate rats. *Investig. Ophthalmol. Vis. Sci.* **2018**, *59*, 2586–2603. [[CrossRef](#)]
217. Mellough, C.B.; Collin, J.; Queen, R.; Hilgen, G.; Dorgau, B.; Zerti, D.; Felemban, M.; White, K.; Sernagor, E.; Lako, M. Systematic comparison of retinal organoid differentiation from human pluripotent stem cells reveals stage specific, cell line, and methodological differences. *Stem Cells Transl. Med.* **2019**, *8*, 694–706. [[CrossRef](#)]
218. Ohlemacher, S.K.; Iglesias, C.L.; Sridhar, A.; Gamm, D.M.; Meyer, J.S. Generation of highly enriched populations of optic vesicle-like retinal cells from human pluripotent stem cells. *Curr. Protoc. Stem Cell Biol.* **2015**, *32*, 1H.8.1–1H.8.20. [[CrossRef](#)]
219. Ohlemacher, S.K.; Sridhar, A.; Xiao, Y.; Hochstetler, A.E.; Sarfarazi, M.; Cummins, T.R.; Meyer, J.S. Stepwise differentiation of retinal ganglion cells from human pluripotent stem cells enables analysis of glaucomatous neurodegeneration. *Stem Cells* **2016**, *34*, 1553–1562. [[CrossRef](#)]
220. Ovando-Roche, P.; West, E.L.; Branch, M.J.; Sampson, R.D.; Fernando, M.; Munro, P.; Georgiadis, A.; Rizzi, M.; Kloc, M.; Naeem, A.; et al. Use of bioreactors for culturing human retinal organoids improves photoreceptor yields. *Stem Cell Res. Ther.* **2018**, *9*, 156. [[CrossRef](#)]
221. Parfitt, D.A.; Lane, A.; Ramsden, C.M.; Carr, A.-J.; Munro, P.M.; Jovanovic, K.; Schwarz, N.; Kanuga, N.; Muthiah, M.N.; Hull, S.; et al. Identification and correction of mechanisms underlying inherited blindness in human iPSC-derived optic cups. *Cell Stem Cell* **2016**, *18*, 769–781. [[CrossRef](#)] [[PubMed](#)]
222. Pasquini, G.; Cora, V.; Swiersy, A.; Achberger, K.; Antkowiak, L.; Müller, B.; Wimmer, T.; Frasncka, S.A.-K.; Casadei, N.; Ueffing, M.; et al. Using transcriptomic analysis to assess double-strand break repair activity: Towards precise In Vivo genome editing. *Int. J. Mol. Sci.* **2020**, *21*, 1380. [[CrossRef](#)] [[PubMed](#)]
223. Peskova, L.; Jurcikova, D.; Vanova, T.; Krivanek, J.; Capandova, M.; Sramkova, Z.; Sebestikova, J.; Kolouskova, M.; Kotasova, H.; Streit, L.; et al. miR-183/96/182 cluster is an important morphogenetic factor targeting PAX6 expression in differentiating human retinal organoids. *Stem Cells* **2020**, *38*, 1557–1567. [[CrossRef](#)] [[PubMed](#)]
224. Phillips, M.J.; Capowski, E.E.; Petersen, A.; Jansen, A.D.; Barlow, K.; Edwards, K.L.; Gamm, D.M. Generation of a rod-specific NRL reporter line in human pluripotent stem cells. *Sci. Rep.* **2018**, *8*, 2370. [[CrossRef](#)]
225. Quinn, P.M.; Buck, T.M.; Mulder, A.A.; Ohonin, C.; Alves, C.H.; Vos, R.M.; Bialecka, M.; van Herwaarden, T.; van Dijk, E.H.; Talib, M.; et al. Human iPSC-derived retinas recapitulate the fetal CRB1 CRB2 complex formation and demonstrate that photoreceptors and Müller Glia are targets of AAV5. *Stem Cell Rep.* **2019**, *12*, 906–919. [[CrossRef](#)]
226. Quinn, P.M.; Buck, T.M.; Ohonin, C.; Mikkers, H.M.M.; Wijnholds, J. Production of iPSC-derived human retinal organoids for use in transgene expression assays. *Adv. Struct. Saf. Stud.* **2017**, *1715*, 261–273. [[CrossRef](#)]
227. Regent, F.; Chen, H.Y.; A Kelley, R.; Qu, Z.; Swaroop, A.; Li, T. A simple and efficient method for generating human retinal organoids. *Mol. Vis.* **2020**, *26*, 97–105.
228. Ribeiro, J.; Procyk, C.A.; West, E.L.; O'Hara-Wright, M.; Martins, M.F.; Khorasani, M.M.; Hare, A.; Basche, M.; Fernando, M.; Goh, D.; et al. Restoration of visual function in advanced disease after transplantation of purified human pluripotent stem cell-derived cone photoreceptors. *Cell Rep.* **2021**, *35*, 109022. [[CrossRef](#)]
229. Scholler, J.; Groux, K.; Goureau, O.; Sahel, J.-A.; Fink, M.; Reichman, S.; Boccara, C.; Grieve, K. Dynamic full-field optical coherence tomography: 3D live-imaging of retinal organoids. *Light. Sci. Appl.* **2020**, *9*, 140. [[CrossRef](#)]
230. Sharma, T.; Wiley, L.A.; Whitmore, S.S.; Anfinson, K.R.; Cranston, C.M.; Oppedal, D.J.; Daggett, H.T.; Mullins, R.F.; Tucker, B.A.; Stone, E.M. Patient-specific induced pluripotent stem cells to evaluate the pathophysiology of TRNT1-associated Retinitis pigmentosa. *Stem Cell Res.* **2017**, *21*, 58–70. [[CrossRef](#)]
231. Shimada, H.; Lü, Q.; Insinna-Kettenhofen, C.; Nagashima, K.; English, M.A.; Semler, E.M.; Mahgereteh, J.; Cideciyan, A.V.; Li, T.; Brooks, B.P.; et al. In Vitro modeling using ciliopathy-patient-derived cells reveals distinct cilia dysfunctions caused by CEP290 mutations. *Cell Rep.* **2017**, *20*, 384–396. [[CrossRef](#)]
232. Shrestha, R.; Wen, Y.-T.; Ding, D.-C.; Tsai, R.-K. Aberrant hiPSCs-derived from human keratinocytes differentiates into 3D retinal organoids that acquire mature photoreceptors. *Cells* **2019**, *8*, 36. [[CrossRef](#)]
233. Singh, D.; Wang, S.; Xia, T.; Tainsh, L.; Ghiassi-Nejad, M.; Xu, T.; Peng, S.; Adelman, R.A.; Rizzolo, L.J. A biodegradable scaffold enhances differentiation of embryonic stem cells into a thick sheet of retinal cells. *Biomaterials* **2018**, *154*, 158–168. [[CrossRef](#)]
234. Singh, R.K.; Mallela, R.K.; Cornuet, P.K.; Reifler, A.N.; Chervenak, A.P.; West, M.D.; Wong, K.Y.; Nasonkin, I.O. Characterization of three-dimensional retinal tissue derived from human embryonic stem cells in adherent monolayer cultures. *Stem Cells Dev.* **2015**, *24*, 2778–2795. [[CrossRef](#)]
235. Singh, R.K.; Ocelli, L.M.; Binette, F.; Petersen-Jones, S.; Nasonkin, I.O. Transplantation of human embryonic stem cell-derived retinal tissue in the subretinal space of the cat eye. *Stem Cells Dev.* **2019**, *28*, 1151–1166. [[CrossRef](#)]
236. Singh, R.K.; Winkler, P.A.; Binette, F.; Petersen-Jones, S.M.; Nasonkin, I.O. Comparison of developmental dynamics in human fetal retina and human pluripotent stem cell-derived retinal tissue. *Stem Cells Dev.* **2021**, *30*, 399–417. [[CrossRef](#)]

237. Sridhar, A.; Hoshino, A.; Finkbeiner, C.R.; Chitsazan, A.; Dai, L.; Haugan, A.K.; Eschenbacher, K.M.; Jackson, D.L.; Trapnell, C.; Birmingham-McDonogh, O.; et al. Single-Cell transcriptomic comparison of human fetal retina, hPSC-derived retinal organoids, and long-term retinal cultures. *Cell Rep.* **2020**, *30*, 1644–1659.e4. [[CrossRef](#)]
238. Sridhar, A.; Ohlemacher, S.K.; Langer, K.B.; Meyer, J.S. Robust differentiation of mRNA-reprogrammed human induced pluripotent stem cells toward a retinal lineage. *Stem Cells Transl. Med.* **2016**, *5*, 417–426. [[CrossRef](#)]
239. Sridhar, A.; Steward, M.M.; Meyer, J.S. Nonxenogeneic growth and retinal differentiation of human induced pluripotent stem cells. *Stem Cells Transl. Med.* **2013**, *2*, 255–264. [[CrossRef](#)]
240. Tornabene, P.; Trapani, I.; Minopoli, R.; Centrulo, M.; Lupo, M.; De Simone, S.; Tiberi, P.; Dell’Aquila, F.; Marrocco, E.; Iodice, C.; et al. Intein-mediated protein trans-splicing expands adeno-associated virus transfer capacity in the retina. *Sci. Transl. Med.* **2019**, *11*, eaav4523. [[CrossRef](#)]
241. VanderWall, K.B.; Huang, K.-C.; Pan, Y.; Lavekar, S.S.; Fligor, C.M.; Allsop, A.R.; Lentsch, K.A.; Dang, P.; Zhang, C.; Tseng, H.C.; et al. Retinal ganglion cells with a glaucoma OPTN(E50K) mutation exhibit neurodegenerative phenotypes when derived from three-dimensional retinal organoids. *Stem Cell Rep.* **2020**, *15*, 52–66. [[CrossRef](#)] [[PubMed](#)]
242. Vergara, M.N.; Flores-Bellver, M.; Aparicio-Domingo, S.; McNally, M.; Wahlin, K.J.; Saxena, M.T.; Mumm, J.S.; Canto-Soler, M.V. Enabling quantitative screening in retinal organoids: 3D automated reporter quantification technology (3D-ARQ). *Development* **2017**, *144*, 3698–3705. [[CrossRef](#)] [[PubMed](#)]
243. Vig, A.; Poulter, J.A.; Poulter, J.A.; Ottaviani, D.; Tavares, E.; Toropova, K.; Tracawska, A.M.; Mollica, A.; Kang, J.; Kehelwathugoda, O.; et al. DYNC2H1 hypomorphic or retina-predominant variants cause nonsyndromic retinal degeneration. *Genet. Med.* **2020**, *22*, 2041–2051. [[CrossRef](#)] [[PubMed](#)]
244. Völkner, M.; Pavlou, M.M.; Büning, H.; Michalakis, S.; Karl, M. Optimized adeno-associated virus vectors for efficient transduction of human retinal organoids. *Hum. Gene Ther.* **2021**, in press. [[CrossRef](#)]
245. Wahlin, K.J.; Maruotti, J.A.; Sripathi, S.R.; Ball, J.; Angueyra, J.; Kim, C.; Grebe, R.; Li, W.; Jones, B.W.; Zack, D.J. Photoreceptor outer segment-like structures in long-term 3D retinas from human pluripotent stem cells. *Sci. Rep.* **2017**, *7*, 766. [[CrossRef](#)]
246. Wang, S.; Poli, S.; Liang, X.; Peng, G.-H. Longitudinal single-cell RNA-seq of hESCs-derived retinal organoids. *Sci. China Life Sci.* **2021**. [[CrossRef](#)]
247. Welby, E.; Lakowski, J.; Di Foggia, V.; Budinger, D.; Cordero, A.G.; Lun, A.T.; Epstein, M.; Patel, A.; Cuevas, E.; Kruczek, K.; et al. Isolation and comparative transcriptome analysis of human Fetal AND iPSC-derived cone photoreceptor cells. *Stem Cell Rep.* **2017**, *9*, 1898–1915. [[CrossRef](#)]
248. Wiley, L.; Burnight, E.R.; DeLuca, A.P.; Anfinson, K.R.; Cranston, C.M.; Kaalberg, E.E.; Penticoff, J.A.; Affatigato, L.M.; Mullins, R.F.; Stone, E.M.; et al. cGMP production of patient-specific iPSCs and photoreceptor precursor cells to treat retinal degenerative blindness. *Sci. Rep.* **2016**, *6*, 30742. [[CrossRef](#)]
249. Wright, L.S.; Pinilla, I.; Saha, J.; Clermont, J.M.; Lien, J.S.; Borys, K.D.; Capowski, E.E.; Phillips, M.J.; Gamm, D.M. VSX2 and ASCL1 are indicators of neurogenic competence in human retinal progenitor cultures. *PLoS ONE* **2015**, *10*, e0135830. [[CrossRef](#)]
250. Xian, B.; Luo, Z.; Li, K.; Li, K.; Tang, M.; Yang, R.; Lu, S.; Zhang, H.; Ge, J. Dexamethasone provides effective immunosuppression for improved survival of retinal organoids after epiretinal transplantation. *Stem Cells Int.* **2019**, *2019*, 7148032. [[CrossRef](#)]
251. Xie, H.; Zhang, W.; Zhang, M.; Akhtar, T.; Li, Y.; Yi, W.; Sun, X.; Zuo, Z.; Wei, M.; Fang, X.; et al. Chromatin accessibility analysis reveals regulatory dynamics of developing human retina and hiPSC-derived retinal organoids. *Sci. Adv.* **2020**, *6*, eaay5247. [[CrossRef](#)]
252. Zeng, Y.; Li, M.; Zou, T.; Chen, X.; Li, Q.; Li, Y.; Ge, L.; Chen, S.; Xu, H. The impact of Particulate Matter (PM<sub>2.5</sub>) on human retinal development in hESC-derived retinal organoids. *Front. Cell Dev. Biol.* **2021**, *9*, 607341. [[CrossRef](#)]
253. Zerti, D.; Dorgau, B.; Felemban, M.; Ghareeb, A.; Yu, M.; Ding, Y.; Krasnogor, N.; Lako, M. Developing a simple method to enhance the generation of cone and rod photoreceptors in pluripotent stem cell-derived retinal organoids. *Stem Cells* **2019**, *38*, 45–51. [[CrossRef](#)]
254. Zerti, D.; Molina, M.M.; Dorgau, B.; Mearns, S.; Bauer, R.; Al-Aama, J.; Lako, M. IGF1Ps mediate IGF-1’s functions in retinal lamination and photoreceptor development during pluripotent stem cell differentiation to retinal organoids. *Stem Cells* **2021**, *39*, 458–466. [[CrossRef](#)]
255. Zhang, X.; Thompson, J.A.; Zhang, D.; Charnig, J.; Arunachalam, S.; McLaren, T.L.; Lamey, T.M.; De Roach, J.N.; Jennings, L.; McLenachan, S.; et al. Characterization of CRB1 splicing in retinal organoids derived from a patient with adult-onset rod-cone dystrophy caused by the c.1892A>G and c.2548G>A variants. *Mol. Genet. Genom. Med.* **2020**, *8*, e1489. [[CrossRef](#)]
256. Zhang, X.; Zhang, D.; Thompson, J.A.; Chen, S.; Huang, Z.; Jennings, L.; McLaren, T.L.; Lamey, T.M.; De Roach, J.N.; Chen, F.K.; et al. Gene correction of the CLN3 c.175G>A variant in patient-derived induced pluripotent stem cells prevents pathological changes in retinal organoids. *Mol. Genet. Genom. Med.* **2021**, *9*, e1601. [[CrossRef](#)]
257. Zheng, C.; Schneider, J.W.; Hsieh, J. Role of RB1 in human embryonic stem cell-derived retinal organoids. *Dev. Biol.* **2020**, *462*, 197–207. [[CrossRef](#)]
258. Zhu, Y.; Carido, M.; Meinhardt, A.; Kurth, T.; Karl, M.; Ader, M.; Tanaka, E.M. Three-Dimensional neuroepithelial culture from human embryonic stem cells and its use for quantitative conversion to retinal pigment epithelium. *PLoS ONE* **2013**, *8*, e54552. [[CrossRef](#)]

259. Zou, T.; Gao, L.; Zeng, Y.; Li, Q.; Li, Y.; Chen, S.; Hu, X.; Chen, X.; Fu, C.; Xu, H.; et al. Organoid-Derived C-Kit<sup>+</sup>/SSEA4<sup>−</sup> human retinal progenitor cells promote a protective retinal microenvironment during transplantation in rodents. *Nat. Commun.* **2019**, *10*, 1205. [[CrossRef](#)]
260. Eiraku, M.; Takata, N.; Ishibashi, H.; Kawada, M.; Sakakura, E.; Okuda, S.; Sekiguchi, K.; Adachi, T.; Sasai, Y. Self-organizing optic-cup morphogenesis in three-dimensional culture. *Nature* **2011**, *472*, 51–56. [[CrossRef](#)]
261. Furue, M.K.; Na, J.; Jackson, J.P.; Okamoto, T.; Jones, M.; Baker, D.; Hata, R.-I.; Moore, H.D.; Sato, J.D.; Andrews, P.W. Heparin promotes the growth of human embryonic stem cells in a defined serum-free medium. *Proc. Natl. Acad. Sci. USA* **2008**, *105*, 13409–13414. [[CrossRef](#)]
262. Yamazoe, H.; Kobori, M.; Murakami, Y.; Yano, K.; Satoh, M.; Mizuseki, K.; Sasai, Y.; Iwata, H. One-Step induction of neurons from mouse embryonic stem cells in serum-free media containing vitamin B12 and heparin. *Cell Transplant.* **2006**, *15*, 135–145. [[CrossRef](#)]
263. Colombres, M.; Henriquez, J.P.; Reig, G.F.; Scheu, J.; Calderón, R.; Alvarez, A.; Brandan, E.; Inestrosa, N.C. Heparin activates Wnt signaling for neuronal morphogenesis. *J. Cell. Physiol.* **2008**, *216*, 805–815. [[CrossRef](#)]
264. Bejoy, J.; Wang, Z.; Bijonowski, B.; Yang, M.; Ma, T.; Sang, Q.-X.; Li, Y. Differential effects of heparin and hyaluronic acid on neural patterning of human induced pluripotent stem cells. *ACS Biomater. Sci. Eng.* **2018**, *4*, 4354–4366. [[CrossRef](#)]
265. McCabe, K.; Gunther, E.; Reh, T. The development of the pattern of retinal ganglion cells in the chick retina: Mechanisms that control differentiation. *Development* **1999**, *126*, 5713–5724. [[CrossRef](#)]
266. Zheng, L.; Zhang, J.; Carthew, R. Frizzled regulates mirror-symmetric pattern formation in the *Drosophila* eye. *Development* **1995**, *121*, 3045–3055. [[CrossRef](#)]
267. Liu, C.; Nathans, J. An essential role for frizzled 5 in mammalian ocular development. *Development* **2008**, *135*, 3567–3576. [[CrossRef](#)]
268. Wong, K.A.; Trembley, M.; Wahab, S.A.; Viczian, A.S. Efficient retina formation requires suppression of both Activin and BMP signaling pathways in pluripotent cells. *Biol. Open* **2015**, *4*, 573–583. [[CrossRef](#)]
269. Todd, L.; Palazzo, I.; Squires, N.; Mendonca, N.; Fischer, A.J. BMP- and TGFβ-signaling regulate the formation of Müller glia-derived progenitor cells in the avian retina. *Glia* **2017**, *65*, 1640–1655. [[CrossRef](#)]